A FRACTAL UNIVERSE MODEL

Patrick Driessen
190 rue Berthelot, B-1190 Brussels, Belgium.
Email: patrick.driessen@infinitesolutions.be

ABSTRACT

When interpreted in terms of a particular fractal model, regularities in the ratio of typical lengths and times between particles and galaxies are found which suggest that self-similarity between these two scales could exist. To establish the fractal model, we first review briefly some of the evidence *pro* and *contra* the local quasar hypothesis (LH). Forceful arguments have been advanced on both sides, whence we suggest, after others, that two classes of objects should be distinguished. A first class would be constituted of face-on giant elliptical radio galaxies and face-on Seyfert galaxies, with slight to moderate excess redshift. Those are called quasars in the mainstream literature. The second class would contain much smaller (about the size of a galaxy nucleus), faint and compact objects with large excess redshift, which we propose to call Compact Excess Redshift Objects (CEROs). The latter would be emitted by the nuclei of giant spiral and elliptical galaxies. A Unified Ejection Scheme (UES) could possibly unify many observations related to active galactic nuclei (AGN's), namely quasars, Seyferts, Liners and extended radio sources (ERS's). When the relationship between CEROs and galaxies is so understood, a possible link between galaxies and particles emerges: if galaxies not only emit CEROs but are also able to absorb them by a mechanism seen as the time-reversal of the ejection process, then they should interact with each other via CERO exchange. This process would be similar to photon exchange between electrons, where spiral galaxies and CEROs are considered as cosmic scale electrons and photons respectively. Giant elliptical galaxies would reproduce neutrons and protons exchange. Such a fractal model relating particles to galaxies allows the computation of scaling factors with respect to length, time, velocity, mass and angular momentum, with relatively good agreement between various tests of the model. The CERO speed with respect to the intergalactic medium (IGM) should be a constant and fall in the range 1000-4000 km/s. Finally, the CERO exchange force between two spiral galaxies is evaluated and it is shown to be greater than the conventional gravitational interaction. In analogy with the particle scale. New gravitational constants must be defined for each scale, and with the value found for the particle scale, the particle Planck mass, length and time fall respectively very close to the proton mass, the proton Compton length and the proton *Zitterbewegung* characteristic time.

1. THE MODEL

1.1 THE FRACTAL HYPOTHESIS

The early and dispersed works on objects with fractional dimensions were unified by Mandelbrot (1982) who coined the word "fractals", and who demonstrated their relevance to a great number of apparently disconnected fields. One of their most striking properties is self-similarity on different scales. Most man-made fractals are by design perfectly self-similar but, in real-life, this property could be the exception rather than the rule. Thus, whenever a natural fractal structure is suspected, the perfect self-similarity hypothesis should be tested carefully. Although the mathematics of fractals is still in its infancy, the concept has been applied to a growing number of problems with valuable results, and as a consequence of their conspicuousness, the idea that the Universe itself could be a fractal has emerged in some papers scattered through the literature. Even if the fractal universe hypothesis is not always clearly stated, at least these papers convey the intuition that scaling laws could apply between the microcosm and the macrocosm. In that vein, various self-similar models have flourished in the last decade. For example, several authors arrived by different routes at the notion of a cosmic scale Planck constant (Cocke, 1983, 1985; Liu Yong-Zhen, Deng Zu-Gan and Cao Sheng-Lin, 1984; DerSarkissian, 1986a). The hypothesis of quantized rotational velocities in the metagalaxy furnish essentially the same super Planck constant (Liakhovets, 1986). To try to account for the observed redshift quantization in galaxy pairs or in small clusters (Tifft, 1976, 1978, 1980, 1982a, 1982b; Cocke and Tifft, 1983; Tifft and Cocke, 1984), quantum models for the dynamics of interacting galaxies have been constructed (Cocke, 1983, 1985; DerSarkissian, 1984, 1986a, 1986b). Finally, Oldershaw has proposed an elaborate fractal space-time model (Oldershaw, 1985, 1986a, 1986b, 1986c, 1986d, 1987) and he has postulated the following scale transformations for length, time and mass hold between the particle, the stellar and the galactic scale:

$$R_{(n)} = \Lambda\, R_{(n-1)}; \quad T_{(n)} = \Lambda\, T_{(n-1)}; \quad M_{(n)} = \Lambda^D\, M_{(n-1)} \tag{1.1}$$

where $\Lambda = 5.2\ 10^{17}$ is the common scaling factor for length and time and D is a parameter, whose experimental value is about 3.17. The last equation shows that mass scales as L^D, whence it results that D is the so-called fractal mass dimension. Its analogy to the better-known self-similarity dimension is stressed by rewriting it as: $D = \left(\ln\left(M_{(n)}/M_{(n-1)}\right)\right)/\left(\ln\left(R_{(n)}/R_{(n-1)}\right)\right)$. In effect Λ^D gives the number of massive structures from level (n-1) necessary to compose a self-similar structure from level (n).

Neglecting for the moment the stellar scale, for which we feel that the data at our disposal is still too scarce to permit strong predictions either *pro* or *contra* the self-similarity hypothesis (although the situation on that front is evolving rapidly), we notice that those analogies between galaxy scale and particle scale objects have not been pushed very far, as if the fractal hypothesis would not really warrant serious consideration *per se*. In particular, gravitation has always been considered as the sole possible force acting between galaxies. This would invalidate from the start any comparison with the particle level where at least three interactions mediated by particle exchange have been found. Here we wish to explore the particle correspondence in greater detail and present arguments showing that at least one exchange-like force, stronger than the gravitational interaction, may intervene in galactic dynamics, in (perfect?) analogy with particle electrodynamics.

1.2 THE FRACTAL VORTEX MODEL

A full account of our own fractal space-time model is presented elsewhere (Driessen, 1991; see also Driessen, 1986, 2015). We shall introduce here only some of the very basic ideas that are just sufficient to guide us in the exploration of the self-similarity hypothesis. It must be stressed that they represent at this point mere conjectures, which should be judged *a posteriori* on the insights that they furnish and on their agreement with known experimental facts. Basically, part I will consist of a heuristic development of the fractal model, while part II is about its confrontation with observations.

Our views about the space-time structure can be summarized very briefly as follows: the Universe is an imbrication of self-similar vortex structures, whose Riemannian geometry bears a resemblance to the Einstein-Rosen bridge, establishing a connection between the sheets of a two-sheeted space-time (or rather, one single sheet of a given thickness, with two faces). In particular two scales were examined, namely the particle and the galaxy scale, and some qualitative similarities between particles and galaxies were found, provided that both objects contain a central black hole (BH). Actually, we think that it should better be viewed as a traversable wormhole. For example, using the membrane paradigm (Thorne, Price and MacDonald, 1986 and references therein) it can be shown that a galaxy with a (spheroidal) BH horizon needs two complete revolutions of its core to come back to its original topological state (Driessen, 1991), a property similar to spin 1/2 behaviour. This led us to associate tentatively spiral galaxies to electrons. Other types of particles (or galaxies) would be distinguished by the topology of the event horizon in their core. In particular, a possible Riemannian geometry was proposed for the photon core. The mechanism whereby an electron structure can emit and reabsorb a photon structure was provided albeit in a purely qualitative way (Driessen, 1991).

On each scale a medium can be defined which is composed of the sea of structures on the next lower self-similar scale. For example, on the galactic scale the medium is defined as the collection of particles composing stars, the interstellar medium (ISM), and the intergalactic medium (IGM). In the continuum approximation, this medium becomes a fluid embodying the space-time continuum. In other words, the space-time manifold is no more an abstract mathematical concept, it has gained the status of a material representation and galaxies are remarkably stable spinning structures in this fluid. On account of their morphology and their astonishing stability, it is guessed that they are vortex structures in this presumably quasi viscous less fluid. In fact, our model actually promotes comparison of galactic cores with vortex structures in superfluid Helium where the largest part of the body is irrotational and devoid of viscosity, while the viscous fluid is concentrated around vortex cores. Like galaxies, particles become vortex structures in the fluid of the postulated self-similar sub-structures, which we propose to call "fractons" for short. Fractons themselves would be vortex structures, etc … (Without prejudging if the hierarchy stops at any given scale). Generally, a structure at level *n* results from the amalgamation of a critical number of similar structures from level *n-1*, and this is the essence of the vortex fractal model. To unearth its finer details and implications, a reinterpretation of quasars will prove necessary. By quasars we shall collectively denote radio-loud quasi-stellar sources (QSS's) and radio-quiet quasi-stellar objects (QSO's). In the general acceptation quasars are defined as star-like objects on the Palomar Sky Survey prints, with strong continuum emission, broad permitted lines and narrow forbidden ones, and moderate to high redshift. So, incidentally, a large part of this paper will be devoted to a discussion of the redshift controversy (Field, Arp and Bahcall, 1973). While reviewing the evidence accumulated on both sides we were stricken by the validity and forcefulness of most of the arguments. Thus, we understood why opponents on each side felt justified to accept no less than the complete capitulation of the other side. Because the largest body of physicist has decided to keep the cosmological hypothesis for redshifts of all objects (maybe for the lack of a really convincing alternative), many have concluded that the problem is now settled to their advantage. But a detached look at the evidence proposed by the iconoclasts shows, in my opinion, that it cannot be dismissed as a collection of mere coincidences.

1.3 THE UNIFIED EJECTION SCHEME (UES)

For the majority of astronomers, all low- and high-redshift, radio-quiet and radio-loud quasars should be understood as the very luminous nuclei of extremely distant galaxies, the redshift being entirely due to the Universe expansion in what has been termed the cosmological hypothesis (CH). Some of their strongest arguments are, (i) fuzzes have been observed around many low-redshift quasars (Kristian, 1973; Hawkins, 1978; Stockton, 1978; Wehinger and Wyckoff, 1978; Wyckoff et al., 1981; Hutchings et al., 1981, 1982, 1984; Gehren et al., 1984; Malkan, 1984; Romanishin and Hintzen, 1989), and the fuzz spectrum is compatible with star light (Balick and Heckman, 1983; Boroson and Oke, 1984) (ii) for some quasars close to galaxies on the projected sky, absorption lines in the quasar spectrum have been found at the lower redshift of the galaxy (Blades, 1987 and references therein), (iii) some low-redshift quasars display very close (projected distance less than 50 kpc) galaxy companions at basically the same redshift (Heckman et al., 1984). In fact, a significant portion of low-redshift fuzzy quasars reside in groups of associated or even interacting galaxies (Hutchings et al., 1981, 1982, 1984; Wyckoff et al, 1981; Gehren et al. 1984), and it is even suggested that the quasar phenomenon may actually be triggered by interaction (tidal or merger) with gas-rich companions. This solid evidence demonstrates that at least some so-called quasars have cosmological redshifts.

However, soon after the first quasar discovery, a small band of dissident put forth the local hypothesis (LH) which postulated that quasars are in fact much closer objects than their redshift would indicate, probably ejected from the nuclei of galaxies (Terrell 1964, 1966; Hoyle, 1965; Hoyle and Burbidge, 1966; Hoyle, Burbidge and Sargent, 1966; Arp, 1967, 1971; Burbidge et al. 1971; Narlikar and Das, 1980; Sulentic, 1983a, 1983b, 1986). If those objects are effectively ejected by the nuclei of galaxies, they are of course much smaller than galaxies themselves. Since they have a redshift which is usually much greater than the redshift of the emitting galaxy, they must obviously have an excess redshift in addition to their cosmological one. For these reasons, we propose to call them Compact Excess Redshift Objects (CEROs). If the CERO excess redshifts were of purely Doppler origin, one would have to suppose that only our Galaxy could have emitted them to account for the fact that no blue-shifted quasar has ever been observed, but this is not tenable from the Copernician viewpoint. More natural is the idea that all large galaxies are able to emit CEROs but with Doppler redshift always more than offset by another cause at present unknown.

In 1971, a discovery by Arp strengthened the LH: in a particularly close pair of a low-redshift galaxy (NGC4319) and a higher redshift blue compact object MK205, originally signalled by Weedman (1970), Arp claimed to have photographed a luminous bridge connecting the two objects (Arp, 1971a). An interesting objection was raised by Stockton, Wyckoff and Wehinger (1979) who found that a small red companion (RC) just 3" NE to the nucleus of MK205 with stellar absorption lines at the redshift of the MK205 nucleus. This was used as an argument to claim that both where interacting galaxies at their redshift distance in the background of NGC4319. Part of the presumed connection was later attributed to tidal tails in this presumably interacting pair (Cecil and Stockton, 1985). But powerful image processing techniques by Sulentic (1983a) had already revealed a very thin tortuous filament inside the diffuse bridge. It apparently continues an undulating jet emerging from the galactic nucleus which is very suggestive of a precessing jet like those observed in some extended radio-sources. There may even be a second blue object (UV knot with an emission spectrum) in the background which would be also attached to NGC 4319 by a diametrically opposed jet (Sulentic, 1983b).

Simultaneously, a battle over statistics was fought (Arp, 1970; Burbidge et al., 1971; Weedman, 1980; Sulentic, 1981; Webster, 1982; Burbidge et al., 1990), with supporters of the LH claiming to have found more high-redshift QSO's closer to bright low-redshift galaxies than chance would allow, and in the meantime other cases of possible associations emerged (see the review by Narlikar, 1986). For example, Carilli, van Gorkom and Stocke (1989) found a large elongated gas cloud connecting the galaxy NGC 3067 to the nearby (16 kpc on the projected sky) quasar 3C 232 and including both of them. Actually, this system was the first recorded case of HI absorption lines in the quasar spectrum at the lower redshift of a nearby galaxy (Haschick and Burke, 1975). Somewhat later, Ca II absorption lines were also found (Boskenberg and Sargent, 1978) and they were thought to arise in a spherical halo surrounding the galaxy. However, after reviewing the known cases, Bowen et al. (1991b) conclude that there is no evidence for spherical Calcium-absorbing haloes covering the whole space around galaxies at our epoch. Calcium absorption is either confined to the optical disc, or distributed in tails as the discovery of Carilli et al. (1989) clearly shows in the NGC 3067-3C 232 system. Naturally, the tail could result from tidal interaction with another galaxy but none is found in the vicinity (in redshift space) of this system. The only interesting object nearby (on the plane of the sky) is the quasar which sits right in the middle of a transversal expansion of the tail. This suggests that it could be a CERO. Thus, a system which was hailed at the origin as bringing strong support to the CH actually reinforces the LH, and throws some doubt on other absorption cases. Other arguments and references in favour of the LH are collected in recent papers (Narlikar, 1986; Arp et al., 1990; Burbidge et al., 1990), and somewhat older references not cited here can be found in Arp's book (Arp, 1987). The status of the redshift controversy up to 1973 is detailed in Field, Arp and Bahcall (1973).

Anyhow, the balance of evidence presented so far suggests to us that there are serious cases of CEROs related to galaxies with much smaller redshift, and we claim, after Arp (1987), that the UES could be extended further to unify phenomena that seem now more or less disconnected; we have in mind quasars, Seyfert galaxies, Liners and extended radio-sources (ERS's), which are discussed in this order below.

About 2 to 4 % of spiral galaxies have been classified as Seyfert galaxies in relation to their active nuclei. Roughly, two sub-classes have been discovered: Seyfert Type 1 galaxies have broad permitted emission lines, narrow high-excitation forbidden lines and a strong featureless continuum, while Seyferts Type 2 display only narrow permitted and forbidden lines and a very weak continuum (both types are in general radio quiet). Obscuration of the nucleus continuum and of the broad-line region (BLR) in Seyfert 2s could be caused by dusty molecular gas clouds, forming a compact torus at about 1 to 50 pc from the nucleus, that is roughly between the BLR

and the narrow-line region (NLR), as shown recently (Antonucci and Miller, 1985; see also the review by Antonucci, 1993). Thus, apparent dissimilarities between Seyfert classes could entirely arise from different obscuration, viewing angle and geometry of the torus. Once this is admitted, the remaining concern is to understand how Seyfert galaxies relate to normal quiescent spirals. First, let us recall numerical simulations by Sanders and Prendergast (1974) which have shown that the *3kpc* expanding gas cloud in our own Galaxy could have been caused by a violent explosion some $67\ 10^6$ *years* ago, with a total energy release of $3\ 10^{58}$ *ergs*. If the phenomenon has a recurrence period of say 10^8 *yrs*., the total energy emitted over the Galaxy lifetime ($\approx 10^{10}$ *yrs*.) could be comparable to the total yield of a Seyfert galaxy ($\approx 10^{60}$ *ergs*). This suggests that our Galaxy could have had of the order of 100 Seyfert episodes in the past, a conclusion which should hold for other spiral galaxies as well. Such models of recurrent excitation have been proposed by many authors (Ambartsumian, 1958, 1961; Vorontsov-Velyaminov, 1961; Arp, 1966; Sanders and Prendergast, 1974; Sanders and Bania, 1976; Bailey and Clube, 1978; Clube, 1978, 1983). Keel has even argued that low-luminosity active nuclei (AGN's) are present in most if not all spiral galaxies (Keel, 1983). In the scheme proposed by Clube (1983), spiral galaxies undergo repeated Seyfert phases at intervals of 10^8 *yrs*., which subsist for about 10^6 *yrs*. and culminate in a 10^4 *yrs*. long quasar phase. In our model, Clube's "quasar" phase actually corresponds to the emergence of CEROs from the nucleus, a point which will be expanded below.

Liners show moderate activity, with a spectrum of low-excitation emission lines not similar to those of Seyferts or HII regions but rather reminiscent of emission spectra from supernova remnants. The currently held view is that they are photoionized by the power-law source from an AGN but with a smaller ionization parameter than in Seyfert galaxies. They could be either mini-Seyferts or dying Seyferts. For example, they could correspond to the aftermath of CERO ejection, when the active nucleus has been recently switched off but is still simmering weakly. An alternative view is that the supernova-like spectrum is due to shock wave heating. In a particular model (Terlevich and Melnick, 1985; Heckman, 1987) the origin of the shock excitation should be sought in the winds created by intense starburst activity. Sulentic (1988) pointed out that another possible mechanism had been overlooked: shocks in the wake of a high velocity body ejected from the galactic nucleus.

It is possible to sketch a plausible scenario for the unified ejection scheme (UES) in spiral galaxies. First, mass loss from stars in the bulge would result in a large number of low angular momentum dusty molecular clouds (Arp, 1966; Shklovsky, 1971) which may provide the fuel for nuclear activity along the following sequence. Gas would flow inwards to form an accretion disk (Lynden-Bell, 1969; Lynden-Bell and Pringle, 1974). Viscous stresses in the disk innermost region, of probable magnetic origin, would then transport angular momentum outwards and cause the gas to spiral down toward the central black hole. Now, one should wonder if the mass loss rate from bulge stars is consistent with energies involved in Seyfert galaxies. This seems to be the case at least for spirals. For example, Bailey and Clube (1978) evaluated the mass loss rate of our Galaxy at about $0.01\ M_\odot\ yr^{-1}$ in a bulge of about $10^{10}\ M_\odot$ at a distance smaller than 1kpc from the nucleus. The total mass accumulated in 10^8 *yrs*. would be $10^6\ M_\odot$ and with only a nuclear conversion efficiency of 0.7*%,* the energy released would already be sufficient to feed the Seyfert phenomenon, but it is well known that gravitational energy conversion can have much larger efficiencies. The origin of angular momentum loss in the first disk formation phase is still discussed. It could arise for example from some non-axially symmetric gravitational potential. The most plausible form of such a perturbation would be a bar which is known to arise very easily in self-gravitating disk. As computer simulations have shown, such a potential is able to force $0,5\ M_\odot\ yr^{-1}$ of the inner region gas to flow inwards (Simkin, Su and Schwarz, 1980; Schwarz, 1979). This process would be enhanced during encounters with companion galaxies where tidal interaction induces non axially symmetric perturbations.

Those predictions are relatively safe although fine details are still being debated, but beyond that point our model becomes much vaguer because we suspect that the physical theory driving the AGN evolution has yet to be invented (see § 2.8). A very qualitative description has been given in Driessen (1991) where it is guessed that local variations in the flow across the black hole event horizon can lead to quasi-periodical instabilities resulting in the formation of CERO structures of typically say $10^{6\text{-}7}\ M_\odot$ each. The most common case would be that of two CEROs ejected simultaneously in opposite directions to conserve momentum.

After this rapid overview of Seyferts and Liners, we now turn to extended radio-sources (ERS's) which originate from the core of large elliptical radio galaxies or (so-called) quasars, and generally display two large and diffuse lobes at the extremities of well collimated and diametrically opposed jets. Inside the lobes there are kpc scale hot spots, but no compact (pc scale) cores have ever been found. Sometimes, especially for so-called extended quasars, the structure is completely asymmetrical with only one jet and no counter-jet. We first discuss ERS's in radio galaxies and we shall come back to the problem of ERS's in quasars later on. Radio galaxies most of the time display absorption spectra typical of giant elliptical galaxies, leading to the basic questions: (i) is there a relationship between AGN's in Seyfert galaxies and ERS's in radio galaxies, and (ii) why does the Seyfert phenomenon always happen in spiral galaxies while large scale ERS's originate from elliptical galaxies? First, many observations point to a link between radio and Seyfert galaxies. They show that a number of radio galaxies have spectra similar to those of Type 1 or Type 2 Seyfert galaxies (Osterbrock, 1977; Grandi and Osterbrock, 1978) with either broad permitted lines and narrow forbidden lines (Type 1) or only narrow permitted and forbidden lines (Type 2), albeit with some slight differences (Grandi and Osterbrock, 1978). However, let us note that many radio galaxies do not show emission lines, not even the narrow ones (Hine and Longair, 1979). Conversely, Seyfert galaxies are also sometimes radio emitters but at lower power with typical luminosities $10^{21\text{-}25}\ W\ Hz^{-1}$ at *1GHz* (Wilson and Heckman, 1985; Beichman et al., 1985) as compared to the ERS's which have *1 GHz* luminosities in the range $10^{24\text{-}29}\ W\ Hz^{-1}$, and their lobes are much smaller ($\approx$ *1 kpc*) than the typical *100-500 kpc* scale for ERS's. Finally, the strict separation of Seyferts in spiral galaxies and ERS's in large elliptical galaxies is also questioned (Balick and Heckman, 1982; Beichman et al. 1985; Heckman et al. 1982). For example, about 10 % of known Seyfert nuclei are found in galaxies which could be classified as elliptical (Adams, 1977; Bradt et al., 1978; Caldwell and Phillips, 1981).

This evidence strongly suggests that the Seyfert and ERS phenomena are intimately related, which can be understood in the framework of the above model for the Seyfert emission. If the energy to feed the monster effectively originates from mass loss of stars in the spheroidal component with low angular momentum, then the following correlations become quite plain: firstly, it has been observed that Seyfert nuclei preferentially occur in early-type rather than late-type spiral galaxies (Heckman, 1978; Adams, 1977; Simkin et al., 1980), and secondly, elliptical galaxies display only a spheroidal component. Galaxies with a bigger spheroid would spend a larger fraction of their life-time in the AGN phase and would produce the most powerful radio sources (for an exhaustive account of the unified view-point, see the review by Lawrence, 1987). Thus, the difference between radio-quiet Seyferts and ERS's seems to be mostly a case of variation in the maximum intrinsic power achievable by the source and the fractional time spent in the active phase, but both phenomena would have basically the same origin. They would represent different manifestations of ejected CEROs, albeit at different powers and periodicities, with jets (vortex tubes in our model) of various radio powers connecting the CERO to the galactic nuclei. As shown in section 2.9, the ejection frequency is inversely proportional to the galactic mass, and periods could vary from $10^{7\text{-}8}$ *yrs*. in spirals to $10^{4\text{-}5}$ *yrs*. in ellipticals. Considering the large difference in available energy, ejection velocities could also differ considerably; from 0.01c in Seyfert galaxies to *0.5-0.7c* in giant elliptical galaxies (although, once freed from the vortex tube attaching them to the parent galaxy, all CEROs would move with the same speed, a point that will be made clear below).

1.4 OBJECTIONS TO THE UNIFIED EJECTION SCHEME

Three immediate and strong objections can be raised however against the extension of the UES to strong radio sources. First, the UES requires large amounts of gas in the spheroid and it is thus a surprise to find so little gas in most giant ellipticals where ERS's almost exclusively arise. The problem had already been noticed by Faber and Gallagher (1976) who argued that normal mass loss process from old population stars in the average elliptical galaxy is expected to produce *0.1-1* $M_\odot\ yr^{-1}$ of gas. Such a quantity not being observed, the gas must be either stored somewhere or it must be removed periodically or continuously from the system. Some possible process for the removal of gas (formation of new stars, hot gas at a few million degrees, clouds of very cold gas) have been discussed by Faber and Gallagher (1976) but none seems able to remove the gas produced in only 10^9 *yrs*. Sanders (1981) has proposed a pulsed wind mechanism: a long period ($5\ 10^8$ - 10^9 *yrs*.) of gas accumulation would be followed by cooling and star formation, giving rise to a shorter ($\approx 10^8$ *yrs*.) period of intense wind driven by a burst of supernova activity. In our model, if the accumulated gas can be transported to the nucleus, CERO ejection immediately follows. When expelled from the core of the parent galaxy, CEROs proceed through the spheroidal bulge and collect large amounts of gas because of their rather impressive mass which is estimated below at roughly $10^{6\text{-}7}\ M_\odot$. It is plausible that repeated ejections could entrain $10^{8\text{-}9}\ M_\odot$ out of the galaxy in $10^{7\text{-}8}$ *yrs*. Thus, CEROs may act as strong gas extractors, and possess a gaseous "fuzz" soon after departure. It is probably relevant to this picture that most clusters have been found to contain a hot ($\approx 10^8$ *K*), low-density ($\approx 10^{-3}$ atoms cm^{-3}), X-ray emitting gas (see Sarazin, 1986 for a review) concentrated around giant elliptical galaxies. Furthermore, X-ray emission lines from heavy elements suggest that a large portion of this gas came from stars in the galaxies. Not only may this gas trace past ejections but it may also provide part of the next lunch for the monster. Indeed, cooling flows have been observed that supply gas toward the centre of the galaxy (a good synthesis is given in Fabian et al., 1984).

The second objection arises from the fact that CEROs have never been found inside hot spots of ERS lobes, although it should be noted that in a few cases some have been observed nearby the lobes on the projected sky (Arp, 1987). As pointed out early by Burbidge (1967), hot spots are surprisingly persistent flat-spectrum sources which contain highly energetic electrons implying local reenergization far from the galactic core. This led him to suggest that they should contain massive objects (CEROs in our scheme), but actually they are not resolved below *1 kpc* nor do they exhibit emission lines. There is a plausible and elegant solution to this problem, and it also relates to the possibility of gas entrainment: when the CERO emerges from the galaxy, it is supposedly enshrouded in a dense gaseous cocoon whose ionized ejecta could feed the radio source lobes. Even if only a moderate fraction of dust mixed with the gas is present, it may be sufficient to block the CERO typical radiation, namely the broad and narrow lines, and the continuum (remember that CEROs are extremely small and faint objects in our model). Progressively, the CERO radiation pushes the cloud away and some relics are left trailing behind. The well-known broad-line spectrum then progressively appears as the CERO departs from the galactic neighbourhood. This scenario is corroborated by the fact that very broad absorption lines have been found at $z_{abs} \approx z_{em}$ in some radio-quiet quasars (BAL QSO's) and the actual consensus is that they result from gas ejected by the quasar itself (see the review by Turnshek, 1987). We also note that some indirect observations would be compatible with the presence of CEROs in the lobes: (i) at least 16 sources in the 3CR catalogue have multiple hot spots (Laing, 1981). (ii) Optical synchrotron emission from a faint diffuse object *(2 kpc* scale) has probably been found in the southern lobe of 3C33 (Meisenheimer and Röser, 1986) signalling the existence of at least *100 Gev* electrons. Their lifetimes are so short that they must map the region where the acceleration takes place. A smooth extrapolation between the radio and optical data requires a sharp break in the spectrum at about 10^{14} *Hz*. Lobe confinement and local particle reacceleration would be much simpler to explain if a massive and active object of $10^7\ M_\odot$ was present in the hot spot. Now, similar featureless spectra with a break around the same frequency have been found in a new class of extremely red quasars which are strong flat-spectrum radio emitters, variable on a time scale of weeks or less and which frequently lack emission lines (Rieke et al., 1979; Bregman et al., 1981). These red QSO's show a very steep decline in the spectrum between IR and optical wavelengths, with a spectral index around 3. They are easily detected in the IR but not optically and are much redder ($V\text{-}K \approx 6$) than a typical elliptical ($V\text{-}K \approx 3$). Again, they could be CEROs.

On the direct observational side, at least one possible case of a CERO inside a radio lobe (Kronberg et al., 1977) is known: 3C303 presents one compact lobe whose centre coincides with the nucleus of a 17th magnitude N-galaxy with redshift z = 0.141. Another

extended lobe contains three ultraviolet stellar-like objects with visual magnitude 20.0, 21.7 and 21.8 which have been labelled C, G and H. Object C is a bit off-centre from the lobe brightest spot, but still well in the radio contour and was shown to be a probable QSO with emission lines at $z = 1.57$. Object G lies nearly at the very centre of the lobe, and no lines have been detected. Object H is nearly outside the lobe and its spectrum is not known. The radio emission dies gradually away at the outer extremities in contrast to limb brightening in most sources. This may be linked to the fact that we are able to see the UV-excess objects. Maybe the lobes are dissipating, unmasking the CEROs which were previously obscured inside. We notice in that respect that it is precisely object G, the most inside the lobe, which shows no spectral features.

However, some objects currently classified as quasars appear to seriously threaten our model because they do not fit easily in the picture outlined above, and this is the third and most serious objection to the UES that we shall now discuss. A stringent test of the validity of our view is that quasar jets should always be intrinsically one-sided, because they supposedly connect CEROs to their parent galaxy. Being relatively slow meandering vortex tubes in our model, rather than relativistic beams, jets emitted by galaxies cannot come to an abrupt ending at shock fronts in the vacuum, and they must terminate on another vortex structure (the ejected CERO). In contrast, current theories assimilating radio-loud quasars to ERS's in very distant giant elliptical galaxies require beaming to explain asymmetry and two relativistic jets must always exist (the conventional relativistic beam model does not easily accommodate intrinsically one-sided jets).

Now, two-sided jets are definitely observed in a population of objects with quasar characteristics. Typically, one strong jet points towards a bright edge-brightened lobe on one side, and on the opposite side a somewhat weaker lobe may trace the terminating point of a fainter (or earlier) jet. Our goal here is to show that double-lobed QSS's are actually radio galaxies with jets close to the line of sight, which are affected by a slight amount of excess redshift (likewise, it is likely that some Seyfert 1 galaxies could pose as fainter QSO's). These objects will be called hereafter quasars in contrast to the CEROs which are supposedly emitted by galaxies. To establish the proposition, it must be demonstrated that a continuum of properties links radio galaxies to QSS's (and Seyfert galaxies to QSO's), but this is precisely what cosmological redshift supporters have attempted to do for quite a long time. In particular they reported optical fuzzes underlying most low-redshift quasars (Kristian, 1973; Wyckoff et al., 1981; Gehren et al., 1984; Hutchings et al., 1984; Malkan, 1984; Romanishin and Hintzen, 1989) and have shown a smooth transition between the luminosities of the most luminous Seyfert 1s and QSO's on one side, and the most luminous broad-line radio galaxies and QSS's on the other side (Lynden-Bell, 1971; Arakelian, 1971; Weedman, 1977). Their findings are more or less consistent with a picture where all radio-loud quasars reside in giant elliptical galaxies and all radio-quiet ones in spiral galaxies (see § 1.5 below). Our basic belief is more restricted, nevertheless many of their arguments can be turned around to suit our purpose which is to show that only *some* radio galaxies masquerade as double-lobed quasars (although all double-lobed quasars are radio-galaxies), and only *some* Seyferts as radio-quiet QSO's (but most radio-quiet QSO's are not Seyferts). In this respect we first note that the BLR is conspicuous in quasars although it is not often seen in radio galaxies, thus implying in the unified picture that quasars have more or less face-on orientation with OVVs and BL Lacs maybe representing the most extreme cases. It could also explain why quasars are much more asymmetrical than ERSs because of Doppler boosting of the incoming jet. Beaming cannot amplify the BLR emission lines, but it can enhance the UV/optical synchrotron emission from the base of the jet. In this picture, the featureless continuum progressively swamps the star light and the BLR emission as the jet comes closer and closer to the line of sight. In OVVs, some weak (with respect to the continuum) emission lines would still be visible, while in BL Lacs, they would be completely swallowed by the continuum. But it is unlikely that orientation alone can explain the extreme luminosities of some quasar nuclei with respect to the fuzz. What these objects represent is the peak of the active phase in galaxies rather than a separate population with intrinsically more luminous nuclei. For quasars in spiral galaxies there are indications that the extreme activity could be triggered by large amounts of gas being fed to the nucleus, a process maybe enhanced by tidal interaction with companions, or by merger with small gas-rich companions (Hutchings et al., 1982), or by direct collision between two gas-rich large spirals (Sanders et al., 1988). It is still not yet totally clear if this could be true for quasars in elliptical galaxies but the original idea that spheroidal galaxies might become active by accretion of gas was proposed very early (Shklowsky, 1962, 1971) and has received since some strong supporting evidence. Prominent dust lanes more or less perpendicular to the ejection axis are observed in some radio galaxies (Cen A is the prototype). They could be indicators of large amount of gas being funnelled to the nucleus during the active phase and it has also been noted that gas-rich elliptical galaxies are generally active (Sanders, 1981). Let us also remember that a low-redshift ($z=0.107$), infrared-loud but radio-quiet quasar (IRAS 13349 + 2438) has been discovered (Beichman et al., 1986), and these authors claim that the enormous infrared energy could come from dust heated by the continuum. It would reside in a gaseous cocoon around the quasar. Finally, notice that radio galaxies are much weaker in the infrared than quasars. This also indicates that the dust enshrouded phase in quasars is a transient of short duration.

While star mass loss is barely sufficient to provide the fuel for a giant elliptical like M87 which requires only $0.01\ M_\odot\ yr^{-1}$, it is inadequate to sustain quasars which may require from 1 to $100\ M_\odot\ yr^{-1}$, although if some excess redshift is present as we argue below, the requirements may be somewhat diminished. But in many cases, it seems that an extrinsic source is required. Two interesting processes could be (i) cooling flows from the hot intra-cluster gas which could accrete as much as $10\text{-}100\ M_\odot\ yr^{-1}$ onto the central giant ellipticals and cD's in clusters (see the reviews by Fabian et al. 1984; Sarazin, 1986; and also, Sarazin and O'Connell, 1983) and, (ii) the capture of gas-rich dwarf companion galaxies suggested in another context by Schweizer (1980). Merger with large spirals or direct gas stripping from colliding spirals, while theoretically possible, are unlikely because large spirals are seldom seen in the central part of clusters where giant ellipticals and cD's reside.

Another obstacle to the unifying viewpoint is that the NLR, also typical of quasars, is not seen in some radio galaxies. When it is seen, it is weaker than in quasars of comparable extended radio luminosity, by about a factor 5 (Browne, 1987), although a few cases

of radio galaxies with narrow lines nearly as strong as in quasars are known. But the NLR is difficult to hide, because it lies further away than the torus. We suspect that dust lanes evoked above could be present in most of them and obscure the narrow lines in galaxies seen from a plane more or less perpendicular to the ejection axis.

In the face-on orientation close to the jet axis, beaming could be significant, but nevertheless, there are indications that alone it cannot explain the very strong asymmetries, large sizes and powers in some sources: (a) jet speeds may be mildly or even non-relativistic, yet a few (non blazar) sources show extreme asymmetries requiring at least velocities $v \geq 0.9c$ for beaming to operate, (b) the deprojected average size of a sample of ultraluminous quasars put them at the extreme fringe of the linear size distribution for other quasars and radio galaxies (Barthel, 1987) and (c) estimated powers at redshift distances in low-redshift quasars are on the average larger than in radio galaxies and inverse Compton self-absorption could be a problem (Hoyle, Burbidge and Sargent, 1966).

Most of these objections (ultraluminous apparent velocities, large sizes and powers, the Compton catastrophe) could be removed if a hitherto unknown cause of excess redshift operated to make the sources appear at larger distances than they really are, as dissidents repeatedly stressed. It would arise from the same basic physical process that seems to occur in high-redshift CEROs and even in some classes of otherwise apparently normal spiral galaxies (Arp, 1987). Various observations seem to imply that it is positively correlated with (i) the gas column density along the photon path, and (ii) the degree of shock excitation in the gas, but it must be more subtle than simple scattering on gas atoms (Arp, 1990b). For example, Arp (1990a) has shown that Sc I galaxies with well delineated and thick spiral arms seem to have large excess redshift (large gas density in the arms), and large redshift differences were found by Jaakkola (1971) and Tifft (1972) between spirals and ellipticals located in the same clusters. It is probably of importance that first-ranked elliptical galaxies, usually devoid of gas, follow Hubble's law rather precisely. Small but significant redshift differences have been found by Tifft between arms (difference in gas densities and path length), and small excited galaxies are generally more redshifted than their large companions (the fact that they show early type absorption and emission lines indicates that they contain a lot of excited gas (Arp, 1987)). Finally, the galaxies NGC55 and NGC300 appear slightly redshifted with respect to hydrogen clouds that they may have ejected (Arp, 1987), and this could be explained if the temperature of these clouds is much smaller than the temperature of the disk gas. So according to this view, if quasars represent special phases in face-on radio galaxies when they are surrounded by an excited gaseous cocoon, they must necessarily have some excess redshift. Finally, the effect of decreasing CERO redshift with separation from nearby galaxies (see Burbidge et al., 1990, and references therein) could be explained by the progressive depletion of the gaseous cocoon. Note that some authors have proposed tired light mechanisms for the excess redshift (see Vigier, 1988, and references therein).

The extremely strong asymmetries in some ERS imply the further hypothesis that flip-flop ejection may take place. Rudnick and Edgar (1984) observe a deficit of symmetric sources with a strong avoidance behaviour: where a peak of radio emission is found on one side, no peak is found on the other side at the same distance from the nucleus. This they argue, is a proof that the lobes are formed by alternating ejection from the nucleus. Their model predicts velocities below about $0.12c$. Lonsdale and Morison (1983) have shown how to discriminate between young compact lobes, with typical spectral index 0.5-0.7, and ageing extended lobes with index 0.9-1.1. Thus, it became possible to approximately trace the history of successive ejections, and for asymmetric sources, they found that the picture is compatible with an alternate ejection model with flow speeds $< 0.3c$ and switching time of order 10^6 yrs. In some cases, it would seem that a string of a few successive ejections to the same side occur before the direction switches.

One possible mechanism for flip-flop has been discovered by Wiita and Siah (1981) albeit in the framework of a modified twin plasma beam model. By numerical simulations, they showed that when the relativistic plasma source is offset with respect to the confining gas cloud centre along the polar axis, the backward beam will be pinched and may even be suppressed. To obtain a periodic flip-flop, they suppose that the plasma source orbits around the gas cloud centre-of-mass. When applying their idea to the ERS in M87, they find a plausible period of 10^4 yrs. which could explain an uneven distribution between the two lobes if the lifetime of the source is of order 10^6 yrs. They also point out that misalignment between the jet and the hypothesized counter-jet is another indirect evidence for intrinsic asymmetry.

To conclude, it would seem that excitations in spirals and giant ellipticals can be accounted for by the same UES: the nuclei of both species would be able to emit CEROs. It should be stressed again that CEROs strongly differ from galaxies in our model: they have very different internal structures (Driessen, 1191) and can in no way evolve to become galaxies. This is the main difference between our model and Arp's scheme (Arp, 1987) which postulates that ejected CEROs expand and terminate as galaxies.

1.5 DIFFICULTIES OF THE CONVENTIONAL PICTURE

Our arguments in §1.4 could still be used to claim that *all* radio-loud quasars are radio galaxies (which is probably true for double-lobed ones but may not be for core-dominated ones) at large distance and *all* radio-quiet ones are Seyfert galaxies. Yet we shall show below, that even if allowance is made for beaming (and flip-flop?) to explain asymmetries etc.., other incongruities arise when all quasars are forced into the galaxy classification scheme as in the conventional unified picture. To avoid constant repetition, all data will be reduced hereafter to a Robertson-Walker space-time with $H_0 = 75\ km\ s^{-1}\ Mpc^{-1}$ and $q_0 = +1$. This does not reflect a belief in some cosmological model, but simply a trend in recent papers and should facilitate comparison of magnitudes and distances.

(a) Diameters

If radio-loud CEROs were at their cosmological distance, the average isophotal diameter at the surface brightness level of μ_r = 26 mag arsec^{-2} for the postulated radio galaxies underlying them would be $D = 128 \pm 34\ h_{75}^{-1}$ kpc (Gehren et al., 1984). In this sample, some have fairly normal diameters compared to the $D \approx 60 \pm 4.5\ h_{75}^{-1}$ kpc found by Sandage (1972a) for first-ranked cluster galaxies (cD galaxies excluded). But the median is too large for them to pertain to that category, and, as reflected by the large variance, a non-negligible number have diameters in the range *160-180* h_{75}^{-1} *kpc* which is rather extreme, even if they were super-giant cD galaxies. What is also striking is the considerable spread in radii compared to those of first-ranked cluster galaxies. For the same authors, the radio-quiet version in their sample would reside in smaller galaxies with spiral-like disks, of average diameter $37 \pm 8\ h_{75}^{-1}$ *kpc* (Gehren et al., 1984). Again, this is somewhat larger than the *25 kpc* usually quoted for the largest nearby spiral galaxies. Thus, the fuzzy quasars selected by Gehren et al. seem to reside in larger than usual galaxies with greater spread in dimensions.

(b) Absolute Magnitudes

Still following Gehren et al. (1984), the average magnitude of the fuzz underlying radio-loud quasars is $\langle M_R \rangle = -22.8 \pm 0.7$. This should be compared to the average magnitude of first-ranked cluster galaxies and radio galaxies. Sandage finds $\langle M_R \rangle = -24.11 \pm 0.37$ for first-ranked cluster elliptical galaxies (Sandage, 1973; $H_0 = 50$ km s^{-1} Mpc^{-1}, $q_0 = +1$) which translates to $\langle M_R \rangle = -23.22 \pm 0.37$ for $H_0 = 75$ km s^{-1} Mpc^{-1}. He also derived $\langle M_V \rangle = -22.98 \pm 0.49$ for radio galaxies (Sandage, 1972b; $H_0 = 50$ km s^{-1} Mpc^{-1}, $q_0 = +1$). Using a colour difference $M_R - M_V = -0.81$ identical to those of first-ranked cluster galaxies (Sandage, 1973), and converting to $H_0 = 75$, gives $\langle M_R \rangle = -22.91 \pm 0.49$ for radio galaxies. Thus, the postulated galaxies underlying radio-loud quasars seem to be on the average fainter than the first-ranked elliptical galaxies and even fainter than radio galaxies in general. This is surprising since they have larger than average radii! We also note the greater scatter of magnitudes for radio-loud quasars as compared to first ranked ellipticals and radio galaxies. For the radio-quiet version Gehren et al. (1984) find $\langle M_R \rangle = -20.5 \pm 1.3$ which compares well to the average $\langle M_R \rangle = -20.12 \pm 1$ for normal spirals and ellipticals (Sandage and Visvanathan, 1978; converted to $H_0 = 75$ kms^{-1}Mpc^{-1}).

(c) Conclusion

Even without mentioning the well-known enormous scatter of quasars around the mean Hubble diagram determined by first-ranked cluster galaxies (see for example Burbidge et al., 1990), it can be argued that the larger than usual spread in quasar characteristics pleads in favour of two separate populations, as suggested before (Rowan-Robinson, 1972, 1973; Arp, 1977; Burbidge 1979, 1980). The fact that a bimodal distribution cannot be demonstrated is probably due to the complications introduced by excess redshift in variable portion in both classes. When it will become possible to subtract it correctly, we believe that the fuzz around quasars (radio galaxies) will be slightly diminished and the diameter of the underlying galaxy will be brought back into the correct range. For CEROs, with large excess redshift, the fuzz diameter will become much smaller than a galactic diameter when scaled to its local distance. The latter case will be illustrated in the next section.

1.6 STATISTICAL DIFFERENCES BETWEEN CLASSES

In table I, a small list of (probable) CEROs very close to galaxies on the projected sky has been assembled. They have been picked up from the cases published by Arp and co-workers. We needed the diameter of their haloes, so that we retained only the systems which were sufficiently close to allow measurement of at least some CERO diameters (a few arcsec). So, this sample is heavily biased in favour of the largest and brightest companion QSO's. In fact, we kept only the cases where the companion galaxy is not further away than *30 Mpc*, which is basically the distance to NGC 4319. To ensure a large probability that the selected objects effectively interact with the galaxies, we kept only those which are closer to the galaxy than *20 kpc* in the local hypothesis. To the list we added the couple NGC 3067 - 3C232 discussed by Carilli et al. (1989). The two important parameters were the apparent magnitude and diameter. For the latter we obtained very rough measures from wide field plates published in the literature. This gave only a crude approximation but should be sufficient to obtain the order of magnitude needed for our later comparison with MK205 in §1.10.1. We computed the distance, linear diameter and absolute V magnitude in the local and cosmological hypothesis. For the CH, standard Robertson-Walker cosmological formulae were applied, together with corrections for absorption and reddening (see appendix A). As can be seen, absorption is negligible in most cases but reddening is not. It would not have mattered much until recently because the uncertainty on H_0 was so large. But recent determinations seem to converge on $H_0 = 75$-85 km s^{-1} Mpc^{-1}. For the local hypothesis these corrections (except absorption) must be changed somewhat because the redshift is no longer a distance indicator, but still contributes to the reddening correction. Details of the calculations are given in appendices B and C.

A quick glance at table I reveals that, in the CH, the average CERO diameter (*21.3 ± 13 kpc*) is small compared to those of first-ranked cluster galaxies, but compares well to those of large spiral galaxies, while the mean magnitude $M_V \approx -24 \pm 1.4$ is on the average one magnitude larger than for giant ellipticals. In the LH, diameters are extremely small as expected ($\approx 0.35 \pm 0.34$ *kpc*), even smaller than those of dwarf galaxies, and these objects are also extremely faint ($M_V \approx -12.1 \pm 2.47$), implying that only the closest ones are visible. Nevertheless, they are sufficiently bright that, as objected by Weedman (1976), if CEROs were recently emitted by our Galaxy,

we should see them as the brightest stars! With our numbers we can re-examine his claim. The latest possible bout of nuclear activity in the Milky Way could have happened about $67\ 10^7\ yrs$. ago (Sanders and Prendergast, 1974). Since CEROs presumably move at the speed of $2200\ km\ s^{-1}$ (see § 2.4), they should have crossed a distance of about $150\ kpc$. Supposing an absolute magnitude $-16 < M_V < -9$ (table I), the range of possible apparent magnitude at this distance would be: $5 < m_V < 12$. Hence, they should be seen, unless they fell back onto the nucleus, which is the most likely fate of ejected CEROs as explained in § 1.9.

From this small collection of probable CEROs, we can infer what their general properties should be:

(a) Low visual magnitude ($M_V \approx -12$). Only the closest and brightest are visible.
(b) Mild to high redshift, with the great majority in the range $0.5 < z < 2$.
(c) Mostly radio quiet. If some are radio loud, they should show flat spectra and compact morphology.
(d) Dusty if close to parent galaxy. The cocoon is lost progressively so that the spectrum evolves while the redshift diminishes.
(e) Very small (diameter $\approx 0.3\ kpc$).

GALAXY							HIGH Z COMPANION						LOCAL HYPOTHESIS				COSMOLOGICAL HYPOTHESIS		
	α	δ	l^{II}	b^{II}	A_V mag	z_g	Name	s (")	m_V mag	θ (")	z	K_z^s mag	S kpc	Δ Mpc	d kpc	M_V mag	Δ Mpc	d kpc	M_V mag
(1)	(2)	(3)	(4)	(5)	(6)	(7)	(8)	(9)	(10)	(11)	(12)	(13)	(14)	(15)	(16)	(17)	(18)	(19)	(20)
N470	0117	0309	136.6	-58.7	0.05	0.00790	68	93	19.9	3.2	1.875	-1.02	13.6	30.5	0.47	-13.86	2607	14.1	-24.65
							68D	96	18.2	4.3	1.533	-0.87	14.1	30.5	0.63	-15.42	2419	19.9	-25.92
N1073	0241	0110	171.0	-50.7	0.08	0.00415	BSO1	104	19.8	1.9	1.945	-1.06	7.6	15.2	0.14	-12.48	2640	8.3	-24.85
							BSO2	117	18.8	2.6	0.599	-0.42	8.6	15.2	0.19	-12.79	1497	11.8	-23.27
							RSO	84	20.0	2.3	1.411	-0.84	6.2	15.2	0.17	-12.06	2339	10.8	-23.95
N3034	0952	6955	141.4	40.6	0.15	0.00012	HOAG1	384	20.0	5.6	2.053	-1.13	9.7	5.2	0.14	-10.02	2688	24.0	-24.80
							HOAG2	516	21.0	5.6	2.058	-1.13	13.0	5.2	0.14	-9.02	2690	24.0	-23.81
							HOAG3	576	21.0	3.8	2.033	-1.12	14.5	5.2	0.09	-9.02	2679	16.1	-23.79
							M82-4	576	20.2	3.8	0.850	-0.68	14.5	5.2	0.09	-9.18	1837	18.0	-22.59
N3067	0955	3237	194.2	52.3	0.04	0.00500	3C232	114	15.8	8.0	0.533	-0.34	13.3	24.2	0.93	-16.77	1390	35.2	-26.02
N3079	0959	5557	157.8	48.3	0.00	0.00410	UB4	199	17.4	12.8	1.154	-0.83	19.6	20.4	1.26	-14.99	2142	61.7	-25.92
N3184	1015	4140	178.4	55.6	0.00	0.00190	UB1	284	17.7	6.4	0.152	0.52	12.0	8.7	0.27	-12.82	527	14.3	-21.89
N3384	1046	1254	233.5	57.7	0.06	0.00240	UB1	250	19.4	4.4	1.111	-0.81	9.8	8.1	0.17	-11.01	2104	21.3	-23.89
							UB13	167	20.6	6.5	0.497	-0.30	6.5	8.1	0.26	-9.58	1327	28.1	-21.09
N5107	1319	3848	96.0	77.0	0.00	0.00310	UB1	40	19.5	2.5	0.949	-0.73	3.8	19.9	0.24	-12.72	1946	12.1	-23.39
median..:															0.35	-12.12		21.3	-23.99
variance:															0.34	2.47		13.3	1.44

Tab.I: A short list of probable CEROs very close to galaxies on the projected sky.

(1) Name of the nearby galaxy.
(2) Right ascension (1950.0) of the galaxy, in hours (2 digits) and minutes (2 digits). All coordinates are from Tully (1988).
(3) Declination (1950.0) of the galaxy, in degrees (2 digits) and arc minutes (2 digits).
(4) Galactic longitude.
(5) Galactic latitude.
(6) Absorption inside our own Galaxy, in the V band, taken from Tully (1988). Determined as functions of galactic coordinates with the maps of Burstein and Heiles (1978). The same value has been attributed to all the high redshift companions of a given galaxy.
(7) Redshift of the nearby galaxy. From the catalogue of Burbidge, Hewitt, Narlikar and Das Gupta (1990), denoted hereafter as BHNDG. This value is considered the distance indicator of the galaxy and its CERO companions in the local hypothesis.
(8) CERO name, from BHNDG.
(9) Projected separation from the galaxy in arcsec, from BHNDG.
(10) Apparent magnitude in the V band, from BHNDG.
(11) CERO halo diameter in arcsec. These are rough and heterogeneous measures determined from the wide field plates published in the following papers: (a) N470: Arp, Surdej and Swings (1984), (b) N1073: Arp and Sulentic (1979), (c) N3034 (M82): Arp (1983), (d) N3079, N3184, N5107: Arp (1981), (e) N3384: Arp, Sulentic and Di Tullio (1979).
(12) CERO redshift, from BHNDG.
(13) Selective part of the reddening correction as a function of the CERO redshift z. The definitions and methods of calculation for this and the following columns are exposed in the appendices. It must be stressed that our reddening correction differs from the usual one by a factor *2.5 log (1+z)*. For example, the relation between our K^s and Sandage's K^* (Sandage, 1966) is as follows: $K^s + 2.5 \log(1+z) = - K^*$. We took the K^* values as a function of z directly from Sandage (1966) and interpolated them to our CERO redshifts. It would have been better to repeat Sandage's (1966) analysis on our CERO sample since their photometric properties may differ from those of objects selected by Sandage which may be contaminated by quasars.
(14) Projected linear separation from the galaxy in the local hypothesis, in kpc. Computed from equ. A.9 in appendix A, using the galaxy redshift z_g.
(15) CERO distance in the local hypothesis. This is in fact the distance to the companion galaxy taken from Tully (1988). It is based in most cases on the galaxy redshift z_g, assuming $H_0 = 75$ km $s^{-1}Mpc^{-1}$ and corrected for the attractive influence from the Virgo Cluster.
(16) CERO linear diameter in the local hypothesis. Computed from A.6 in appendix A, using the galaxy redshift.
(17) CERO absolute V magnitude in the local hypothesis. See equ. C.10 from appendix C.
(18) Quasar distance in the cosmological hypothesis. Computed from equ. A.5, using the total shift z, and assuming $H_0 = 75\ km\ s^{-1}Mpc^{-1}$, $q_0 = 1$.
(19) Quasar linear diameter in the cosmological hypothesis. Computed from A.6 with the total shift z.
(20) Quasar absolute magnitude in the cosmological hypothesis. Computed from A.8.

This is clearly not sufficiently different from the properties of quasars to permit a clear-cut distinction from observations alone without reliable distance indicators; that is, a hint of the absolute luminosity and scale. Could radio loudness mark the demarcation line, with radio quiets embodying CEROs? Probably not because radio loudness simply signals the presence of a jet, and even CEROs still in the vicinity of their parent galaxy may still be connected to a jet.

Now, it has been repeatedly suggested by many authors that two quasar classes do exist, and some criteria have been proposed to separate them, either related to the radio-properties alone or based on correlations between radio and spectroscopic properties, namely: (i) radio-quiet versus radio-loud (Bergeron and Kunth, 1984), (ii) extended radio sources (lobe-dominated) versus compact (core-dominated) sources (Miley and Miller, 1979), (iii) steep-spectrum extended sources versus flat-spectrum compact sources (Setti and Woltjer, 1973; Schmidt, 1976; Jaakkola et al., 1975), (iv) the strength of the Fe II lines (Steiner, 1981), (v) emission line dominated fuzzes versus (red) stellar continuum dominated fuzzes (Boroson and Oke, 1984; Boroson, Persson and Oke, 1985). There is now much evidence that these classifications overlap considerably. In particular, Boroson and Green (1992) show that the strongest anti-correlation among all properties is between the Fe II equivalent width and the ratio of the peak of the [OIII] $\lambda 5007$ line to that of $H\beta$. This reinforce previous studies which had shown that Fe II is strong in radio-quiet QSO's (and Seyfert 1s) but rarely seen or weak in radio-loud extended sources, while [OIII] is weaker in the former than in the latter. Naturally, if these correlations were only due to geometrical effects (obscuration by a torus, viewing angle) rather than to a fundamental difference in the source, the whole classification scheme would defeat our purpose. However, Boroson, Persson and Oke (1985) argue rather strongly against that.

Whether this anti-correlation also separates flat-spectrum core-dominated (FSCD) sources from steep-spectrum lobe-dominated (SSLD) sources is still an open question due to the paucity of FSCD samples. Setti and Woltjer (1977) found frequently FeII in FSCDs but not in SSLDs. This was confirmed by Miley and Miller (1979), Steiner (1981), Boroson and Oke (1984) but disputed by Bergeron and Kunth (1984) who did not find much differences between FSCDs and SSLDs. Maybe this is because, as shown by Boroson and Green (1992), FSCDs have properties more or less intermediate between those of SSLDs and radio-quiet QSOs, somewhat closer to those of radio-quiets. But the sample of FSCDs in their study is so small (five objects) that no definitive conclusion can be drawn. Jaakkola et al., (1975) argue that the mass of thermal plasma in FSCDs calculated on the basis of Faraday depolarisation data is several orders of magnitude less than in SSLDs and that the total energy in relativistic particle and magnetic field follows the same trend pointing to the dwarf nature of FSCDs, implying that they are CEROs. On the other hand, Orr and Browne (1982) claimed that FSCDs are just face-on SSLDs. This seems corroborated by the fact that high dynamic range radio maps of FSCDs have revealed in many cases diffuse lobes superimposed on or straddling the dominant core (Antonucci, 1993 and references therein). Also, most FSCDs are now known to be blazars and many present superluminal motions in their milliarcsecond jet. Thus, the situation is very much confused. It could also be that FSCDs exist in CERO and quasar populations, representing the extreme beamed cases of both types, further complicating the picture. Maybe the jet cannot be seen in most QSOs either because it does not exist or because it is too weak. Only when directed straight toward us does it becomes visible because of Doppler boosting.

We may now state quite confidently that all low-redshift radio-loud steep-spectrum double-lobed QSSs are quasars while most high z radio quiet QSOs are CEROs. The low-redshifted radio quiets are certainly contaminated by Seyfert 1s masquerading as QSOs. An indication that we are on the right track is that as we study so-called quasars with larger and larger redshift the fraction of CEROs should increase. This is in agreement with the observed trend that among radio-loud quasars the fractional population of triple (these are quasars) with respect to core and core-lobe steadily decreases with redshift from about 80% at $z = 0.5$ to about 30 % at $z = 1.6$ (Neff, Hutchings and Gower, 1989). Furthermore, an accelerated gas cocoon is part of our model for CEROs, and, interestingly, about 10% of radio quiet QSOs have broad absorption lines, but none is known among radio louds.

However, it should be kept in mind that all these correlations are tentative at best as they have sometimes been extracted from small and not well-defined samples and selection effects may be important. We would feel better if we had some definite characteristic which would enable us to recognize a quasar from a CERO. It is difficult to obtain a totally iron-clad distinction from the radio structure or from spectroscopic differences because the energy sources and environments are likely to be rather similar in all AGN's. A sharper and definite difference most probably resides in the geometrical core structure (the topology of the hole event horizon) as our model indicates (Driessen, 1991) albeit on such a small scale that it may not be resolvable in the near future. Indeed, our model suggests that CERO cores probably display a double structure, with two supermassive objects of say $10^{6\text{-}7}\ M_{\odot}$ each connected by a material bridge. Each "head" has a radius ≈ 1 au and the separation between the heads could be about 137 times larger. This subtends *0.01 mas* at *10 Mpc*, which is clearly too small to be observed with earth-based telescopes. Quasar cores should be like protons and neutrons. For example, a proton-like core should exhibit three substructures corresponding to quark-like cosmic scale objects. There is indeed some evidence that multiple nuclei may reside in radio galaxies and quasars. A striking example is the radio source 3C75 (Owen and O'Dea, 1983) where twin jets emerge from two optical nuclei in the same source. Some other jets are well represented by a precession model (Eckers et al., 1978; Linfield, 1981; Gower et al., 1982) and precession is a natural consequence of multiple orbiting nuclei. Finally, Gaskell (1983) has noticed that in some QSS's the peak of broad emission lines is either redshifted or blueshifted with respect to the narrow lines. He submits that this may indicate the presence of at least two supermassive objects orbiting around each other, each with his own BLR. Interestingly, the best cases of displaced BLR occur in SSLD sources.

1.7 THE CERO EXCHANGE HYPOTHESIS

Now that we have firmer ground to trust the CERO ejection hypothesis, we may notice that CEROs could as well be absorbed by galaxies through a mechanism viewed as the time-reversal of the ejection process. The correspondence with particles follows then readily. If we recall that spiral galaxies seemingly display some of the electron characteristics (Driessen, 1991), the process of absorption and emission becomes strikingly similar to photon exchange between electrons. *Therefore, as a working hypothesis, spiral galaxies will be considered as cosmic scale electrons, and CEROs as cosmic scale photons. Our contention is that spiral galaxies interact "electrodynamically" (on the cosmic scale) via CERO exchange*.

This rather bold hypothesis will appear less so when it will be shown in §1.8 below that some objects in the sky actually display signs of exchange, but in order to read them correctly the model must be first extended to encompass other galaxy types.

1.8 OTHER GALAXY TYPES

There are many other kinds of galaxies besides large spirals, and they should be accounted for, if the model is to be completely consistent. We are thinking about the classes of dwarf spheroidal; dwarf spiral; irregular; lenticular; elliptical; giant elliptical and super-giant cD galaxies.

Let us first consider irregular galaxies which are noticeable for their lack of spirals arms. We are thus led naturally to wonder about the origin of arms. While the density wave mechanism is well accepted as an explanation for the dynamics of spiral arms, a problem is left pending: because of dynamical friction, spiral arms cannot survive much longer than at most two galactic rotations (≈ 5 10^8 yrs.) and they must be regenerated periodically. At present, the origin of the regeneration process is still debated. There has been an interesting albeit unproved proposal in the past. by Ambartsumian (1958, 1965) who was the first to claim that gas ejection from the galactic nucleus combined with differential rotation could provide the required perturbation leading to spiral arm formation. The idea was pursued and elaborated by Arp (1969), and indeed there is some morphological evidence in disturbed galaxies that ejection from the nucleus could in some cases trigger the phenomenon. In fact, Arp's object itself may furnish a striking example: the galaxy NGC 4319 which seems to be caught in the process of CERO emission is at the same time extremely perturbed, and two well delineated, smooth and very open spiral arms appear related to the ejection process. Another impressive example is given on fig. 9.11 of Arp's book (Arp, 1987): a spiral has ejected a long and well collimated jet, and the galaxy has again formed two very pronounced and distorted spiral arms giving a strong impression of recoil. The jet is usually interpreted in terms of a tail extracted from a spiral arm by interaction with another galaxy. But no galaxy of similar size and redshift is seen in the immediate vicinity. There is only a single plume and it is manifestly emerging from the nucleus rather than from one of the arms. In another case, two curved jets of radio emission associated with gaseous emission filaments are seen emerging from the spiral galaxy NGC 4258 (van der Kruit, Oort and Mathewson, 1972). The authors argue that these arms probably lie in the same plane as the (visible) spiral arms. Their numerical simulations have shown that the peculiar phenomenon may have resulted from gas clouds violently ejected about 18 10^6 years ago by a gigantic explosion *(≈10^{58} ergs*) along two opposite directions, and interacting with the quiescent interstellar gas in the rotating disk of the galaxy. The explosion

did not last much more than about 1 million years, and the rate of outflow was about 100 solar mass per year. The life-time of this kind of structure would be at most 50 million years. In about 100 million years they could develop in spiral arms if a large fraction of the interstellar gas has been swept up by the ejected clouds: to form arms of say $10^9 M_\odot$, the explosion must have expelled about $10^8 M_\odot$. In our model, the clouds are trailing behind formerly ejected CEROs at about 2200 km/s (see § 2.4 below) and this is consistent with the observed cloud velocities which range from *800* to *1600 km/s*.

While there exists as yet no formal proof demonstrating clearly the relationship between spiral arm formation and CERO emission, there are at least some indications that this may be the correct view. The predicted period of the two processes roughly coincides. Usually no more than 4-6 spiral arms are currently observed, and if the arms survive about $5\ 10^8$ *yrs*., provided that they are usually formed in pairs by two diametrically opposed CERO ejection, then 2-3 regeneration could take place in this period. Thus, the regeneration process should happen no more frequently than every $2\ 10^8$ *yrs*. Now, the period of recurrent activity in the nucleus of our Galaxy has been estimated by Sanders and Prendergast (1974) at a few 10^8 yrs., Bailey and Clube (1978) independently proposed $\approx 10^8$ *yrs*. and Arp (1987) estimated the time scale of CERO ejection as a few 10^7 *yrs*., while our own computation below gives $\approx 6\ 10^7$ *yrs*. (see § 2.3). One could say that the two period are somewhat of the same order although the ejection period seem consistently lower than the regeneration period. This would indicate that not every CERO ejection is able to trigger spiral arm formation. Indeed, CEROs leaving along or close to the polar axis would presumably not affect the galaxy axial symmetry, and this is probably the most frequent occurrence. But on the other hand, even in the absence of a formal numerical simulation, we would be surprised if the ejection of a 10^7 solar mass object, along an axis close to the galactic plane, would not profoundly disturb the disk structure.

After this digression about spiral arms, let us come back to the discussion of irregular versus spiral galaxies. In view of what we have just said, the fact that irregular galaxies do not display spiral arms and are generally much less massive than spiral galaxies would imply that the mass concentration in their nuclei is insufficient to initiate the formation of a super-massive BH ($5\ 10^6$ *to* $10^8 M_\odot$) which in turn could become active and eject CEROs. In the framework of the particle analogy, irregulars would have no "electric" charge, and a clue as to their origin is obtained by looking at the local group. Small irregulars seem to crowd preferentially around large spiral galaxies, in a region of maximum extension about 200 kpc from the spiral galactic nucleus. But remember that in our scheme, CEROs emerge from spiral galaxies enshrouded in a cocoon of gas and dust. The fierce CERO radiation progressively blows the cocoon away, so that after a CERO ejection, large hydrogen clouds, dust and some stars are left behind in the CERO trail.

Such a phenomenon may have been observed by Carilli et al. (1989) with a galaxy (NGC 3067) and an active object (3C232) included in the same elongated HI cloud. Remember also the gas cloud close to 3C273 in the jet direction. It has a H I mass $\approx 4\ 10^9 M_\odot$, and a total estimated (dynamical) mass of $2.1\ 10^{10} M_\odot$. According to Giovanelli and Haynes (1989), "the data is suggestive of two main clumps in the process of merging", and they have interpreted the cloud as a proto-galaxy. It is likely that two clouds ejected away from 3C 273B are now aggregating to form an irregular galaxy. Finally, there are at least two other cases of trailing gas clouds near M33 and NGC 300, close to the possible trails of ejected CEROs (Arp, 1987). Therefore, in view of this evidence there is a strong suspicion that in general the clouds left over from CERO ejections recondense to form the small irregulars found around spiral galaxies (on the particle scale, this ejecta would have no charge, no quantized spin, and a very small mass, as a result they would be extremely difficult to detect around electrons. In fact, it is not even clear that they could be considered as *bona fide* stable particles). A good argument in that direction is that irregulars are very rich in gas and their metallicity is extremely weak as if no star formation had taken place in their distant past. Most of their resolved stars appear to be population I objects. However, in our model they should contain a trace of population II stars which were collected from the bulge of the parent galaxy. As suggested before in section 1.4, dwarf galaxies may be recaptured and feed the central monster with gas triggering a new bout of activity, and so on.

Dwarf elliptical galaxies differ strongly from irregulars. First, they are made up almost exclusively of old stars although the colours of NGC185 and NGC205 reveal a small population I component in their centres. Gas cannot be measured unequivocally by direct detection of the 21 cm radiation for example, but from the population I in NGC185 and NGC205, a small amount of gas can be estimated at $4\ 10^4 M_\odot$ and $8\ 10^4 M_\odot$ respectively (Hodge, 1963; 1970). For comparison, the total masses of dwarf elliptical galaxies are found in the range $1\text{-}200\ 10^5 M_\odot$. It has been noted that dwarf elliptical galaxies preferentially crowd around giant elliptical galaxies, so perhaps they would result from the same extraction process (entrainment by a CERO) but from giant elliptical galaxies. But it is difficult to explain why a typical dwarf elliptical like M32 orbit a typical spiral like M31.

Let us now consider giant elliptical and super-giant cD galaxies which usually lie at the centre of clusters with fainter and smaller galaxies apparently in orbit around them. The companions are mainly composed of small elliptical and irregular galaxies plus a few spiral galaxies. The cD galaxies have exceptionally bright cores and large haloes which extend sometimes up to 2 Mpc (Oemler, 1976). Our contention is that giant elliptical and super-giant cD galaxies represent the cosmic scale equivalent of atomic nuclei with increasing order of complexity in their nuclei. The smallest one would have a proton-like nucleus while others would have multiple nuclei representing amalgams of proton- and neutron-like structures. They would interact via CERO exchange with the electron-like spiral galaxies around. Here again, irregulars would come from recondensation of the gas entrained by ejected CEROs. When more than one giant or super-giant is found within a cluster, we have a molecular like object.

The case of the average size elliptical and SO galaxies, remains a mystery, as there is apparently no easy way to relate them to known particles, except if there is an evolutive sequence linking them to spiral galaxies.

Another problem is posed by dwarf spiral galaxies nearby large spirals (Arp, 1969). In some cases, the companion is nearly as large as the main galaxy and the system would resemble a pair of spin-up spin-down electrons found in atomic orbital (naturally it remains to be proven that galactic spins are so arranged). But in most cases the very large difference in size makes it difficult to interpret them both in terms of electrons.

After this tour of galaxy types, let us come back to our main issue: can we rely on observations to support the CERO exchange picture? It is indirect and weak to be sure but nonetheless interesting. Since the explanation of plumes in spiral galaxies as structures produced by tidal interaction with colliding companions (Toomre and Toomre, 1972), most material extensions from spiral and elliptical galaxies (jets, plumes, tails, loops …) have been explained in these terms, but at least for a few cases extracted from Arp's atlas (Arp, 1966) this interpretation seems to be inappropriate.

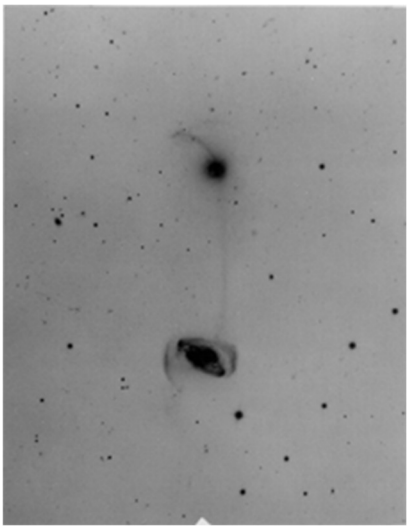

Figure 1: plate 104 in Arp's atlas (Arp, 1966).

The clearest case is that of plate 104 (NGC5216+18) where a faint, thin filament goes all the way from the nucleus of a spiral to the nucleus of an elliptical. Its morphology is not what one would expect from a plume or a spiral arm: the curvature is weak, it does not emerge from a spiral arm, but from the nucleus and the width does not change noticeably with distance. In fact, the galaxy has two well-formed spiral arms, with no apparent extensions, and, where the southern arm crosses the jet in projection, arm and jet are nearly perpendicular. We think that the jet in this precise case traces the path of a CERO (or CEROs) ejected from the elliptical (the jet is somewhat straighter close to the elliptical nucleus, then curves gently to meet the spiral nucleus as if it had been influenced by the spiral gravitational attraction when coming closer) and which is currently being absorbed by the spiral nucleus.

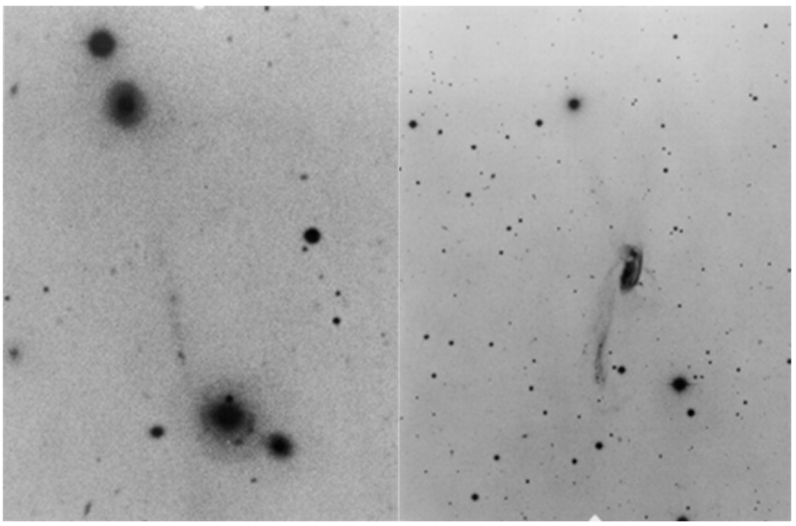

Figure 2: On the left, plate 103 in Arp's atlas (Arp, 1966). On the right, plate 102.

On plate 103 (see fig.2 above), another very straight and thin jet connects two elliptical galaxies, and finally on plate 102 one finds a more intricate situation with a central spiral ejecting a long thin filament from its nucleus toward a southern diffuse object (a dwarf galaxy?). Another filament apparently coming from the periphery of the spiral goes northward toward the nucleus of an elliptical, which itself emits on the opposite side another jet terminating on a compact blue object. So, this case it not so clear-cut. Other examples

are given in Arp (1972). A particularly striking one is that of NGC7603 ($cz = 8700\ km\ s^{-1}$) which has strong emission lines characteristic of a Seyfert, and a curved filament connecting it to a small companion galaxy. The latter has a nearly stellar nucleus and a very low surface-brightness fuzz around. The companion shows absorption lines at $cz = 16800\ km\ s^{-1}$. Finally, small companion galaxies are sometimes found at the end of arms of large spiral galaxies (Arp, 1969). In these cases, the jet has probably been emitted close to the spiral plane and is curved by differential rotation. Arp (1968) has also noted the existence of lines of galaxies along the axis determined by the jets in radio sources. For example, all giant ellipticals in the vicinity of M87 fall more or less along the line fixed by M87 jet and counter-jet. Arp interpreted this as ejection of proto-galaxies from a central galaxy. In contrast, we consider that jets mark the trace of CEROs exchanged by these aligned galaxies.

1.9 REFINEMENTS OF THE MODEL

Some refinements can be brought to the general picture. The first point answers a question put forth by Weedman (1976): why would ejected CEROs remain in the neighbourhood of their parent galaxy. The solution resides in the presence of jets. For example, a sinuous (presumably precessing) filament seems to connect MK205 to NGC4319 (Sulentic, 1983a, 1983b). No less than four jets originate from NGC1097 (Arp, 1976) and the very centre of our own Galaxy shows fossilized jets emanating from the nucleus. Although they have not been seen in most Seyfert galaxies, we can speculate that jets are nearly always present in active galaxies, but that most remain too faint to be seen with our present means. If this is true then spiral and elliptical galaxies should be surrounded by "clouds" of CEROs linked to the parent galaxy by jets which are vortex tubes in our model. These tubes are stretched as CEROs move away, thus the centrifugal force on their periphery increases and a restoring force is exerted on the CEROs (Driessen, 1991). This would explain why CEROs remain around the galaxy. In principle, vortex tubes cannot be broken as long as there is no viscosity, and the extreme stability of galaxies implies that viscosity is nearly non-existent in most parts of the "fluid". However, close to the galactic nucleus there should be some dynamical viscosity, so that sometimes jets are torn apart. In this case the CERO is liberated and it escapes with constant velocity because of its peculiar structure (Driessen, 1991). Yet we suspect that in most cases the restoring force will cause the CERO to fall back toward the galaxy nucleus where it will be reabsorbed. The whole process of emission and reabsorption strikingly evokes Feynman's self-energy diagrams, thus maybe the argument can be used in reverse to shed an interesting light on the problem of virtual photons. If Feynman's self-energy diagram embody physical truth, one should wonder why virtual photons surround the electron which has emitted them, and how it is possible that the electron can reabsorb the photon at a later time. After all, photons should escape with the velocity of light, and the electron should never be able to catch up on them. But if departing photons are still tied to the electron by a vortex tube, a strong restoring force is exerted which may cause them to fall back onto the electron. Such linked photons are called virtual because they are not separate proper photon structures. There is only one single structure composed of the electron, the jets and the attached photons. In addition, such tied up photons have inertia (mass).

Another point demanding clarification is the flip-flop mechanism. Each CERO ejection provokes a recoil of the emitting galaxy, and an acceleration which, as we suggest, provokes the emission of a CERO in the opposite direction, in analogy with the mechanism of *Bremstrahlung* radiation by electrons. The resulting erratic motion evokes the *Zitterbewegung* of particle physics. Now, the profound physical reason for the flip-flop mechanism could be inspired from Wiita and Siah's proposal (Wiita and Siah, 1981): when ejection takes place on only one side, the nucleus recoils and for some time it will be offset from the centre of the plasma torus. Consequently, the jet along the polar axis in the opposite direction will be pinched and may be suppressed.

But naturally, this model also has trouble explaining the majority of symmetric sources. Thus, we have to suppose that in general emission will be simultaneous in opposite directions (momentum is conserved, no recoil of the nucleus). From time to time, a perturbation provokes a retardation of the jet formation on one side while it continues on the other side. The nucleus recoils, thus a pinch is followed by complete suppression of the active jet, etc… Hence, we could envision a process where a few CEROs are ejected in rapid succession (at about 10^4 *yrs*. interval) on one-side of the major axis of an elliptical galaxy, followed by a switch to the other side after $10^{5\text{-}6}$ *yrs*., and so-on. In spiral galaxies the numbers would be *2-6* 10^7 *yrs*. and $10^{8\text{-}9}$ *yrs*. respectively.

Coincident with a bout of ejection, two open spiral arms are generated. They are smooth at first but then star formation begins. The galaxy quickly looks like an Sc. Then the arms wind up progressively, and at the same time each successive emission depletes the galaxy from its gas. It consequently passes in reverse the stages in Hubble's classification from Sc to Sa. Presumably, when it is totally depleted, ejection stops, and the galaxy takes on a more relaxed appearance (maybe a So), until mass loss from stars replenishes it and the process repeats itself.

A word about the merger picture currently in vogue may be necessary because we feel that it has been used (and maybe abused) to try to explain almost any difficult observation. Our model can predict which kind of merger should be possible. Alladin (1965) was able to show by numerical simulation that colliding galaxies tend to stick, and this was confirmed by numerical simulations (see the reviews by Ostriker, 1977 and Toomre, 1977). This was one of the justifications for interpreting NGC7258 for example as the result of the merger of two disk galaxies (Schweizer, 1982). The loops and tails which are so preeminent in NGC1316 for example (Schweizer, 1980) could mark the trail of CEROs falling back onto the nucleus. Now, deep inelastic collision of two spirals is not prohibited by our model but their merger into one single entity would be equivalent to the fusion of two electrons and has not been observed in particle physics. The likely explanation is that the vortex cores in these objects cannot merge, because of spin-spin interaction, a fact which has not been taken into account in simulations. On the other hand, cannibalization of dwarf galaxies by large spirals or giant ellipticals is quite possible (the dwarfs have no BH cores) and is favoured in our model as one likely culprit of the triggering of an AGN in the large

galaxy. Capture of a large spiral by a giant elliptical is a rare but possible event which would correspond to electron capture by the nucleus.

1.10 A CRITICAL REVIEW OF THREE TEST CASES

We conclude this first part by critically reviewing the evidence presented for three important test cases, namely MK205, 3C273 and NGC7603, in light of our model. In each case, we first discuss some of the most relevant observations, compare the object to our test sample and then try to decide which object pertains to the CERO or quasar class. The dimensions and magnitudes of the objects surveyed are given in table II, both in the local and cosmological hypothesis (LH and CH).

1.10.1 ARP'S NGC4319 SYSTEM

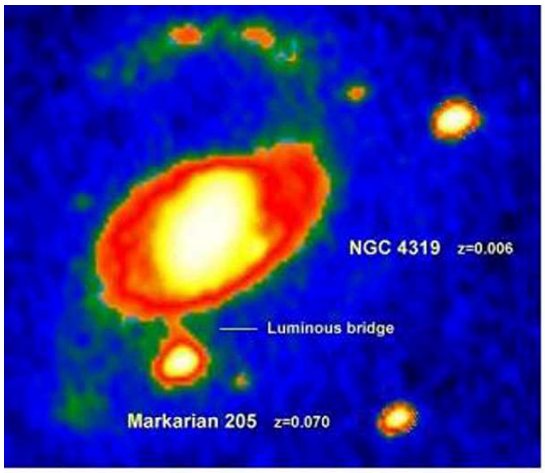

Figure 3: NGC 4319 seemingly connected to MK205 by a luminous bridge.

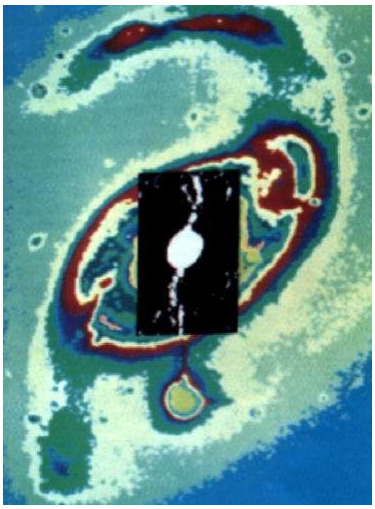

Figure 4: Image processing by Sulentic (1983c) shows an undulating luminous bridge joining the core of NGC4319 to MK205.

NGC4319

NGC4319 has a late type absorption spectrum, plus the single emission line [NII] 6584 (except in the UV knot), and practically no H_α! The limit is $H_\alpha / NII < 0.3$ (Sulentic and Arp, 1987b) and it may indicate shock excitation due to a violent ejection as suggested by Sulentic. The fact that the galaxy is depleted of its hydrogen agrees well with our model of gas extraction by ejected CEROs. Another remarkable fact about this galaxy are its two remarkable spiral arms, wide open and neatly scissored at their bases. This must have been caused by the ejected CEROs but probably did not arise simply because the CEROs crossed the arms. Indeed, the appearance is that of an ejection out of the galactic plane. In our model, a CERO, is composed of two vortex heads, connected by a vortex tube. We must suppose that the velocity induced by the vortex heads in the plane perpendicular to their spins is able to disrupt the galaxy arms.

MK205

The halo appears elliptical with dimensions 20"x14" (Sulentic and Arp 1987a) which means a major diameter of *24 kpc* at the redshift distance of *266 Mpc* and *2.7 kpc* at the distance of NGC4319 (table II). Thus, on dimensions alone, MK205 could be either a large spiral galaxy or a medium elliptical in the CH. In the LH, it could be a dwarf galaxy, or a rather large ejected CERO with a size one order of magnitude larger than the average size (0.35 kpc) of our test population of probable CEROs, with the exception of 3C232 which also stands out as particularly bright and large.

MK205 has been detected by Sulentic (1986) as a weak unresolved radio source. The 20cm radio luminosity is $L_{20} = 10^{22.4}$ *W Hz*$^{-1}$ in the CH. This would be the similar to that of normal galaxies but vastly inferior to typical luminosities of radio-loud quasars or radio galaxies. In the LH, the luminosity becomes $L_{20} = 10^{20.2}$ *W Hz*$^{-1}$, which is extremely weak. Finally, the size of the *6 cm* radio source is less than *170 pc* at the distance of NGC4319 and about *1.5 kpc* at the redshift distance.

MK205 has the emission line spectrum typical of a low-redshift QSO or a Seyfert 1 galaxy (Weedman, 1970, 1971; Stockton, Wyckoff and Wehinger, 1979; Sulentic and Arp, 1987b), with a strong ultraviolet excess (*B-V= +0.40, U-B = -0.94*; Weedman, 1973). In the CH, we applied the same reddening correction as to our other quasars and we found an absolute magnitude $M_V = -23.70$ (table II), brighter than most Seyferts, and even brighter than the average radio galaxies and first-ranked elliptical galaxies in clusters. In the LH, it has $M_V = -18.76$, fainter than most Seyferts, but still considerably brighter than the average of *-12.72* that we found for our selected CEROs.

No CaII K absorption lines at the redshift of NGC4319 have been found in the spectrum of MK205 down to the 2σ limit of *38 mÅ* in ground-based observations (Bowen et al., 1991a). Ca II is a weak line but it is clearly present in the high latitude (42°) line-of-sight to MK205 from our galactic halo. Thus, the non-detection was quite surprising since the line-of-sight passes at about *4 kpc* from NGC4319 nucleus and probes both the halo and the disc. For comparison, a line-of-sight transverse to our own Galaxy seen face-on, near the solar position would give a median equivalent width of *220 mÅ* (Bowen et al., 1991a). Actually, this was sufficiently unsettling to prompt Bowen et al. (1991a) to recognize that one of the possible explanations is that MK205 lies in front of the galaxy. Another plausible cause would be that the ISM is more highly ionized in NGC4319 than in the galactic halo. Later, really weak Mg II and C IV lines were found with the HST (Bahcall et al., 1992). But the latter also cite 17 resonance lines from low-ionization states of usually abundant ions that were not detected. Finally, absorption lines like MgI 5175 and Ca + Fe 5268 have been found in the MK205 halo, but they are generally weaker than in the spectrum of the red companion (see below). The optical spectrum of the halo is compatible with starlight (Sulentic and Arp, 1987b).

The Red Companion (RC)

Stockton, Wyckoff and Wehinger (1979) found a red companion about 3" NNE of MK205. It clearly distorts the outer isophotes of MK205 in the general region where the Sulentic and Arp connection should reach MK205. If assumed to have an apparent angular diameter of 1" and $m_B = 18.5$, it has a diameter of *0.26 kpc* and $M_B = -14.76$ in the LH (table II). In the CH, it has a diameter of *2.3 kpc* $M_B = -19.69$, similar to those of red compact galaxies. The spectrum shows various absorption lines typical of late-type stellar contribution (Stockton, Wyckoff and Wehinger, 1979; Sulentic and Arp, 1987b), namely MgI 5175, Ca II 5268, Na D, etc... In addition, prominent [OIII] 4959,5007 emission lines were observed by Sulentic and Arp (1987b) who found that their strength was greater than in the halo spectrum of MK205, although it should be noted that they were not seen by Stockton, Wyckoff and Wehinger (1979). The redshift of the companion is slightly smaller than that of MK205 at $z = 0.0709 \pm 0.0005$.

The UV Knot

The observed dimension and apparent magnitude are rather similar to that of the RC, with about *2"* and $m_B = 19.5 \pm 0.5$ (Sulentic and Arp, 1987a), considering that some of its emission could be absorbed if it passes through the halo of NGC4319. It is situated *18"* north-northwest of NGC4319, in a direction diametrically opposed to MK205, but at about half the distance. So, if it is the result of an ejection, it is more recent. It has a spectrum characteristic of low-excitation HII region, with no OIII 5007, only H_α, H_β, et NII 6548 et 6854. Sulentic could not detect any compact radio emission (Sulentic, 1986). If both MK205 and the UV knot have been emitted by NGC4319 as suggested by Sulentic and Arp (1987a), why would they differ so much in dimension and magnitude?

Conclusions

There have always been nagging doubts about MK205 being a *bona fide* quasar. Most of observations do not make MK205 identification easy. First, its redshift is small for a CERO candidate. In the CH, it seems far too bright to be a Seyfert at its redshift distance or even a radio galaxy, while its dimension of *24 kpc* show that it is certainly not exceptionally large. In the LH, it is much smaller and fainter than the large Seyferts, but still larger and brighter than all of our test CEROs. Cecil and Stockton (1985) have argued that it must be at its redshift distance because the Red Companion (RC) is at nearly the same redshift and could be a dwarf compact galaxy in interaction, extracting plumes of material from MK205, one of which would have been incorrectly interpreted by Sulentic as the bridge. This explanation appears contrived, especially since, to my knowledge, simulations of encounters between dwarf

elliptical galaxies and a larger galaxy are not able to create plumes. It seems to me that the arguments and computer processed pictures presented by Sulentic and Arp (1987a) and by Sulentic (1983a, 1983b), to show that it interacts with NGC4319, are overwhelming. Furthermore, the observed absorption lines at NGC4319 redshift are so weak that they are hardly compatible with the line-of-sight to MK205 passing right through the disk of NGC4319. Rather, they suggest, as in the case of the 3C232-NGC3067 system, that a tail of gas may have been extracted from the galaxy and brought toward MK205, causing the absorption there. However, MK205 does not display most of our CERO characteristics: it is too large, bright and diffuse. Its appearance is more akin to that of small galaxies often found in orbit around large spiral galaxies, with in addition, a Seyfert-like nucleus. But on the contrary, the RC shows many of the characteristics that one would have expected from red CEROs. In the LH, it is small and compact, of about the same size as our average CERO. Its magnitude falls in the possible range, the redshift is nearly equal to that of MK205, and it shows bright emission lines.

Thus, let me suggest a new interpretation of the system: MK205 is a dwarf Seyfert galaxy endowed of some excess redshift, interacting with NGC4319 via CERO exchange. The red companion is a CERO that has been ejected by NGC4319 and which is on the verge of absorption by MK205.

Actually, the complete picture may even be more complicated than that. A careful look at the surprising last picture in Cecil and Stockton's figure 2 (Cecil and Stockton, 1985) reveals, in addition to the RC northward of MK205 core, another possible compact object southward and apparently merging with it (it is called feature c in Cecil and Stockton's fig. 3). A sharp very luminous arc (feature g) connects it to the red companion. Cecil and Stockton argue that it could be a purely artificial feature resulting from internal reflection from the filter, but it could alternatively be quite real signalling a fascinating system!

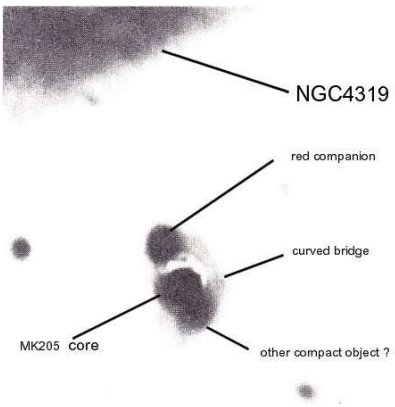

Figure 5: The region around the core of MK205, according to Cecil and Stockton (1985).

We suggest that the RC, the curved bridge and the other compact object precisely describe the structure that we have predicted for the cosmic scale photon (or the CERO, see fig. 6 below).

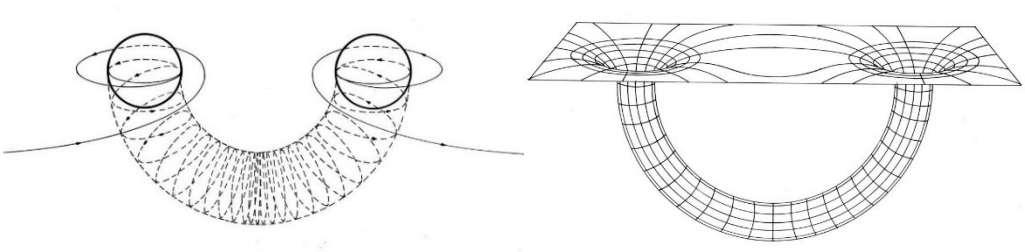

Figure 6: The photon (CERO) structure that I predicted (Driessen, 1983, 2020). On the left, a “head” of the electron type is connected to a head of the positron type by a bridge (extending in in other dimensions). It is probably completed by a visible bridge between the heads, as on fig. 5 above. On the right, the same structure is represented on a slice in two dimensions, plus a z extension. One recognizes a wormhole structure joining two regions of the same space-time sheet. To be complete, one should draw another space-time sheet below.

1.10.2 THE 3C273A-3C2773B SYSTEM

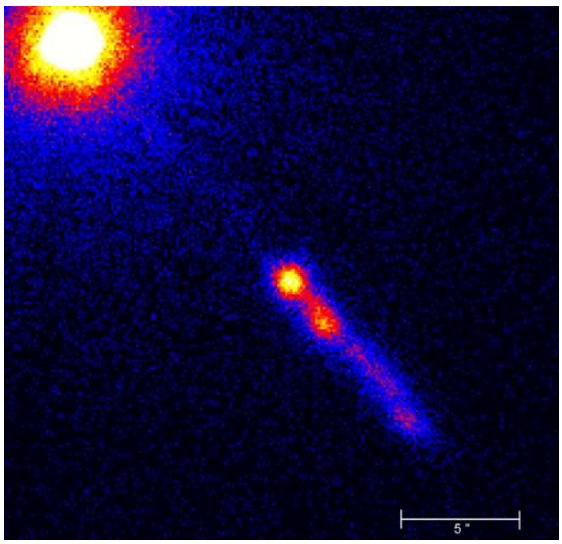

Figure 7: The quasar 3C273B, and its jet. Note the hotspot, named 3C273A, inside the jet. The picture was obtained in X-rays.

The quasar 3C273 is not considered as much an *experiment Crucis* as the former system but still it is interesting because of the claim of Arp and Burbidge (1990) that it could lie at the Virgo cluster distance. This is the hypothesis that we want to test here, from which we hope to extract a clue as to its nature. 3C273B is usually interpreted as a low-redshift quasar emitting a radio-loud jet toward the hot spot, 3C273A. For 3C273B, at cosmological distance $\Delta = 545\ Mpc$, the data are (table II): diameter of the nebulosity $D = 100\ h_{75}^{-1}\ kpc$, apparent and absolute magnitude $m_R = 16.3$, $M_R = -23.2$, while for the whole quasar itself, the magnitude is $M_V = -26.80$ ($m_V = 12.9$). At the distance of Virgo A ($\Delta = 16.8\ Mpc$), the diameter becomes $D = 3.6\ kpc$ and the magnitude for the nebulosity and quasar are $M_R = -16$ (Wyckoff et al., 1981) and $M_V = -19.1$ respectively. Thus, in the CH, the fuzz has the correct magnitude for a first-ranked elliptical but it is exceptionally large for a radio galaxy. It is also too large and too bright in the LH to be a CERO! The optical luminosity was estimated at $10^{46}\ erg\ s^{-1}$ in the CH and at $1.3\ 10^{43}\ erg\ s^{-1}$ locally. For comparison, the total optical plus X-ray flux from Seyfert 1 nuclei is given at $10^{43\text{-}45}\ erg\ s^{-1}$ and at $10^{46\text{-}47}\ erg\ s^{-1}$ for bright QSO's (in the CH). It is also possible to evaluate the velocity in the jet. Apparent motions for blobs ejected from the nucleus of 3C273B have been measured at $\mu = 0.79 - 1.20\ mas\ yr^{-1}$ (Porcas, 1987; Zensus, 1987). This represents superluminal apparent velocities of $v_{app} = \mu z / H_0 (1+z) = 9.1c - 13.33c\ h_{60}^{-1}$ ($q_0 = 1$) at cosmological distance, but locally this becomes $v_{app} \approx \mu \Delta = 0.26c\text{-}0.4c$.

Thus, the case for 3C273B is still very much undecided. Arguments in favour of a CERO are: (a) its apparent position in the Virgo cluster on the projected sky (b) the discovery reported by Giovanelli and Haynes (1989) of an elongated H I cloud in the southern part of the Virgo Cluster, which following Arp and Burbidge (1990) lies close to 3C273 on the projected sky (*260 kpc* if 3C 273 is at the distance of the Virgo Cluster); furthermore the well-known jet from 3C 273B points towards the cloud and its axis nearly coincides with the cloud axis (c) the fact that it has been called the most strongly asymmetric source and (d) its well-known superluminal behaviour which perhaps implies that it is closer than its redshift indicates. Arguments for it being a radio galaxy at its redshift distance are: (a) it has a relatively small redshift and it is radio loud with a non-compact radio structure, (b) the large fuzz magnitude and diameter found in the LH forbid that it could be emitted by the nucleus of a Virgo galaxy (c) the hot spot in 3C273A looks suspiciously like those observed in the lobes of other extended radio sources attached to well-known strong radio galaxies of the Fanaroff-Ryley Type II. It has strong brightening at the edge, and the spectrum presents a cut-off at $10^{14}\ Hz$ with an overall shape similar to those of certain red QSO's (Henry et al., 1984; Röser and Meisenheimer, 1986). Finally, 3C273A has been observed in the optical region showing that Tev electrons are energized locally. This suggests that a compact object resides there, presumably a CERO in our model. (d) Absorption lines at the redshift of Virgo have been found in the spectrum and, (e) the apparently superluminal blobs are moving from 3C273B (the compact source) toward 3C273A (the hot spot). This is not compatible with a model where 3C273B would be ejected from a galaxy in the Virgo cluster.

All things considered; it seems more likely that 3C273B is a small radio galaxy ejecting a CERO hidden in the 3C273A hot spot. Maybe it has some excess redshift and, in that case, it could still be part of the Virgo cluster. The aligned gas cloud could be a relic from an earlier ejection of a CERO more or less along the current jet axis.

1.10.3 THE NGC7603 SYSTEM

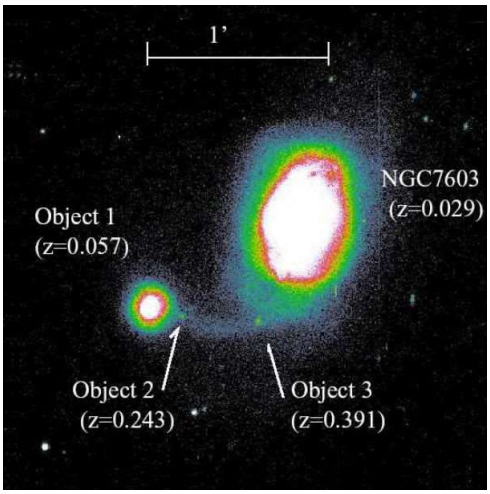

Figure 8: The NGC7603 system.

Of all systems explored by Arp and collaborators, this is probably the most interesting. Two galaxies, NGC7603 and object 1 on the picture, with different redshifts, $z = 0.029$ and $z = 0.057$ respectively, are found to be connected by a luminous filament (Arp, 1971b). In this filament, there are two compact objects (2 and 3) of high redshifts (López-Corredoira and Gutiérrez, 2002).

Objects 2 and 3, are emission line sources. Due to the overall aspect of the spectra and the broadening of the $H\beta$ line, the authors note that they could be classified as broad line objects (Seyfert 1 or quasar). But due to other characteristic of their spectra, they suggest that they should be HII galaxies. However, we strongly doubt this classification, because why would ordinary HII galaxies be so much redshifted with respect to the galaxies. For our part, we suppose that they are CEROs, with their spectra partially obscured by a gaseous cocoon (also containing stars), which they entrain from the small ejecting galaxy (object 1) towards the large absorbing galaxy (NGC7603). This would explain the large difference in size between the two galaxies. If this picture is correct, it would considerably increase our belief in the CERO exchange model.

What is important also is that we have no less than four objects with very different redshifts, connected by a luminous bridge (no one dared argue that the compact objects 2 and 3 are background sources). This kills in one stroke the idea that all redshifts are entirely cosmological.

GALAXY							HIGH Z COMPANION						LOCAL HYPOTHESIS				COSMOLOGICAL HYPOTHESIS		
	α	δ	l^{II}	b^{II}	A_V mag	z_g	Name	s (")	m_V mag	θ (")	z	K_z^s mag	S kpc	Δ Mpc	d kpc	M_V mag	Δ Mpc	d kpc	M_V mag
(1)	(2)	(3)	(4)	(5)	(6)	(7)	(8)	(9)	(10)	(11)	(12)	(13)	(14)	(15)	(16)	(17)	(18)	(19)	(20)
N4319	1219	7536	125.4	41.7	0.08	0.00620	MK205	42	14.5	20.0	0.071	0.77	5.7	28.2	2.72	-18.76	266	24.1	-23.70
							RC	39	$(18.5)_B$	1.9	0.071	0.16	5.3	28.2	0.26	-14.15	265	2.3	-19.08
							UVK	18	$(19.5)_U$	2.0	_____	_____	2.4	28.2	0.27	-12.84	___	____	
	_____																		
N4420	1224	0227	288.5	64.7	0.00	0.00520	3C273B	4770	12.9	44.0	0.158	0.50	386.5	16.8	3.57	-19.09	545	100.5	-26.80

Tab. II: **Analysis of Arp's system and the 3C273 system.**

(1) Name of the nearby galaxy. In the local hypothesis, 3C273 could be situated in the Virgo Cluster, close to NGC4420 (BHNDG).
(2) Right ascension (1950.0) of NGC4319 for Arp's system (Tully, 1988) and of 3C273B (BHNDG, 1990) for the second system.
(3) Declination (1950.0).
(4-7) As in table I.
(8) Name of compact object.
(9) Projected separation from the galaxy in arcsec, from BHNDG. For the red companion to MK205 (RC) and the UV knot (UVK), the separations have been estimated from the plates in Sulentic (1983b).
(10) Magnitude in the V band, from BHNDG. For the red companion to MK205, only $m_B = 18.5$ is known (Sulentic and Arp, 1987a). The same authors give $m_U = 19.5$ for the UV knot.
(11) Apparent halo diameter in arcsec, measured on the plates of: (a) RC: Cecil and Stockton (1985), (b) UVK: Sulentic (1983b). The halo dimensions of MK205 are estimated at *20"x14"* in Sulentic and Arp (1987a).
(12-20) As in table I. For MK205, we compute a blue magnitude ($M = M_B$) and accordingly we compute the blue reddening correction, starting from Sandage's (1966) K^*_B. For the UV knot, we compute a U magnitude ($M = M_U$) without reddening correction.

2. OBSERVATIONAL EVIDENCE

2.1 NOTATIONS AND GALAXY SAMPLES

The self-similarity hypothesis will now be put on a stronger footing in the next sections by looking at length, time, speed, mass, angular momentum and charge scales. There are at least two very promising scales, namely particles and galaxies, but an intermediate stellar scale might exist according to Oldershaw. For example, he deduced his length and mass scaling factors from a comparison between the solar system and a highly excited Rydberg atom (Oldershaw, 1986a). In the spirit of the present model, a scale would rather be defined by objects endowed with intrinsic spin angular momentum. Stellar mass black holes might be our candidates of choice. At least two such objects have been found: the well-known SS433 and the newly discovered 1E1740.7-2942 close to the galactic centre (Mirabel et al.,1992). Both emit radio jets strikingly similar to those of extended radio sources on the galactic scale. It is extrapolated that millions of such objects could exist in the Galaxy alone but as usual observations lag far behind speculations. We have no intention to study this hypothetical scale here for it would be rather perilous to extract predictions from only two objects. Thus, the following sections will concentrate exclusively on the particle and galactic scale, and all predictions will be derived from comparison of measurements on these ranges. We shall gain in consistency, but there will be a price to pay in that a somewhat contorted calculation scheme will result, mainly because the gravitational constant has been measured only on the ill-defined stellar scale.

It should be immediately obvious that our body of hypothesis implicitly entails that particles display a large scatter in their dimensions and masses similar to those of galaxies. So, the current assumption that there exists something like a single, perfectly well-defined electron, with always the same mass and radius, should be dismissed, although it has become standard practice to speak of *the* electron mass, *the* electron radius, etc.... Indeed, it should not be forgotten that measurements made on the microscopic scale invariably involve enormously large particle numbers and are of purely statistical nature, but it is also precisely what makes them so reliable.

For the galactic scale, one will inevitably dispose of much smaller statistics involving only nearby objects as long as the distance scale will not be known with higher precision. Ideally, one should dispose of a relatively large and homogeneous sample of not-too-distant galaxies with the three values of radius, mass and angular momentum furnished together in a coherent way (and in particular with the same H_0 value), but to my knowledge, this is not yet available, due to the ambiguity on the dark matter amount. One early line of attack concentrated on "exact" mass and angular momentum calculations of the few galaxies for which velocity curves and accurate photometry were available at the time, when it was still more or less assumed that rotation curves would join a Keplerian fall-off at large radii. For example, Takase and Kinoshita (1967) used Brandt's analytical fits to the velocity profile (Brandt, 1960; Brandt and Belton, 1962) to compute the mass and angular momentum for some 16 spiral galaxies and a few other galaxies. But in the late seventies it became evident that curves remained flat or even slowly rising at least up to a few Holmberg's radii (Roberts, 1976; Bosma, 1978; Rubin et al. 1978), and this invalidated Brandt's formulae. The work of Nordsieck (1973a, 1973b) represented an improvement because he replaced the spheroid method used in Takase and Kinoshita's (1967) work by Toomre's thin disk method (Toomre, 1963) which is better suited to disk galaxies, and where the surface mass density directly derives from the measured velocity curve. Yet the latter did not extend very far, so that Nordsieck (1973b), hereafter denoted as NS, proposed three possible extrapolations to take into account the mass beyond the last measured point. We adapted his results (table III) so as to represent the extrapolation which corresponds to an asymptotically flat rotation curve as explained in the legend of table III.

Another approach relied on much larger samples with mass and angular momentum statistically related to measurable quantities. For example, a collection of 213 galaxies compiled by Dai Wen-Sai, Liu Ru-liang and Hu Fu-Xing (1979), called here DLH, where all galaxies are closer than 55 Mpc. For 175 of those galaxies, the so-called "indicative" mass values M_i, based on 21-cm neutral hydrogen line observations, came from Balkowski (1973). Starting with Heidman (1968), several authors have claimed that it correlates well with the "true" total mass M; that is, $M = \nu M_i$ with $\nu = 0.8\text{-}2$. As regards the computation of angular momentum, one disposes of two measurable quantities. First, the width of the 21-cm line gives the maximum rotational velocity V_m, which was taken by DLH from Bottinelli and Gouguenheim (1974). And second, the radius at which the rotational speed reaches its maximum is called R_m, and it can be obtained from Holmberg's radius R_H (Holmberg, 1958) via the approximate statistical relation: $R_m \approx 1/3\ RH$ (DLH, 1979). Using Brandt's formula (Brandt, 1960; Brandt and Belton, 1962) with index $n = 3$, DLH computed the density of angular momentum and found $j = J/M = 0.879\ V_m R_m$. Although Brandt's curves cannot be relied upon, such a statistical relation should nevertheless hold in general as is evident from dimensional analysis (Nordsieck, 1973b), but with an unknown coefficient. Indeed, j must be a linear function of a characteristic speed and radius of the system. Since the velocity curve can be rather well approximated by a linear increase up to R_m, followed by a flat $V \approx V_m$ part, it is clear that R_m and V_m should be the relevant quantities, thus $j = \mu V_m R_m$.

Ngc	Type	R_H	Δ	M	J	j	R_m	V_m	j/R_mV_m
Name		kpc	Mpc	$10^{10}M_\odot$	$10^{73}gcm^2s^{-1}$	$10^{29}cm^2s^{-1}$	kpc	kms^{-1}	
(1)	(2)	(3)	(4)	(5)	(6)	(7)	(8)	(9)	(10)
Gal.	Sbc	____	0.0	21.0	25.17	6.03	8.5	220	1.05
224	SAb	24.1	0.69	21.0	27.63	6.62	8.03	282	0.95
681	SABab	15.4	23.0	5.0	2.46	2.47	5.13	164*	0.95
1084	SAc	15.8	19.2	3.3	1.23	1.87	5.27	158*	0.73
1808	SABO/a	____	10.0	6.2	3.07	2.49	4.36*	194	0.95
1832	SBbc	____	25.3	7.1	4.11	2.91	3.18*	206*	1.44
2903	SABbc	16.1	7.9	9.6	6.20	3.25	5.37	228	0.86
3031	SAab	16.8	3.3	17.0	16.58	4.91	5.6	262*	1.08
3504	SABab	____	19.8	1.4	0.23	0.83	2.22*	164*	0.74
3521	SABbc	16.8	8.5	15.0	12.89	4.32	5.6	303	0.83
4490	SBdp	10.9	8.3	1.22	0.21	0.87	3.63	129	0.60
5005	SABbc	15.5	14.4	13.0	9.82	3.80	5.17	293*	0.81
5055	SAbc	16.8	7.2	7.8	4.11	2.65	5.6	279*	0.55
5194	SABcp	14.9	7.2	6.8	3.68	2.72	4.97	137	1.29
7331	SAbc	28.5	14.4	10.8	8.60	4.01	9.5	279	0.49
median..:		17.42		9.75	8.40		5.48	220	0.89
variance:		4.8		6.5	8.7		1.9	60	0.26

Tab. III: Statistics for spiral galaxies adapted from Nordsieck (1973b).

(1) NGC reference number.
(2) de Vaucouleur's classification (de Vaucouleurs G. and de Vaucouleurs A., 1964)
(3) Linear disk radius in kpc obtained from Holmberg's (1958) angular radius at the *26.5 mag arcsec*$^{-2}$ isophote. Not corrected for inclination and absorption.
(4) Distance in Mpc. When it was based on redshift, a Hubble constant of *75 km s*$^{-1}$ *Mpc*$^{-1}$ was assumed.
(5) Mass derived from the rotation curve with Toomre's thin disk method (Toomre, 1963), and extrapolated beyond the points where the velocity was measured, assuming a constant disk M/L with increasing radius. We took Nordsieck's (1973b) median extrapolated value to which we added his quoted uncertainty. This corresponds to an extrapolation with constant velocity beyond the last measured point (Nordsieck, 1973a).
(6) Extrapolated angular momentum, derived from Toomre's (1963) thin disk method. We first used the same extrapolation procedure as for the mass, starting from Nordsieck's (1973b) values. We then converted the results to CGS units, using $10^{12}\ M_\odot$ *kpc km/s* = $0.0614\ 10^{73}\ gcm^2s^{-1}$. As pointed out by Nordsieck, this represents only the disk angular momentum.
(7) Density of angular momentum $j = J/M$.
(8) Turn-over radius in the rotation curve, where the velocity reaches its maximal value. It was deduced from the statistical relation $R_M = 1/3\ R_H$ (DLH, 1979). The cases marked with an asterisk have been taken from DLH (1979) and reduced to the distance quoted here. For the Galaxy, we took a turn-over radius of 8.5 kpc from Nordsieck's (1973b) fig. 1.
(9) Maximum rotational velocity at radius R_m and beyond, in kms^{-1}, taken from Bottinelli and Gouguenheim (1974). The cases marked with an asterisk come from DLH (1979). For the Galaxy, the value usually quoted now is *220 km/s* at *8.5 kpc*.
(10) Coefficient j/R_mV_m. The mean and variance give an idea of the statistical relationship between j and R_mV_m. Thus, the extrapolated disk angular momentum is apparently rather well described by $J = 0.9\ M\ R_m\ V_m$.

In this paper a statistical method quite in the way of DLH, based on the relatively large Balkowsky (1983) sample will be applied. We chose this sample because distance measurements were mostly independent on H_0, and whenever H_0 had to be used, it agreed with our preferred value ($H_0 = 75\ km\ s^{-1}\ Mpc^{-1}$). Secondly, we kept only disk galaxies, and amongst those we further selected only S_a, S_b and S_c types, which can be called spiral galaxies beyond any doubt. We decided to exclude S_d to S_m types because in most cases the spiral arm structure is not observed clearly, and as a consequence those galaxies do not necessarily emit CEROs allowing to the discussion in § 1.8. In fact, the mass, radius and angular momentum seem to be consistently lower for the latter species, and the frontier with irregular galaxies (which should not be included in our statistics) is ill-defined. Our final sample is presented in table IV. The statistical analysis was made in two steps: first the correlation coefficient μ was estimated from Nordsieck's "exact" mass and angular momentum results in table III. Thus, we added columns with R_m and V_m values and computed $j/R_m\ V_m \approx 0.89 \pm 0.26$. Considering that Nordsieck's mass and angular momentum should not be taken too faithfully, we then decided to use simply $J_i \approx M_i\ R_m\ V_m$ in table IV to compute an indicative angular momentum for this much larger

sample where rotation curves are not known. Naturally it would have been much more satisfactory to do Nordsieck's calculations again on some 70 galaxies with presently known deep rotation curves, but this is outside the scope of the present paper.

As a matter of convention, quantities associated with the particle and the galactic scale will be denoted by indices (0) and (2) respectively. Index (1) will be reserved for future studies of the possible stellar scale, and when no ambiguity arises, particle quantities will be denoted by lower case letters devoid of indices in order to simplify the notations. For example, the (average) electron mass will be noted $M_{(0)} = m$. Likewise, upper case notations will be reserved for galactic scale quantities, so that the mass of the average spiral galaxy will be written $M_{(2)} = M$. One notation problem remains for the gravitational constant on the stellar scale, which is traditionally denoted by the uppercase G. Here we shall need to define two such constants on the galactic and particle scale (see § 2.7) and we shall accordingly use $G_{(2)} = G$ for the galactic scale, $G_{(0)} = g$ for the particle scale, and simply keep $G_{(1)} = 6.67\ 10^{-8}$ $cm^3 g^{-1} s^{-2}$ for the hypothetical stellar scale. The value adopted for Hubble's constant is $H_0 = 75\ km\ s^{-1}\ Mpc^{-1}$. We did not bother to give error estimates on our calculations because they are so model dependent that a slight change in the interpretation would often result in a large change of the results, and to state errors would convey a false sense of security. All values quoted below should be regarded as rough orders of magnitudes.

2.2 LENGTH SCALE

2.2.1 BOHR RADIUS

The first Bohr orbit in the hydrogen atom has a radius equal to $a_0 = 0.529\ 10^{-8}\ cm$. For higher atomic number Z, the size of the inner shell electron orbit decreases as Z^{-1}, whereas the radius of the outer shell remains of order a_0. On the galactic scale a_0 should thus correspond to the outer radius A_0 of regular type clusters. Simple condensations in clusters (sometimes called groups) do not qualify because they usually contain one or two large galaxies with many dwarf companions, and in our view, dwarfs do not correspond to any known particles, as explained in § 1.8. For example, the local group would yield a radius around *1 Mpc*, but it contains no giant or super-giant elliptical, and most of the members are irregulars which do not rate as electron-like galaxies as we formerly supposed. In our model, a true (atomic-like) cluster should be composed of at least one giant elliptical or super-giant cD plus a number of spiral galaxies, and eventually a flock of small ellipticals and irregulars (possibly relics from past CERO ejections). Because atomic-like systems on this scale should also conserve about the same external size irrespective of the number of spiral galaxies they contain (that is; irrespective of the nucleus "charge"), it is not important to select only those clusters which are truly hydrogen-like with only one spiral gravitating around a giant elliptical.

To give an idea of the order of magnitude and structure of regular clusters, let us consider the well-known Coma cluster. The central condensation of Coma is contained within a radius of about $2.7\ h_{75}^{-1}\ Mpc$, with a low-density fringe which may extend possibly to $\approx 7\ h_{75}^{-1}\ Mpc$ and a very low-density highly irregular supercluster which has been detected up to $23\ h_{75}^{-1}\ Mpc$ (see for example Bahcall, 1977 for a review). This hierarchy of structures seems common for regular rich clusters. Zwicky and Karpowicz (1966) reported that the largest clusters in Zwicky's catalogue have a radius about $3.3\ h_{75}^{-1}\ Mpc$, but Zwicky's method of estimating cluster radii may have underestimated them and the scatter is large anyway.

For lack of a precisely defined value, we shall retain Zwicky's estimate so that the scaling factor for length becomes:

$$\Lambda_L = A_0/a_0 = 1.94\ 10^{33} \tag{2.1}$$

The validity of this result will be checked *a posteriori* in § 2.10 below.

Name	type	Δ	θ	R_H	R_m	V_m	M_i	J_i
		Mpc	(')	kpc	kpc	kms^{-1}	$10^{10}M_\odot$	$10^{73}gcm^2s^{-1}$
(1)	(2)	(3)	(4)	(5)	(6)	(7)	(8)	(9)
24	5	10.0	6.0	8.73	2.91	143.0	4.28	1.09
224	3	0.7	182.9	18.62	6.21	282.0	35.52	38.16
253	5	2.6	30.1	11.38	3.79	197.0*	7.41*	3.40
598	6	0.8	79.2	9.22	3.07	123.0	3.37	0.78

772	3	7.2	9.9	10.37	3.46	275.0	18.79	10.96
1055	3	6.0	10.4	9.08	3.03	151.0	4.96	1.39
1097	3	15.1*	11.5	25.26	8.42	287.0	49.95	74.07
1187	5	14.5	7.6	16.03	5.34	294.0	33.21	32.02
1300	4	13.2	7.4	14.21	4.74	170.0	9.95	4.92
1365	3	10.0	13.2	19.20	6.40	221.0	22.56	19.58
1532	2	21.9	10.0	31.85	10.62	215.0	35.60	49.88
1637	5	7.6	7.7	8.51	2.84	236.0	11.41	4.69
1784	5	13.8	5.6	11.24	3.75	225.0	13.69	7.08
1792	4	13.2*	5.0	9.60	3.20	191.0	8.46	3.17
1964	3	12.0	7.3	12.74	4.25	94.0	2.75	0.67
2090	5	20.6*	5.9	17.68	5.89	157.0	10.48	5.95
2139	6	15.1	3.3	7.25	2.42	240.0	10.07	3.58
2146	2	8.7	8.0	10.12	3.37	105.0	2.69	0.58
2280	6	15.1	6.7	14.71	4.90	228.0	18.45	12.66
2403	6	2.1	26.8	8.19	2.73	138.0	3.77	0.87
2541	6	4.6	7.8	5.22	1.74	139.0	2.43	0.36
2613	3	6.9	9.3	9.33	3.11	129.0	3.77	0.93
2683	3	7.9	10.2	11.72	3.91	154.0	6.73	2.48
2776	5	15.8	4.3	9.88	3.29	294.0	20.55	12.21
2782	1	32.7*	3.7	17.60	5.87	218.0	20.15	15.81
2835	5	7.6	9.1	10.06	3.35	117.0	3.32	0.80
2841	3	10.0	10.2	14.84	4.95	329.0	38.58	38.52
2903	4	8.3	13.1	15.81	5.27	228.0	19.82	14.62
2997	5	7.6	10.9	12.05	4.02	286.0	23.65	16.67
3031	2	3.0	31.0	13.53	4.51	236.5*	5.37*	3.51
3079	4	12.6	8.7	15.94	5.31	220.0	18.53	13.30
3169	1	21.9	6.0	19.11	6.37	262.0	31.47	32.24
3198	5	7.2	10.4	10.89	3.63	162.0	6.86	2.48
3310	4	12.6	4.3	7.88	2.63	214.0	8.71	3.00
3319	6	7.6	7.9	8.73	2.91	115.0	2.78	0.57
3344	4	8.3	9.2	11.11	3.70	265.0	18.71	11.27
3359	5	9.1	8.4	11.12	3.71	212.0	12.05	5.81
3368	2	9.5	10.3	14.23	4.74	287.0	28.22	23.58
3486	5	6.0	9.3	8.12	2.71	143.0	4.03	0.96
3521	4	6.6	12.4	11.90	3.97	303.0	26.24	19.36
3556	6	10.5	9.7	14.81	4.94	165.0	9.70	4.85
3596	5	7.2	5.4	5.65	1.88	246.0	8.20	2.33
3627	3	8.3	12.3	14.85	4.95	213.0	16.22	10.49
3628	3	6.9	14.5	14.55	4.85	136.0	6.51	2.64
3631	5	13.2	7.2	13.82	4.61	173.0	9.96	4.87
3718	1	10.5	7.5	11.45	3.82	293.0	23.61	16.21
3726	5	11.5	7.8	13.05	4.35	162.0*	7.76*	3.36
3938	5	14.5	6.7	14.13	4.71	140.0	6.70	2.71
3992	4	12.0	9.1	15.88	5.29	258.5*	25.12*	21.10
4096	5	13.2	7.8	14.97	4.99	159.0	9.12	4.44
4144	6	9.1	6.4	8.47	2.82	90.0	1.68	0.26
4157	3	15.1	7.6	16.69	5.56	202.0	16.40	11.31
4217	3	13.8	6.3	12.64	4.21	266.0	21.54	14.82
4244	6	4.0	13.6	7.91	2.64	110.0	2.30	0.41
4303	4	11.0	10.1	16.16	5.39	152.0	9.01	4.53
4321	4	10.5	9.8	14.97	4.99	400.0	57.62	70.57
4535	5	10.5	9.7	14.81	4.94	166.0*	9.77*	4.92
4559	6	7.9	10.6	12.18	4.06	171.0	8.57	3.65
4826	2	9.5	11.6	16.03	5.34	220.0	18.67	13.47
4941	2	12.0	4.7	8.20	2.73	140.0	3.88	0.91
5033	5	6.9	11.0	11.04	3.68	175.0	8.14	3.22
5194	4	7.6	13.4	14.81	4.94	137.0	6.70	2.78
5236	5	4.0	16.2	9.42	3.14	417.0	39.39	31.67
5247	4	19.1	7.4	20.56	6.85	107.0	5.73	2.58
5248	4	15.1	7.6	16.69	5.56	202.0	16.42	11.33
5301	3	18.2	4.9	12.97	4.32	185.0	10.73	5.27
5371	4	20.0	5.8	16.87	5.62	423.0	72.33	105.60
5474	6	5.8	7.2	6.07	2.02	35.5*	0.14*	0.01
5523	6	17.4	5.3	13.41	4.47	432.0	60.05	71.18
5676	4	14.5	5.0	10.54	3.51	133.0	4.47	1.28
5713	4	13.2	3.8	7.30	2.43	127.5*	5.01*	0.95
5879	4	13.2	5.9	11.33	3.78	127.0	4.44	1.31
5899	5	33.1	3.3	15.89	5.30	497.0	94.04	151.90
5907	5	6.3	11.6	10.63	3.54	260.0	17.26	9.76
5921	4	18.2	6.3	16.68	5.56	183.0	13.44	8.39
5962	5	19.1	4.0	11.11	3.70	228.0	13.95	7.23
6015	6	15.1	5.7	12.52	4.17	163.0	7.97	3.33

6207	5	18.2*	3.7	9.79	3.26	178.0	7.50	2.67
6217	4	16.6	3.4	8.21	2.74	225.0	9.99	3.77
6239	3	15.3	3.8	8.46	2.82	109.0	2.43	0.46
6503	6	5.8*	9.9	8.35	2.78	107.0	2.30	0.42
6643	5	22.9	4.8	15.99	5.33	178.5*	9.33*	5.45
6835	1	20.9	3.3	10.03	3.34	193.0	9.01	3.57
6946	6	10.5	16.0	24.43	8.14	159.0	14.86	11.81
6951	4	12.6	6.8	12.46	4.15	452.0	61.15	70.47
7137	5	24.4*	2.3	8.16	2.72	210.0	8.67	3.04
7217	2	14.5	7.6	16.03	5.34	99.0	3.84	1.25
7218	6	12.0	3.8	6.63	2.21	181.0	5.25	1.29
7314	4	15.8	5.7	13.10	4.37	176.0	9.77	4.61
7331	4	9.1	12.9	17.07	5.69	279.0	31.99	31.18
7361	5	17.2*	4.0	10.01	3.34	122.0	3.60	0.90
7418	6	20.2*	4.8	14.10	4.70	187.0	11.92	6.43
7448	4	15.1	3.4	7.47	2.49	330.0	19.50	9.83
7625	1	24.5*	2.7	9.62	3.21	183.0	7.80	2.81
7640	5	7.2	11.7	12.25	4.08	137.0	5.51	1.89
7741	6	10.0	6.7	9.74	3.25	170.0	6.75	2.29
Median :				12.65	4.22	204.74	15.55	13.27
Variance:				4.4	1.4	85.3	16.3	23.5

Tab. IV: Statistics for spiral galaxies adapted from Balkowsky (1973) and Bottinelli and Gouguenheim (1974).

(1) NGC classification.
(2) Morphological type from G. and A. de Vaucouleurs *Reference Catalogue* (1964). Only the following types in Balkosky's (1973) original list have been retained: 1=Sa, 2=Sab, 3=Sb, 4=Sbc, 5=Sc, 6=Scd.
(3) Distance in Mpc, taken from Balkowski (1973). Most of these have been determined by methods independent of Hubble's constant. The numbers marked with an asterisk have been calculated from redshift with $H_0 = 75\ km\ s^{-1}Mpc^{-1}$.
(4) Photometric angular diameter in Holmberg's (1958) system, also taken from Balkowsky (1973). Reduced to face-on view at the galactic pole, in units of arcmin.
(5) Corresponding linear radius in kpc, without cosmological correction.
(6) Radius at the turn-over point in the velocity curve, statistically equal to about $1/3\ R_H$ (DLH, 1979), in kpc.
(7) Maximum rotational velocity in kms^{-1}, from Bottinelli and Gouguenheim (1974).
The numbers marked with an asterisk have been taken from Tully's (1988) rotational velocity W_R^i which is found statistically to be equal to $2\ V_m$.
(8) Indicative total mass M_i in units of $10^{10}M_\odot$, deduced from 21cm observations by Balkowski (1973). The few masses marked with an asterisk have been taken from Tully's total mass which is also an indicative mass based on 21 cm observations (Tully, 1988). As argued by Heidmann (1968), Balkowsky (1973), DLH (1979) and others (see the references in DLH), the indicative mass is of order of the "true" total mass and statistically related to it.
(9) Indicative disk angular momentum in units of $10^{73}gcm^2s^{-1}$, computed with the statistical relation: $J_i = M_i\ R_m\ V_m$.

2.2.2 ASSOCIATIONS OF QUASARS AND GALAXIES

Possible associations of QSO's and galaxies have been studied for years, and supporters of the local hypothesis contend that there is a larger than normal density of high-redshifted quasars around bright galaxies. In our model, this is perfectly natural since a spiral (or a giant elliptical) should always be surrounded by a collection of "virtual" CEROs (here a CERO would be called "virtual" if it is still attached to its parent galaxy by a vortex tube as illustrated by the filament threading the bridge in Arp's object). In fact, the situation mimics "virtual" photon clouds around electrons. In these conditions, the galaxy should experience a kind of *Zitterbewegung* due to successive recoils from virtual CERO emission as discussed in § 1.9. Burbidge, Hewitt, Narlikar and Das Gupta (1990) have shown that there is an excess of pairs of a low-redshift galaxy coupled to a high-redshift quasar (CERO in our model), with a separation peaking between *20* to $60\ h_{50}^{-1}\ kpc$. The spread of the CERO distribution around spiral galaxies can thus be taken as $L \approx 40\ h_{75}^{-1}\ kpc$. It should be compared to the electron Compton wavelength $\lambda_e = 3.86\ 10^{-11}\ cm$, since it is well known that the electron "spread" is due to virtual photon emission as illustrated by Feynman's self-energy diagrams. From the comparison of L and λ_e, the following scale factor obtains:

$$\Lambda_L = L/\lambda_e \approx 3.20\ 10^{33} \tag{2.2}$$

2.2.3 ASSOCIATIONS OF SPIRALS WITH IRREGULARS

The unified emission scheme suggests that hydrogen clouds are dragged along with ejected CEROs (see § 1.8). They finally detach from them and recondense to form irregular galaxies found around spiral galaxies, so that the spread of these small galaxies around a spiral should give another lose tracer of the galactic "wavelength". For example, around our Galaxy there is a dense sub-system composed of 15 dwarf galaxies. For example, Zaritsky et al. (1989) have studied their radial velocities and distances with the intention to put strong constraints on the dynamical mass of our Galaxy. The median distance of those satellites established from their numbers is *95 kpc* which yields a scaling factor

$$\Lambda_L \approx L'/\lambda_e = 7.6\ 10^{33}. \tag{2.3}$$

It should be stressed that *95 kpc* represents the peak of the local distribution which may in fact extend up to *200 Kpc* or more. For example, Dressler (1976, 1980) has found sub clustering at the scale $320\ h_{75}^{-1}\ kpc$ in a sample of 65 clusters.

2.2.4 THE ELECTRON RADIUS

Let us try and compare the typical radius of the average spiral galaxy ($R_{(2)} = R$) with the radius of the average electron ($R_{(0)} = r$). Our first task is to evaluate the average galactic radius. Because galaxies do not show sharply defined boundaries, rather arbitrary radii have been defined which often depend on a luminosity cut-off. For example, Holmberg's (1958) radius R_H extends to the *26.5 mag* per square degree which may be considered as the cut-off of visible matter. Another radius, R_{25}, goes only to the 25th magnitude and is more commonly used now. Other radii are (i) the exponential scale length of the disk surface brightness R_D, (ii) the turn-over radius in the velocity curve R_M, (iii) the limiting radius R_{HI} of gaseous HI which can be traced as far away as $R_{HI} \approx 1.5\ R_H$. Now if the galaxy is effectively surrounded by a spherical dark matter halo, the mass defining radius could extend up to $R_g \approx 100\ kpc$ (see § 2.5). We do not know a priori which one of these radii should represent the galactic radius to be compared with the electron radius, so we shall rather arbitrarily start with Holmberg's radius and will check our results *a posteriori*.

From table IV, the sample of spiral galaxies gives an average Holmberg radius $\langle R_H \rangle = 12.65 \pm 4.4\ kpc$. For the NS sample, a disturbingly large average of *17.5 kpc* is found in table III, but the NS sample could be less controlled as regards distance determination. Moreover, the sample is small and heavily biased in favour of large galaxies for which rotation curves were more easily measured.

For electrons, a natural length called the classical radius $r_0 = e^2 / m\ c^2 \approx 2.818\ 10^{-13}\ cm$, can be constructed from the fundamental constants of electromagnetic theory by equating the electron self-energy e^2/r_0 to the rest energy mc^2. Inherent in this definition is the assumption that the whole of the electron mass is of electromagnetic origin, but that does not help much in understanding which characteristic size it does represent. In particular, it is a cause of concern that r_0 somewhat exceeds the proton radius ($r_p \approx 1.5\ 10^{-13}\ cm$) although the proton mass is considerably larger than the electron mass. However, this could still be sustained if, as our model presumes, the electron has the flat morphology of a spiral galaxy while the proton is spheroidal like an elliptical galaxy and accumulates more mass up to a given radius. Indeed, Holmberg's radius for large spiral galaxies is just about half of the giant elliptical radius ($\approx 30\ h_{75}^{-1}\ kpc$, Sandage 1972a), and if the full extension of the spiral disk radius encompassing HI clouds should be considered, then spiral and elliptical galaxies truly become of the same size. Another argument indicates that r_0 could indeed represent a physically interesting low energy radius. The elastic cross-section for Compton scattering (in our model it corresponds to elastic scattering of CEROs on spiral galaxies) is expressed by the Klein-Nishina formula (see for example Bjorken and Drell, 1964) which, at low energies, tends to $\sigma \approx (8\pi/3)\ r_0^2$. Writing $\sigma = \pi\ r_{eff}^2$, we find that low-energy photons probe an effective radius: $r_{eff} = R_{(0)} = (8/3)^{1/2}\ r_0 \approx 4.60\ 10^{-13}\ cm$. Taking $r = r_{eff}$ furnishes the following length scaling factor:

$$\Lambda_L = R/r_{eff} \approx 8.48\ 10^{34} \tag{2.4}$$

It is disturbing that the latter determination differs so much from the former ones, by as much as one order of magnitude. Possibly, the whole model is incorrect, or alternatively this suggests that we should have chosen a smaller defining radius for galaxies (a bulge radius for instance). But maybe we should also have considered dwarf spiral galaxies in our statistics. Indeed, dwarf spiral companions have been found attached to large spiral galaxies by a jet (Arp, 1972, 1980) or an extended arm (Arp, 1969). As stated in section § 1.8 these systems very much resemble the spin-up, spin-down electron pairs filling atomic orbitals. Thus, dwarf spirals should also be able to eject and absorb CEROs. As dwarf galaxies have radii typically in the range *1-5 kpc*, and if one dwarf spiral is counted for each large one, the average radius could be halved. Both effects combined could reduce Λ_L by a factor *10 - 20*, bringing it more in line with the former determinations. Yet it is not clear that objects with such widely different radii could all be interpreted in terms of cosmic electrons. However, we favour this interpretation because there is apparently no alternative: they could not be seen as an electron (the dwarf) orbiting a proton (the large spiral), because the cosmic Bohr radius would be at most *500 kpc* which is way too small and not compatible with other Λ_L determinations, even if they were as low as 10^{33}. But if dwarf spirals had been counted from the start in our statistics, we would have run the considerable risk of also including dwarf irregulars (which should not be included) outnumbering spirals by a large factor. Indeed, the fainter end of the luminosity function is not well

known but it seems to imply an ever-increasing number of small galaxies. Hence, we decided finally not to include them. In these conditions, the average of our four determinations (2.1-4) gives:

$$\Lambda_L \approx 2.44\ 10^{34} \tag{2.5}$$

2.3 TIME SCALE

It has been argued above that radio jets in ERS's, and the optical bridge in Arp's object are manifestations of the same process, namely CERO emission by galaxies. On the other hand, it is now well established (Rudnick and Edgar, 1984) that at least for some extended radio sources, the emission mechanism is a flip-flop, with one ejection to one side, then to the other side, and so on (see § 1.4 and 1.9). Each ejection provokes a recoil of the emitting galaxy, and a similar process supposedly holds good for spiral galaxies. The resulting erratic motion is reminiscent of the electron *Zitterbewegung* due to virtual photon emission for which the typical time scale is (Bjorken and Drell, 1964):

$$T_{(0)} = \tau = h/(2mc^2) \approx 6.44\ 10^{-22} s. \tag{2.6}$$

This should be compared to the period of CERO emission by spiral galaxies which is evaluated in a three-step procedure as follows:

(a) The cumulative duration of all postulated Seyfert episodes in the typical spiral galaxy *is* $T_t = p\ T_{lf}$, where p is the percentage of Seyfert galaxies compared to ordinary quiescent spiral galaxies, and T_{lf} is the life-time of the average galaxy. The evaluation for p is difficult because successive determinations have led to ever increasing results as more and more Seyferts were discovered (Sargent, 1972; Huchra and Sargent, 1973; Simkin, Su and Schwarz, 1980). The value usually quoted is $p \approx 2\text{-}4\%$, and $p \approx 3\ 10^{-2}$ will be assumed henceforth.

(b) Next, we try to evaluate the duration T_0 of one single Seyfert phase. In the apparently exploding galaxy NGC4258, van der Kruit, Oort and Mathewson (1972) estimate the energy release at $E \approx 3\ 10^{58}$ *ergs*. For our Galaxy, the total energy of the last period of activity has also been evaluated by Sanders and Prendergast (1974) at $E \approx 3\ 10^{58}$ *ergs*. We assume that this is typical of large spiral galaxies undergoing Seyfert activity. This energy is emitted in radiation plus the kinetic energy of the entrained gas and of the departing CERO. The latter is found to be $EQ = (1/2)\ M_Q\ V_Q^2 \approx 5\ 10^{56}$ *ergs*, where we have taken $M_Q \approx 10^7\ M_\odot$ and VQ $\approx 2.2\ 10^3$ *kms*$^{-1}$ (this value will be justified below in § 2.4). Thus, the CERO kinetic energy represents a very small fraction of the total energy, and can be neglected. The power emitted radiatively would be typically $P \approx 5.010^{44}$ *ergs*$^{-1}$ for Seyfert galaxies, so that we find for the duration T_0 of one Seyfert episode: $T_0 = E/P \approx 1.9\ 10^6$ *yrs*. Almost the same result is obtained by another indirect route (Bailey and Clube, 1978): Seyfert nuclei involve speeds $\approx 10^3$ *kms*$^{-1}$ in a volume of typical extension ≈ 1 *kpc* around the nucleus, producing a typical time scale of the same order.

(c) Finally, we introduce the average number $n = T_t/T_0$ of Seyfert episodes over a whole galactic life-time. Thus, the elapsed time between two Seyfert episodes can be calculated as $T = T_{lf}/n = T_0/p \approx 6.34\ 10^7$ *yrs*.

Our result is intermediary between the $\approx 10^7$ *yrs*. advocated by Arp (1987) for explosive events in spiral galaxies, maybe leading to spiral arm regeneration, and the somewhat higher values $\approx 10^{8\text{-}9}$ *yrs*. favoured by other authors (Bailey and Clube, 1978; van der Kruit, Oort and Mathewson, 1972). These values are not incompatible with our own, if we recall that our prediction is for CERO ejection in all possible directions and that only those ejections close or into the galactic plane have a chance to regenerate spiral arms. The latter should be less frequent than the former.

As a by-product, it is possible to evaluate the average number $n = T_t/T_0$ of Seyfert episodes. For this we need a knowledge of the galactic life-time T_{lf}. The inverse of Hubble's value furnishes in principle an upper limit: $H_0^{-1} = 1.3\ 10^{10}$ *yr*s. Our Galaxy has a life-time $T_{lf} \approx 1.2\ 10^{10}$ *yrs*., and it is usually postulated that other galaxies formed at about the same epoch. But the oldest star ages are currently estimated at *1.3 to 1.7* 10^{10} *yrs*. (Sandage and Cacciari, 1990), and so are apparently larger than the Universe life-time! In view of this contradiction, we shall take the largest possible value $T_{lf} \approx H_0^{-1} \approx 1.3\ 10^{10}$ *yrs*., yielding $T_t \approx 4.5\ 10^8$ *yrs*. for the total duration of all Seyfert events over the life-time of the average spiral. From this one obtains $n \approx 240$, which is relatively large compared to other predictions of about 100 episodes (see § 1.3). Admittedly our time-based estimations are poorer than the space-based ones and we have found no other way to check this single time-scale calculation. The reason should ultimately be found in the fact that, on the macroscopic scale, it is (relatively) easy to measure precise lengths, but it is much harder to evaluate long periods of time because one has to rely on small statistics over few objects frozen at different evolutionary stages.

If the above period $T_{(2)} = T \approx 6.34\ 10^7\ yrs$. can be trusted, one obtains the scaling factor:

$$\Lambda_T = T/\tau \approx 3.11\ 10^{36}\ yrs. \tag{2.7}$$

2.4. VELOCITY SCALE

CEROs are viewed here as cosmic scale photons, and consequently they should propagate at constant speed (denoted $C_{(2)} = C$) with respect to the (asymptotic) space-time continuum, which, on this scale, is identified with the intergalactic medium (IGM). The latter is composed of particles embodying the self-similar structures of the next lower self-similar scale. The CERO speed should be a characteristic constant of this medium, and to derive it from the photon speed, we need the velocity scaling factor which is:

$$\Lambda_V = \Lambda_L / \Lambda_T \approx 1/127 \tag{2.8}$$

where we have used (2.5) and (2.7). This gives a CERO velocity of:

$$C_{(2)} = \Lambda_V C_{(0)} = \Lambda_V c \approx 2354\ km\ s^{-1}. \tag{2.9}$$

It should be noticed that the velocity scaling factor (2.8) is strikingly close to $\alpha \approx 1/137$. Reasonable variations of the parameters given above produce variations of $1/\Lambda_V$ in the range *40 - 600* so that the near equality found here may be an accident. However, as Λ_V should clearly become a new dimensionless constant, of no less importance than α, it would be very disturbing to get two fundamental constants with close but different numerical values, and it is tempting to suppose instead that Λ_V is exactly equal to α. However, we cannot exclude the possibility that Λ_V should be a function of α. Assuming that $\Lambda_V = \alpha$ exactly, the CERO velocity can be calculated very precisely as: $C_{(2)} = \alpha C_{(0)} = \alpha c = 2187.7\ km\ s^{-1}$, which will be called the "theoretical" value. A direct experimental verification of this prediction would be difficult using present day technology. For example, at the Virgo cluster distance, namely $16.8\ h_{75}^{-1}\ Mpc$, with a fully transverse displacement, CEROs would cross *1 mas* in about *33.8 years*. This is still at the threshold of our measuring power. At the distance of M31 (*0.7 Mpc*) the *1 mas* crossing-time becomes only *1.4 yrs*.

One important difference between this essay and Oldershaw's work, reside in the fact that speeds do not scale in the latter since Oldershaw supposes that $\Lambda_L = \Lambda_T$, whence $\Lambda_V = 1$ and $C_{(2)} = C_{(0)} = c$. From our point of view, such a position is untenable as it would imply infinite CERO redshifts. With our value for the CERO velocity, it is clear that only a very small fraction of the CERO redshift comes from the Doppler effect.

Oldershaw finds another purported self-similar scale at $\Lambda_{OL} \approx 3\ 10^{17}$, intermediate between the particle and the galaxy scale, but we are not yet convinced that it is possible to find objects on the stellar scale which are perfect self-similar replicates of particles or galaxies. However, for the direct scaling between particles and galaxies, a unique ratio can be extrapolated from his work, simply by squaring his value for the scaling factor, to take into account the fact that one of his levels has been skipped here:

$$\Lambda^2_{OL} \approx 3\ 10^{35}. \tag{2.10}$$

Reassuringly, this is close to the geometrical mean of our length and time scaling factors: $\Lambda^2_{OL} \approx (\Lambda_L \Lambda_T)^{1/2}$.

2.5 MASS SCALE

It is our goal here to compare the average spiral mass to the electron mass, but estimations of galactic masses are notoriously unreliable because of the discrepancy between the luminous mass and the dynamical mass deduced from the velocity profile. Within Holmberg's radius, *M/L* values ranging from 4 to 6 have been found for spiral galaxies, but they still appear to increase considerably beyond R_H (for reviews, see Faber and Gallagher, 1979; Trimble, 1987). Ostriker and Peebles (1973) noticed that cold self-gravitating disks were strongly unstable with respect to the bar instability, while about 1/3 of the disks are observed without bars. They suggested that disks may be stabilized by a massive halo of dark matter (DM). Subsequent analysis led to the conclusion that the halo may have a spheroidal form and that it contains most of the mass. Alternatively, the galaxy structure, and in particular the flat rotation curve, could be driven by a new dynamic (Milgrom, 1983; Bekenstein and Milgrom, 1984; Sanders, 1986).

Supposing that there is a halo, its mass is difficult to estimate precisely because rotation curves remain flat or slowly raising up to the last measured point implying a linearly increasing mass with radius. Some lower limits have been found. For example, the constraint that the escape speed from the Galaxy must exceed the largest speed of stars in the solar neighbourhood ($\approx 500\ km\ s^{-1}$) yields a halo radius $R_h \geq 40$ kpc and a mass $4.6\ 10^{11} M_\odot$ (Binney and Tremaine, 1987) for our Galaxy. Modelization of the dynamics of the Magellanic stream are consistent with a halo extending at least to *100 kpc* (Lin and Lynden-Bell, 1982). A large number of other determinations are recapitulated in Trimble (1987). They range from *12* to *118 kpc* in radius and $2\ 10^{11}$ to $3\ 10^{12}\ M_\odot$ in mass. The main difficulty is that any probe of the gravitational potential can only probe the mass inside its radius. Results extracted from

Nordsieck's sample in table III and from Balkowsky's sample in table IV give respectively *0.975* and *1.5* 10^{11} $M_\odot$, but these are certainly lower limits in view of more recent results.

We suggest here another method to estimate the total mass of a spiral galaxy not encumbered by the usual limitations. First the quasi-perfect linear increase of the mass with radius implies a quasi-perfect $1/r^2$ dependence in the halo density. Let us suppose that it does not stop abruptly at some radius but that it merges smoothly with the haloes of other galaxies and finally with the intracluster medium. Thus, the mass of one galaxy is unbounded. When we compute the mass of a galaxy, we do not want to include in it the infinite contribution of the "vacuum", and a finite result can be obtained by subtracting the "vacuum" mass from the galaxy mass. This is equivalent to limiting the calculation down to the radius at which the halo density reaches the intra-cluster gas density ρ_g. Contribution from this gas must not be counted in the mass of the spiral because it pertains to the mass of the giant elliptical lying at the cluster centre. Likewise, the elliptical mass should be estimated up to the radius where the cluster gas density reaches the inter-cluster density.

A convenient analytical form of the halo density is:

$$\rho(r) = \rho_0 \, [\, 1 + (r/r_c)^2]^{-1}. \tag{2.11}$$

It has the correct r^{-2} behaviour at large r and goes down below ρ_0 at small r to account for the fact that the luminous mass seems able to produce the rotation curve there. The free parameter r_c is the core radius, difficult to estimate because dynamical effects from the halo are not very sensitive to it. On the other hand, using the fact that the mass at radius r behaves asymptotically as $M(r) \sim r \, V_M^2 / G_{(1)}$ we can compute the density $\rho(r) \sim V_M^2/4\pi G_{(1)} r^2$. Thus, equating this to the asymptotic expressions for ρ furnishes $\rho_0 \sim (1/4\pi G_{(1)}) \, V_M^2/r_c^2$ and:

$$\rho(r) \sim (1/4\pi G_{(1)}) \, V_M^2/r^2. \tag{2.12}$$

Now it is an easy matter to find that the radius R_g at which ρ attains the average cluster density ρ_g is given by:

$$R_g \approx V_M / (4\pi G_{(1)} \rho_g)^{1/2} \tag{2.13}$$

and that the halo mass contained inside this radius is:

$$M_g \approx V_M^3 / (4\pi G_{(1)}^3 \, \rho_g)^{1/2}. \tag{2.14}$$

As seen in Sarazin (1986) for example, there is hot gas filling more or less regular clusters with density about $10^{-3} \, h_{50}^2$ *atoms/cm*^{3} ($\rho_g = 3.8 \, 10^{-27} \, h_{75}^2$ *g cm*$^{-3}$). Taking a typical velocity $V_M \approx 220$ *km/s* then yields $R_g \approx 127$ *kpc* and $M_g \approx 1.43 \, 10^{12} M_\odot$. This should probably be considered an upper limit because there are many spiral galaxies smaller than our Galaxy.

In view of this and other estimations, a reasonable order of magnitude for the average spiral mass is $5 \, 10^{11} M_\odot$, which, when compared to the electron mass $m = 9.109 \, 10^{-28}$ *g* furnishes a ratio:

$$\Lambda_M = M_{(2)} / M_{(0)} = M/m \approx 1.1 \, 10^{72}. \tag{2.15}$$

Mass should be a derived quantity in a purely geometrical model, related to the curvature of space-time, thus it seems natural to express Λ_M as a function of Λ_L, using (2.5) and (2.15):

$$\Lambda_M = \Lambda_L^{2.095} \tag{2.16}$$

where $D = 2.095$ is the fractal mass dimension. Its value strongly differs from Oldershaw's result as he found an exponent superior to *3* (see § 1.1). Our own result agrees with our vision of electrons as flattened, nearly 2-dimensional objects, similar to spiral galaxies and scaling very closely as L^2. It would not be surprising if this ratio did not hold for elliptical galaxies, in view of their very different shape, and thus the Universe could be a multi-fractal with several self-similarity dimensions. Unfortunately, it does not seem possible to find a reliable measure of the mass of giant elliptical galaxies at the present time, to be compared to the proton mass. Older measurements of cluster masses relied on the virial theorem where the gravitational constant $G_{(1)}$ was used. Values of order $10^{13} M_\odot$ with an upper limit of a few $10^{14} M_\odot$ are usually quoted for the giant elliptical galaxies or super-giant cD's in rich clusters (see for example Wolf and Bahcall, 1972), and maybe as much as $10^{15} M_\odot$ for the whole cluster. Recent measurements of relative velocities between different nuclei of dumbbell galaxies (Valentijn and Casertano, 1988) have shown that if the dumbbell nuclei can be treated as point mass, a total mass of $\approx 10^{13} M_\odot$ is required just for the centres, but as the rotation curve seems to be rising, the total mass could be larger. Finally, for M87 a direct mass estimate can be obtained because the halo of X-ray emitting gas should be bound to the galaxy. Fabricant and Gorenstein (1983) show that M(r) rises linearly with *r* out to more than *300 kpc* where the mass attains $M \approx 3 \, 10^{13} M_\odot$. In our model, the average total mass of a proton-like elliptical galaxy should be *1836* times

the mass of the average (electron-like) spiral, because the dimensionless ratio m_p/m_e should be conserved by scaling. Using the average spiral mass, one finds: $M_{ell} = 1836\ M \approx 9.2\ 10^{14}\ M_\odot$. This high value is plausible if the giant elliptical masses make up most of the cluster mass ($\approx 10^{15}\ M_\odot$) in the same way that in atoms, nucleon masses determine the essential part of atomic masses.

Another dimensionless constant of interest is the ratio between the galactic mass $M_{(2)\,G}$ and the mass of the central black hole $M_{(2)\,BH}$, which will be used in § 2.7 below. Recent infrared and submillimetre measurements of the gas dynamics in the region between *0.5* and *10 pc* of our Galaxy centre fit a central point mass of $M_{(2)\,BH} \approx 2.5\text{-}4\ 10^6\ M_\odot$ (Crawford et al., 1985; Genzel and Townes, 1987; Serabyn et al., 1987). Stellar velocities and velocity dispersion do not seem to follow the trend set up by the gas, however, and could still be explained by a dense distribution of stars (Rieke and Rieke, 1988). Yet these authors admit that if the core radius of the central stellar distribution is larger than *0.1 pc* (say ≈*0.6 pc*), then a central black hole of $\approx 2\ 10^6\ M_\odot$ remains a viable alternative. In M31, stellar velocities and velocity dispersions in the nucleus imply a possible central mass of $10^{7\text{-}8}\ M_\odot$ for Kormendy (1988), if the nucleus is an ellipsoid as one might expect, and $3\text{ - }7\ 10^7\ M_\odot$ for Dressler and Richstone (1988) Finally, spectroscopic studies of the variable Seyfert 1 galaxy NGC 5548 imply the existence of a central supermassive engine of $\approx 2\ 10^6\ M_\odot$ (Crenshaw and Blackwell Jr., 1990). Thus, all considered, the possible range is large, between $\approx 2\ 10^6$ and $10^8\ M_\odot$, with a most probable value of say $5.0\ 10^6\ M_\odot$, whence:

$$M_{(2)\,G}/M_{(2)\,BH} \approx 1.0\ 10^{5.} \tag{2.17}$$

2.6 ANGULAR MOMENTUM SCALE

Angular momentum scales as ML^2T^{-1}, so one can predict a scaling factor of order of $\Lambda_J = \Lambda_M \Lambda_L^2 \Lambda_T^{-1} \approx 2.1\ 10^{104}$. The resulting angular momentum of the typical spiral galaxy should be: $J = \hbar\!\!\!^{-}\ /2 = \Lambda_J\ \hbar\ /2 \approx 1.1\ 10^{77}\ gcm^2s^{-1}$ (notice that Ħ corresponds to ħ and not to *h*). Moreover, we can also predict that the angular momentum of all galaxies, except the irregulars which in our view are not *bona fide* galaxies, but including the elliptical galaxies, must be quantized in unit's $\hbar\!\!\!^{-}\ /2$ because all particles have angular momenta in units of ħ /2. This might explain why large elliptical galaxies are constrained to surprisingly small rotation velocities.

Our predicted $\hbar\!\!\!^{-}$ value is three orders of magnitude larger than the statistical indicative angular momentum resulting from Balkowsky's sample in table IV which was $J \approx 13.27\ 10^{73}\ gcm^2s^{-1}$ and which agreed well with the NS average $J \approx 8.4\ 10^{73}\ gcm^2s^{-1}$ in table III. Yet, it should be remembered that the "exact" calculations of NS were done at a time where the rotation curves were not known up to very large radii and they may have underestimated J. Notice however that Takase (1967) has found the discordant result $J \approx 2.7\ 10^{75}\ gcm^2s^{-1}$ for M31 somewhat closer to our prediction. It is also interesting to compare our $\hbar\!\!\!^{-}$ value with predictions of other authors, namely Liu Yong Zhen et al. (1984), Cocke (1983), DerSarkissian (1986a) and Liakhovets (1986); they estimated the cosmic quantum of action at $\hbar\!\!\!^{-} = 4.18;\ 2.4;\ 50$ and $42.2\ 10^{73}\ gcm^2s^{-1}$ respectively. The large discrepancy between the measured and predicted angular momentum could originate from lots of potential problems, the most obvious being that the hypothetical DM halo is coupled to the disk rotation and thus contributes mightily to the total momentum. This hypothesis can be tested by a somewhat naive calculation. We consider a simple spherical halo model extending to R_g as found in § 2.5, and suppose that each mass element moves with constant speed V_M. The halo angular momentum is then approximately:

$$J_h \approx VM \int \rho(r)\ r^3 \sin^2\theta\, dr\, d\theta\, d\phi \tag{2.18}$$

where the integration is about a sphere of radius R_g. Using formulae of § 2.5, it is easy to show that:

$$J_h \approx (32\ \rho_g\ G_{(1)}^2)^{-1}\ V_M^5 = (\pi/8)\ M_g\ R_g\ V_M. \tag{2.19}$$

With the numerical values of § 2.5, one finds $J_h \approx 9.6\ 10^{75}\ gcm^2s^{-1}$. Considering that our radius R_g may be underestimated because ρ_g is probably overestimated, and that $\hbar\!\!\!^{-}$ may be overestimated because Λ_L is probably a bit too high, this is an encouraging result which may indeed suggest that the main cause of the difference between the disk momentum and the predicted total momentum resides in a rotating halo with speed V_M.

2.7 THE STRENGTH OF THE COSMIC SCALE EXCHANGE FORCE

The three fundamental constants on the particle scale e, ħ and c, form a complete set in the sense that only one dimensionless combination can be composed from them, the famous fine structure constant $\alpha = e^2 / \hbar\ c \approx 1/137$ which is of foremost importance since it is not affected by scaling. In the fractal model, one can define corresponding constants on the galactic scale:

(a) the charge for CERO exchange between galaxies: $E_{(2)} = E$.
(b) the basic quantum of angular momentum: $\hbar\!\!\!^{-}_{(2)} = \hbar\!\!\!^{-}$.
(c) the CERO velocity: $C_{(2)} = C$.

$\hbar$ and C have already been evaluated above. The galactic charge E is understood here as the strength of the CERO exchange force between two galaxies, exactly like the electron charge e relates to the strength of the photon exchange force. It is an easy task to evaluate it starting from the scaling relation between E and e:

$$E^2 = \Lambda_M \Lambda_L^3 \Lambda_T^{-2} e^2. \tag{2.20}$$

Taking the scaling factors from (2.5), (2.7) and (2.15), one finds:

$$(\Lambda_E)^2 = \Lambda_M \Lambda_L^3 \Lambda_T^{-2} \approx 1.64\ 10^{102} \tag{2.21}$$

hence, with $e^2 \approx 2.3\ 10^{-19}\ g\ cm^3\ s^{-2}$, the charge E is such that:

$$E^2 = 3.79\ 10^{83}\ g\ cm^3\ s^{-2} \tag{2.22}$$

E, $\hbar$ and C constitute a new set on the galactic scale, constrained by the same dimensionless ratio: $\alpha = E^2 / \hbar C \approx 1/137$. E gives an *absolute* measure of the strength of the exchange force, but it would be more interesting to compare it to the gravitational interaction strength. Thus, it is now time to introduce gravitation in the picture. It is traditionally defined by the two constants $G_{(1)} = 6.67\ 10^{-8}\ cm^3 g^{-1} s^{-2}$ and c. But $G_{(1)}$ has been measured on an as yet ill-defined intermediate scale. Noticing that $G_{(1)}$ scales with the basic dimensions [L], [M] and [T], we suggest that two other gravitational constants should be defined:

(1) $G_{(0)} = g$ on the particle scale, where gm^2 would measure the gravitational interaction "strength" between two electrons.
(2) $G_{(2)} = G$, where GM^2 measures the gravitational interaction "strength" between two spiral galaxies.

Those constants are constrained by the scaling law $GM^2 = (\Lambda_E)^2\ gm^2$ which is not very useful as long as neither G nor g are known. A measure of the *relative* strength of the exchange force is given by the dimensionless ratio: $\gamma = e^2/gm^2 = E^2/GM^2$. The difficulty is that there is no easy way to relate $G_{(1)}$ to either G or g without considering the intermediate stellar scale. Indeed, the well-known $G_{(1)}$ works quite well for objects typically the size of asteroids or planets, or even stars. But having no definite proof of a self-similar relationship between stellar size black holes (typically $\geq 3\ M_\odot$) and galaxies or particles, we cannot establish a precise scaling factor between the gravitational constants.

There is an indirect way out of this stalemate, provided that the following reasonable postulate is made: noticing that in Einstein's general relativity, the BH mass is related to its radius by $R_{(1)\,BH} = 2G_{(1)}M_{(1)\,BH} / c^2$, it is suspected that similar relationships (at least as far as orders of magnitude are concerned) should hold for the BH radii in the cores of electrons and galaxies, whenever the adequate gravitational constants are considered:

$$R_{(0)\,BH} \approx 2\ g\ M_{(0)\,BH} / c^2 \tag{2.23.a}$$

$$R_{(2)\,BH} \approx 2\ G\ M_{(2)\,BH} / C^2 \tag{2.23.b}$$

It should be noticed however that these relations are not really consistent with the conventional relation $R_{(1)\,BH} = 2G_{(1)}M_{(1)\,BH} / c^2$, where light speed on the microscopic scale is mixed with quantities from the stellar scale. Allowing to our postulate, the correct relation should rather be in this case $R_{(1)\,BH} = 2G_{(1)}M_{(1)\,BH} / C_{(1)}^2$, where $C_{(1)}$ is intermediate between c and C, provided naturally that an intermediate scale does really exist! At present, direct experimental measurements of $R_{(1)\,BH}$ are not available, and the imprecision on $R_{(2)\,BH}$ is too large so that it is difficult to assess the relevance of our hypothesis.

A second postulate is that electron and spiral galaxies have the same structure. In that case, the "classical" electron and galactic radii are given by:

$$R_{(0)\,CL} \approx e^2 / m\ c^2 = r_0 \tag{2.24.a}$$

$$R_{(2)\,CL} \approx E^2 / M\ C^2 = R_0 \tag{2.24.b}$$

Let us now compute:

$$R_{(2)\,G} / R_{(2)\,BH} \approx (E^2/M\ C^2)\ (C^2/2\ G\ M_{BH}) \approx 0.5\ (E^2/G\ M^2)\ (M/M_{BH}) \tag{2.25}$$

where (2.23.b) and (2.24.b) have been used with $R_{(2)\,G} \approx R_{(2)\,CL}$. Thus, one gets:

$$\gamma \equiv E^2/GM^2 = 2\,(R_{(2)\,G}/R_{(2)\,BH})\,(M_{BH}/M) \tag{2.26}$$

The first ratio $R_{(2)\,G} / R_{(2)\,BH}$ can be evaluated approximately: repeated observations of the radio source Sagittarius A at the geometrical centre of our Galaxy have pointed to the existence of a super-massive BH, whose size should be less than $3\ 10^{14}$ *cm* ≈ *20 au* (Davies et al., 1976; Kellerman et al., 1977; Brown and Lo, 1982). Variations in radiation output over less than half an hour have never been observed in any AGN, implying a lower limit on the size of the emitting plasma region of about *3.6 au*, and it is usually agreed that the maximum radiation from accreting disks comes from a zone on the disk at about *3* Schwarzschild's radii. So, we shall take the hole radius to be of the order of *1 au* or less, and the ratio becomes:

$$R_{(2)\,G}/R_{(2)\,BH} \approx 12.65\ kpc/1\ au \approx 2.61\ 10^9. \tag{2.27}$$

The ratio M / M_{BH} has been evaluated at the end of § 2.5 (see equ. 2.17), where it was found to be around $1.0\ 10^5$. When both ratios are entered into (2.26), one finds:

$$\gamma \approx 5.22\ 10^4 \tag{2.28}$$

Thus, the CERO exchange force between two spiral galaxies appears to be several orders of magnitude larger than the gravitational interaction. This implies that the dynamics of a spiral galaxy "gas" is not driven at all by the gravitational interaction, but instead that the gas of galaxies should rather behave as an electron gas. Notice that the CERO exchange force here should be *repulsive* if the analogy with particle physics is correct: both galaxies have the same sign for the "charge". On the contrary, the exchange interaction between a giant elliptical galaxy of the proton type and a spiral should be attractive and responsible for cluster cohesion.

Starting from γ it is now possible to find

$$G = E^2 / \gamma M^2 \approx 7.34\ 10^{-12}\ cm^3 g^{-1} s^{-2} \tag{2.29}$$

The validity of this result can be checked backwards easily. We shall compute the black hole radius in the galactic core with $R_{(2)BH} \approx 2\ G\ M_{(2)\,BH} / C^2$. Using the computed values for *G, C* and taking $M_{(2)\,BH} \approx 5.0\ 10^6\ M_\odot$, one obtains $R_{(2)\,BH} \approx 0.18$ *au* which is reasonably close to our original rough estimation of *1 au*, considering the uncertainties involved. This G value applies to the study of galactic interactions in clusters. If we are now confronted with a profusion of gravitational constants, it is precisely because the effective interaction strength scales with the basic dimensions. Again, the very concept of such a quantity breaks down, and, as we shall see below, it may be possible to subtract *G* and *g* from the list of independent fundamental constants.

Finally, it is interesting to compare the newly found interaction to the force obtained when the gravitational constant on the galactic scale is taken as $G_{(1)}$. A new ratio is introduced: $\delta = E^2/G_{(1)} M^2 = \gamma (G_{(2)}/G_{(1)}) \approx 5.74$. Thus, the exchange force is somewhat stronger than the gravitational force usually considered in astrophysical calculations on the cluster scale, a fact which could be of importance to explain at least part of the missing mass in clusters. But again, the numbers quoted here should not be taken at face value for we have been playing with a crude model. Precise prediction must await a theoretical approach. Here we simply want to point out that it is dangerous to speak of a missing mass problem in clusters when all calculations are based on a gravitational constant which has been tested only on the stellar scale.

Obviously, the dimensionless ratio γ holds on the particle scale also, from which the microscopic gravitational constant can be computed:

$$g \approx 5.33\ 10^{30}\ cm^3 g^{-1} s^{-2} \tag{2.30}$$

The same result would have been obtained starting from the scaling law $GM^2 = (\Lambda_g)^2\ gm^2$. The existence of *g* had been already predicted by Oldershaw (1987) who claimed that g is equal to $1.85\ 10^{31}\ cm^3 g^{-1} s^{-2}$. He pointed out that strong gravity theories of elementary particles furnish essentially the same result (Sivaram and Sinha,1979). With our values of the microscopic gravitational constant, the BH radius in the *electron* core can be calculated with the help of (2.23.a) and it is found to be in both cases:

$$R_{(0)\,BH} \approx 2\ g\ M_{(0)\,BH} / c^2 = (2gm/c^2)\ (M_{(0)\,BH}/M_{(0)}) \approx 1.08\ 10^{-22}\ cm. \tag{2.31}$$

where it has been assumed that $M_{(0)\,BH}/M_{(0)} = M_{(0)\,BH}/m = M_{(2)\,BH}/M_{(2)} = 1.0\ 10^5$ from which it immediately results that the mass of the postulated BH in the electron core is: $M_{(0)\,BH} = 9.1\ 10^{-33}\ g$.

2.8 LIMITATIONS OF THE MODEL

If we repeat the above treatment for the e-p and p-p cases, we find the following constants:

$$\gamma' = e^2/g\ m\ m_p \approx 2.84\ 10^2, \tag{2.32.a}$$

$$\gamma'' = e^2/g\ m_p^2 \approx 1.55\ 10^{-2} \tag{2.32.b}$$

where we have used: $m_p/m \approx 1836$. This implies that the interactions are roughly of the same order, but as they also both possess an r^{-2} dependence, and a monopole-monopole character, it is tempting to write $(e_{meas})^2 = e^2 + g\ m_1\ m_2$ for the *measured* effective interaction strength between two masses m_1 and m_2 submitted to a compound of the two forces. But then a manifest impossibility arises because the charge would depend on the masses of the participants in the interaction (for example the effective electron charge in the e^--e^- interaction would differ from the effective proton charge in the p-p interaction), a property which is clearly not observed.

In fact, the additive formula is wrong, and the relations 2.28, 2.32.a, 2.32.b simply indicate that the interactions are of the same order. But they are so much intertwined that their effects cannot be separated. It is not even correct to conceive two distinct interactions as we shall now try to demonstrate by going to the galactic scale where the situation can be visualized easily. Thus, let us consider two galaxies exchanging one CERO. The strength of the exchange force roughly depends on:

a) the probability of CERO emission by the first galaxy over the unit time period.
b) the impulse carried away by the liberated CERO (equal to the impulse transferred to the receiving galaxy).
c) the probability for the CERO to arrive at the second galaxy location which is roughly the propagator $1/R^2$.
d) the CERO capture cross-section by the second galaxy.

Clearly, each factor is greatly influenced by gravitational forces exerted between participants. Even before the exchange takes place, both galaxies induce tidal gravitational perturbations into each other, which may trigger the CERO emission as described in § 1.3. This pre-interaction propagates with velocity c, which is about 100 times larger than the speed C of the CERO exchanged. In other words, even before the exchange, the galaxies are already aware of each other. When the CERO emerges from the first galaxy, it is held in leash by the vortex tube but also by the gravitational attraction exerted by the emitting galaxy. As it approaches the second galaxy, the probability of capture is greatly enhanced by the gravitational force exerted by the target galaxy. Thus, gravitation drives the dynamics of the process all along and when the global force between two galaxies is considered, it is impossible to disentangle it from the exchange effect.

After this digression about galaxies, let us come back to particles. Even if it does not seem possible in the present state of our knowledge to make precise predictions for the mixed electron-proton case, some general conclusions can still be drawn. First, gravitational and photon-exchange effects most probably do not differ as usually claimed by about 40 orders of magnitude, and actually merge in a single force, at energies much lower than usually predicted. The conventional assertion rests on the incorrect use of the gravitational constant $G_{(1)}$ on the particle scale where it clearly does not apply, in view of our results for the simple electron-electron case.

More importantly, our model suggests a breakdown of conventional General Relativity (GR) theory *à la Einstein* on some definite scales, and in particular the particle and the galactic scale. In fact, all objects endowed with intrinsic spin angular momentum do seem to have trouble in GR, notwithstanding the existence of the rotating Kerr solution and the fact that GR very successfully describes intermediate-scale spinless objects like planets, star-planet systems, binary stars, etc.., as more and more refined experiments have shown. Galaxies with their bizarre structures and flat rotation curves do not fit naturally in GR, as well as jets if they are vortex tubes of gravitational (non-magnetic) origin. Solutions representing particles have not been found, but on the other hand, one has stumbled on a whole zoo of non-physical solutions whereas a good theory should select only physical solutions (particles and galaxies). But the simple existence of true singularities should have already cast strong doubts on the validity of GR. If this unconventional view is adopted, a new general relativistic theory must be found which would be able to encompass the galaxy (particle) structures and the dynamics of their CERO (photon) exchange, as well as other types of exchange. Then it would become possible to compute theoretically the exact effective strength of the CERO (photon) exchange force. The fact that the charge of the spiral galaxy (electron) is exactly equal to the charge of the giant elliptical galaxy (proton) would presumably result from a new conservation principle. This is a radical proposal, but certainly not more contrived than the postulate of some dark exotic matter to account for 90 % of the mass in galaxies, or the large families of (non-observed) particles predicted by super-symmetric theories, just to cite two examples. The future theory should contain non vanishing torsion to be able to incorporate spin and it should probably include non-metricity too. Lots of effort in that direction have already been spent with Einstein-Cartan and Weyl type of theories albeit without any really significant success so far. Finally, we would like to stress again, if it is not already clear, that all efforts tending to mould gravitation into the same exchange picture as other interactions are doomed. In fact, the future gravitational theory should be by itself the unified theory describing all particles and their exchange interactions. A similar fate awaits artificial attempts at quantizing gravitation. The quantum behaviour should result from the wave-transmitting properties of the medium discussed in § 1.2.

2.9 FUNDAMENTAL CONSTANTS

A criterion of successful unification is that the resulting theory should contain one unique dimensionless constant (Georgi and Glashow, 1974; Wesson, 1981). Let us call it β. Then choosing a typical physical length L, for example the galactic BH Schwarzschild's radius, as the basic length unit, the unified theory should furnish all other lengths, not only on the galactic scale but on all other scales as well, as functions of L and β. There are indications that $\alpha = e^2/\hbar c$ may play the role of β, as suggested already by Georgi and Glashow (1974) and Wesson (1981). Firstly, α is already the unique constant of electromagnetism. Secondly, notice that it appears ubiquitously on the particle scale, where it is found: (i) as a length ratio between Bohr radius and the electron Compton wavelength, then as another length ratio between the latter and the electron classical radius (ii) as the speed ratio v_1/c *where* $v_1 = e^2/\hbar$ is the electron velocity on the first Bohr orbit (iii) as the energy ratio $(e^2/d)(1/mc^2)$; that is, the electrostatic energy at the Compton distance $d=h/mc$ between two electrons in units of the natural energy mc^2. If the Universe is a fractal, then α should in the same way represent physical ratios on any self-similar scale. Furthermore, α should relate different scales too, otherwise we would be left with other independent dimensionless scaling factors. The fact that simple powers of α relate the various lengths on the particle scale suggests that Λ_L and Λ_T could be simple powers of α. Notice for example how close $\Lambda_L \approx 2.44\ 10^{34}$ falls to $\alpha^{-16} = 1.54\ 10^{34}$ although this may be a pure accident. Finally, another apparent coincidence reinforces the case for α being the unique remaining dimensionless constant. So-called natural dimensions have been discovered by Planck in terms of the basic constants h, c, and $G_{(1)}$:

the Planck mass: $M_{pl} = (\hbar\, c / G_{(1)})^{1/2} = 2.18\ 10^{-5}\ g$ (2.33.a)
the Planck length: $L_{pl} = (\hbar\, G_{(1)} / c^3)^{1/2} = 1.62\ 10^{-33}\ cm$ (2.33.b)
the Planck time: $T_{pl} = (\hbar\, G_{(1)} / c^5)^{1/2} = 5.39\ 10^{-44}\ s$ (2.33.c)

It has always come as a surprise that they do not correspond to anything manifestly known. For example, the Planck mass is ridiculously large if it should relate to the particle scale. But, allowing to our model, one should rather define two new sets in terms of { ħ, g, c} and {*Ħ, G, C*}; that is,

on the particle scale:

the particle Planck mass: $m^* = (\hbar\, c / g)^{1/2} = 2.43\ 10^{-24}\ g$ (2.34.a)
the particle Planck length: $l^* = (\hbar\, g / c^3)^{1/2} = 1.44\ 10^{-14}\ cm$ (2.34.b)
the particle Planck time: $t^* = (\hbar\, g / c^5)^{1/2} = 4.82\ 10^{-25}\ s$ (2.34.c)

on the galactic scale:

the galactic Planck mass: $M^* = (Ħ\, C / G)^{1/2} = 1.34\ 10^{15}\ M_\odot$ (2.35.a)
the galactic Planck length: $L^* = (Ħ\, G / C^3)^{1/2} = 114$ pc. (2.35.b)
the galactic Planck time: $T^* = (Ħ\, G / C^5)^{1/2} = 4.74\ 10^4$ yrs. (2.35.c)

Considering first the particle values, one observes that m^* falls surprisingly close to the proton mass $m_p = 1.67\ 10^{-24}\ g$. We do not believe that this is a coincidence. Indeed, it seems clear that a better adjusted model should yield exactly $m^* = m_p$. The particle Planck length and time approach closely the proton Compton wavelength $\lambda_p = h / m_p c = 2\ 10^{-14}$ cm and the proton *Zitterbewegung* characteristic time $\tau_p = h / m_p c^2 = 7\ 10^{-25}$ s. respectively. This can be shown to result directly from the assumption $m^* = m_p$. Indeed, replacing g expressed in terms of $m^* = m_p$ into (2.34.b) and (2.34.c) yields $l^* = \lambda_p$ and $t^* = \tau_p$. Likewise, on the galactic scale we find a mass close to the predicted (proton-like) giant elliptical mass and a Planck time which is the characteristic *Zitterbewegung* time for proton-like giant elliptical galaxies. The latter should also represent the typical time-scale for CERO emission by those galaxies and it agrees rather well with the experimental values 10^4-10^6 *yrs*. discussed in part I. On the particle scale, *Zitterbewegung* characteristic times are inversely proportional to masses: $\tau_e/\tau_p = m_p/m_e \approx 1836$. Considering the experimental determination of $T_{spir} = 6.34\ 10^7$ *yrs*. for the spiral galaxy characteristic CERO emission period in § 2.3, and the value above $T_{ell} = T^* = 4.74\ 10^4$ *yrs*. for the elliptical period, we find a ratio $T_{spir}/T_{ell} = M_{ell}/M_{spir} = 1337$. Its closeness to m_p/m_e reinforce our belief in the value of a few 10^{14} $M_\odot$ predicted for giant elliptical galaxies in §2.5.

It is clearly a very favourable point of our model that theoretically defined Planck's natural units coincide with known constants. In particular it shows that the gravitational constants g and G are redundant. They are simply redefinitions of the proton mass and proton-like galactic mass respectively. Thus, one is left with only three constants e, ħ and c on the particle scale, from which only one dimensionless constant can be defined, namely α, and this closes our argument. A natural consequence should be that every mass ratio of the theory, and in particular m_p/m_e, is expressible in terms of α.

Let us note further that $m^* = m_p$ entrains $h\ c = g m_p^2$ so that $\alpha = e^2/g m_p^2$ can be alternatively seen as a comparison between the exchange force and the gravitational force exerted between two protons. The equality also entails that our basic formula (2.26) can be rewritten:

$$R_{(2)\,G}/R_{(2)\,BH} = R_{(0)G}/R_{(0)\,BH} = (\alpha/2)\,(m/M_{(0)\,BH})\,(m_P/m)^2 \tag{2.36}$$

Finally, we conclude this part with a discussion of Wesson's (1981) work. He introduces a new dimensionless constant $\eta = G_{(1)} / p\,c$, where p is defined via the universal relation $J = p\,M^2$ which supposedly holds without change from the galaxy to the particle scale. The fact that observations reveal an η value rather close to α is a strong incitation for Wesson to claim that $\eta = \alpha$ exactly. We first remark that if an angular momentum versus mass relation does exist, because p is not dimensionless it is not one but two such relationships that one should write, namely $j = p\,m^2$ on the particle scale, and $J = P\,M^2$ on the galactic scale, and the new dimensionless constant should be defined as: $\eta = g/pc = G/PC$. The equation $j = p\,m^2$ becomes then strikingly similar to Regge trajectories which suggest in turn that in fact many branches exist on each scale, $j = p\,m^2$, $j = p'\,m^2$ etc... The proton branch has $j \approx h$ and $m = m_p$. Thus $p = h/m_p^2$ and $\eta = g/pc = g\,m_p^2/h\,c = 1$!

2.10 THE COSMIC BOHR ATOM

No analogy between particles and galaxies could be considered successful if the quantum behaviour was not compellingly demonstrated for galaxies. As a first step toward that goal, we re-examine our model for the cosmic Bohr atom in this respect. Consider one giant (proton-like) giant elliptical galaxy with one (electron-like) spiral orbiting around the former under the combination of the gravitational attraction (which affects the space-time structure directly and acts continuously) and the CERO exchange force (acting by impulse). The cosmic Bohr radius can be estimated in retrospect by using the average value of the scaling factor for length (2.5), which yields:

$$A_0 = \Lambda_L\,a_0 \approx 41.8\ Mpc \tag{2.37}$$

There is a large difference with the value of 3.3 Mpc we started with in § 2.2.1. This again may signal that Λ_L has been overestimated, as discussed in § 2.2.4. This is probably due to a false apprehension of the galactic radius that should be chosen to correspond to the electron "classical radius". Many indications point to the fact that the spiral galaxy Compton wavelength should be in the range *100-200 kpc*. Thus, the extended galactic radius $R_g \approx 127\ kpc$ computed in § 2.5 should represent this Compton length and accordingly the true classical galactic radius should be α^{-1} times less; that is: $R_{(2)\,G} = \alpha^{-1}\,R_g \approx 1\ kpc$. This is typical of a bulge radius rather than the disk radius we chose originally. To understand why we should have to develop the gravitational theory of CERO-galaxy interaction to the level of precision of quantum electrodynamical theory.

The average speed of the galaxy on the $n = 1$ orbit is $V = \alpha\,C_{(2)} = 17.18\ km\ s^{-1}$ using our computed value of $C_{(2)}$, and $V = \alpha^2\,c = 15{,}96\ km\ s^{-1}$ from the "theoretical" value $C_{(2)} = \alpha\,c$. For binary galaxies, Tifft (1982a, 1982b) finds bunching of redshifts at $72\ kms^{-1}$ and possibly also at $36\ kms^{-1}$ intervals. Mostly for groups of large spiral galaxies with one or more companions, Arp and Sulentic (1985) report peaks in the redshift distribution at $70\ kms^{-1}$ intervals. As supposed implicitly in this section, these redshift differentials should not be due to excess redshift, but to Doppler effect from quantized velocities. However, the values found experimentally do not agree with our prediction but they do not refer to the same systems either. We would like a direct comparison with redshift differentials in Hydrogen-like systems composed of one giant elliptical plus one companion spiral (and not small companion spirals around one large spiral).

Another problem is the smallness of our absolute (not differential) velocity value compared to the velocity dispersion found in clusters ($\approx 800\ kms^{-1}$). We believe that in this case the discrepancy originates from the relatively large redshift differences as function of galaxy type in clusters reported by Jaakkola (1971) and Tifft (1972). These are not due to Doppler velocities but should be caused by the excess redshift alluded to in § 1.4.

Finally, notice that Bohr's quantization condition $\oint \boldsymbol{P}.\boldsymbol{dR} = n\,\hbar$ should hold, and for the first orbit $n = 1$, one has $MVA_0 = \hbar$. The value found this way with $M \approx 12.65\ 10^{10}\ M_\odot$, $V \approx 17.18\ km/s$ and $A_0 = 41.8\ Mpc$ is $\hbar \approx 2.2\ 10^{77}\ gcm^2s^{-1}$ in agreement which the result of § 2.6.

2.11 SMALLER AND LARGER SCALES

Up to this point, we have endeavoured to remain as close as possible to experimentally measurable quantities, but it is not forbidden to speculate that the fractalization of space extends to smaller and larger scales. We have already briefly alluded to fractons as structures pertaining to the scale below particles (§ 1.2). They would compose the supporting medium for particle vortex structures. Using our scaling laws, the typical dimension of a proton-like fracton is found to be $\approx 2\ 10^{-47}\ cm$. This is considerably smaller for example than the traditional Planck length at $\approx 10^{-33}\ cm$ to which no particular significance is attached here but which is usually considered the ultimate limit of the "graininess" of space. The fracton mass would be $\approx 8\ 10^{-100}\ g$, and the fracton ultimate velocity about $3.8\ 10^{12}\ cms^{-1}$, which represents the speed of photon-like fractons.

Likewise, ascending toward larger scales, the model predicts that galaxies should be basic particle-like structures in a larger universe, sometimes also aptly called the "metagalaxy". Some authors predicted that the metagalaxy is rotating, which is an important prediction since rotation would then participate to the metagalaxy dynamics by providing a repulsive centrifugal force. Furthermore, rotation certainly has a meaning in a fractal model: it can be defined with respect to the even larger structure that would contain the metagalaxy.

We can predict a radius $R_{MG} = 9.52\ 10^{56}\ cm$, a mass $M_{MG} = 1.1\ 10^{117}\ g$, and an angular momentum $J_{MG} = 4.61\ 10^{181}\ gcm^2s^{-1}$ for such a stabilized and fully developed meta-galaxy. For comparison, the values reported for the visible Universe are of order $R_{vis} \approx 10^{26\text{-}27}\ cm$, $M_{vis} \approx 10^{55\text{-}56}\ g$ and $J_{vis} \approx 10^{91\text{-}93}\ gcm^2s^{-1}$, (Muradyan, 1980; Sistero, 1983). The considerable difference shows that our Universe is extremely young and that it is probably far from having stabilized into a fully formed "particle". This is confirmed by the very small estimated number of CEROs emitted by galaxies up to the present time (about 200, see § 2.3).

3. CONCLUSIONS

The recurrent apparition of similar ratios when comparing the galactic and particle scale seem to support the idea that the Universe is a fractal, with galaxies and galaxy clusters reproducing self-similarly particle and atomic - (or molecular-) like systems respectively. By taking this hypothesis a step further it was shown that CEROs are good candidates for photon homologue on the galactic scale, and spiral galaxies for electrons. Proton- and neutron-like systems should be associated to giant elliptical galaxies. The interaction which should be responsible for cluster dynamics would be a mixture of the gravitational interaction and of the CERO exchange force, for which it was possible to compute approximately the coupling constant, or, in other words, the "charge" of a spiral galaxy. However, discordant results for the radius of the cosmic Bohr atom and for the quantum of cosmic angular momentum seem to indicate too large a value for the length scaling factor. This in turn might point to the necessity of choosing a smaller characteristic radius for spiral galaxies to be compared to the classical electron radius, or of including dwarf spiral galaxies in our statistics, or both. The first Bohr velocity is much too small compared to velocity dispersion in clusters which we suggest is due to large excess redshift differences as a function of galaxy types in clusters. Thus, more work would be necessary to refine the range of values given here. On the good side we were able to interpret Planck's dimensions on the particle scale in terms of the proton characteristics, showing that the so-called "quantum black hole" is nothing else than the proton. This allowed the prediction that α is the dimensionless constant of the future unified theory. Reflecting backwards, if the trend toward unification is justified, the fractal hypothesis represents a plausible and elegant solution. For if structures reproduce self-similarly on the various scale, one single theory can describe all scales at once. Otherwise, one would have to build different physics for different scales as is customary now.

Furthermore, if the fractal hypothesis was vindicated, it could have profound implications for cosmology. Indeed, as soon as galaxies formed in the early Universe a strong repulsive interaction emerged between spiral galaxies and may have accelerated the expansion. Later on, when the galactic "gas" temperature became sufficiently low, a threshold appeared where atomic-like galactic system decoupled from the "radiation" (free CEROs). Afterwards, cosmic atoms tended to aggregate into molecular-like systems, but because "charge" screening was imperfect, galactic scale "molecules" experienced Van der Waals type of forces, which would explain why clusters further aggregated in super-clusters and even larger filamentary structures.

On the principle that the Universe is economical of structures, and even if the self-similarity evoked here finally proves to be imperfect, it is likely that much new knowledge and innovative ideas could be gained as to the nature of particles by looking at galaxies, and one could benefit from the fact that structures on this scale can be studied in much greater details and at considerably lesser expenses.

ACKNOWLEDGMENTS

I had numerous and enlightening discussions on the subject with J. Demaret and J. P. Swings. I appreciated their constant encouragement during the laborious evolution of this model, and also the possibility of using the facilities at the Liège Institute of Astrophysics. It is also a pleasure to acknowledge the helpful comments of P. Tombal and Y. Derop and some material support from the Hoechst Belgium Company. My hearty thanks go to A. Van Gestel who provided a document leading to the computation of the time scaling factor and to all my friends who had to endure my constant rattle about quasars for more than ten years, especially amongst those A. and F. Coquelet. Finally, I owe enormously to Catherine Burnet for without her constant caring and moral support I would not have been able to complete this work.

APPENDIX A: COSMOLOGICAL CORRECTIONS

The well-known expressions for standard cosmological corrections (see for example Sandage, 1988) are first stated at some length to facilitate comparison with the tired-light case (Appendix B) and the mixed case (Appendix C) below. Let us consider light rays emitted from a quasar at wavelength λ_e and received by an observer at λ_0. The quasar redshift satisfies $1 + z = \lambda_0/\lambda_e$ and arises from the relativistic time dilatation effect described by $dt_0 = (1 + z)\, dt_e$. Let I_e and I_0 be the bolometric intensities (with dimensions erg s^{-1} cm^{-2} sr^{-1}) at the emitter and source respectively. If absorption and scattering are negligible over the light path, then energies emitted and absorbed in a time increment *dt* are related by: $I_e dt_e = (1 + z)\, I_0 dt_0$. This is due to the fact that all photons emitted are collected but each one loses energy on the trip by an amount *(1+z)* as shown by the relationship between λ_o and λ_e. Now using the transformation of time units in the latter relation yields the transport relation:

$$I_e = (1 + z)^2\, I_0 \tag{A.1}$$

For a source emitting only in the narrow range $d\lambda_e$, the bolometric intensity becomes $I_{\lambda_e}\, d\lambda_e$ 1for which (A.1) still applies, hence using $d\lambda_0 = d\lambda_e(1 + z)$, one obtains:

$$I_{\lambda_e} = (1 + z)^3\, I_{\lambda_0} \tag{A.2}$$

The bolometric flux received f_0 is related to the source luminosity L_e by an expression of the type $f_0 = L_e/4\pi R^2$, and the value of *R* computed from that relation is called the luminosity distance. It differs from the proper distance Δ precisely because of relativistic corrections. The correct relationship can be found starting from (A.1) and it is:

$$L_e = (1 + z)^2\, 4\pi\Delta^2\, f_0 \tag{A.3}$$

For monochromatic quantities, one has, using the same trick as before:

$$L_{\lambda_e} = (1 + z)^3\, 4\pi\Delta^2\, f_{\lambda_0} \tag{A.4}$$

In a Robertson-Friedmann-Walker space-time, Δ can be written as $\Delta(z) = cZ(z)/H_0$ where *Z(z)* is an "effective" redshift:

$$Z(z) = \frac{1}{q_0^2(1+z)}\left[q_0 z + (q_0 - 1)\sqrt{1 + 2q_0 z} - 1\right] \tag{A.5}$$

Finally, a radial separation θ can be converted to a linear separations *D* with the formula:

$$D = \Theta \frac{\Delta}{(1+z)} \tag{A.6}$$

This can be used for separations between objects or compact object diameters but not for isophotal diameters determined on the basis of a certain limiting magnitude per square degree. In this case, the more complicated relation can be found in Sandage (1988) for example.

In the optical domain, it is customary to work in the magnitude system. Let m_λ be the apparent magnitude of the source at proper distance Δ and wavelength λ, then by definition:

$$m'_\lambda\,(\Delta') - m''_\lambda(\,\Delta'') = -2.5\, \ln \frac{f'_\lambda(\Delta')}{f''_\lambda(\Delta'')} \tag{A.7}$$

Now let m_{λ_0} 2be the apparent magnitude of the source at proper distance Δ and M_{λ_0} be 3the corresponding absolute magnitude at the conventional luminosity distance of 10 pc. Then, using (A.7) and (A.4), one obtains:

$$m_{\lambda_0} - M_{\lambda_0} = 5(\ln \Delta - 1) + 7.5 \ln(1 + z) + K^s_{\lambda_0}(z) + A_{\lambda_0} \tag{A.8}$$

where a term A_{λ_0} 4has been added to represent the absorption correction inside our Galaxy, and where we have defined the selective (λ dependent) reddening correction as follows:

$$K^s_{\lambda_0}(z) = 2.5\, \ln \frac{L_{\lambda_0}}{L_{\lambda_e}} \tag{A.9}$$

Note that the usual reddening correction is usually defined otherwise (Oke and Sandage, 1968) with one factor $2.5 \ln(1 + z)$ from the right-hand side of (A.8) included into the definition. This part is called the non-selective term and it has been included to

take into account the change in bandwith between emitter and observer. Here we prefer to leave all explicitly z-dependent terms out of K^s for comparison with other equations to follow. Note also that our sign convention agrees with that for giant elliptical galaxies in Oke and Sandage (1968) but is the reverse of Sandage's (1966) reddening correction for QSO's. More explicitly, our K^s is related to Sandage's (1966) correction K^* by: $K^s + 2.5\ln(1+z) = -K^*$. A more rigorous expression than (A.8) should involve the finite band width of the spectral response of the filters used to measure magnitudes (see Oke and Sandage, 1968).

APPENDIX B: CORRECTIONS FOR TIRED LIGHT MECHANISMS

We now consider the other extreme case where the whole redshift z is entirely due to a tired light mechanism in the postulated gaseous envelope surrounding the quasar. It is not necessary to know about the details of this mechanism in order to compute magnitude corrections since the resulting effect is just another redshift. Thus, we still have $d\lambda_0 = d\lambda_e(1+z)$ but the shift does not depend on a relativistic time dilatation. Hence the universe can be considered Euclidean on the relatively short path where it arises, so that $dt_0 = dt_e$. The equations of appendix A can be retraced with this modification in mind, which yields $I_{\lambda_e} = (1+z)^2\, I_{\lambda_0}$ 5and consequently:

$$L_{\lambda_e} = (1+z)^2\, 4\pi R^2\, f_{\lambda_0} \tag{B.1}$$

where R is now the Euclidean distance of the source. Notice that it also differs from the luminous distance because of the $(1+z)^2$ factor. Equation (A.7) becomes here:

$$m_{\lambda_0} - M_{\lambda_0} = 5(\ln R - 1) + 5\ln(1+z) + K^s_{\lambda_0}(z) + A_{\lambda_0} \tag{B.2}$$

with the same formal definition of the selective reddening correction as before.

APPENDIX C: COSMOLOGICAL AND TIRED LIGHT EFFECTS COMBINED

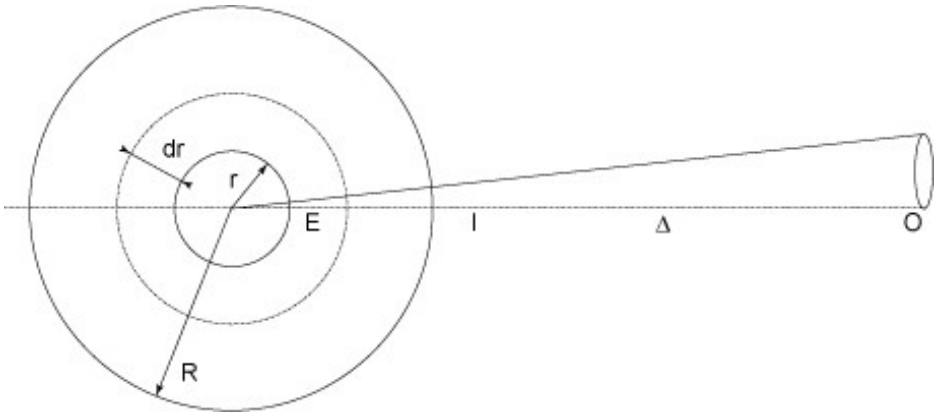

Fig. 8: The quasar core has a typical dimension *r* of order *1 au*. Most of the light is emitted in the BLR and the NLR; that is, in a shell of width *dr* extending to about 1 kpc from the core. A gaseous envelope of external radius $R \approx$ 10-100 kpc is postulated around the core, and this is where most of the excess redshift z_t supposedly arises. This as yet unknown tired-light mechanism displaces the emitted wavelength from λ_e to $\lambda_i = (1+z_t)\lambda_e$. An observer O at proper distance $\Delta \gg R$ sees the light at wavelength $\lambda_0 = (1+z_c)\lambda_i$, where the shift z_c is of purely cosmological origin.

The geometry of the problem is depicted on fig. 8. In the exceptional circumstance that the quasar is found interacting with a galaxy of cosmological redshift z_c, the total quasar redshift z can be separated into a tired light contribution z_t and a cosmological contribution z_c. The tired light effect from E to I shifts the wavelength λ_e at r to the wavelength λ_i at R, with $1 + z_t = \lambda_i/\lambda_e$. In the relatively small distance from r to R, cosmological effects are deemed negligible and the luminosity distance coincides with the proper distance. Cosmological effects shift λ_i at R to λ_0 at Δ with $1 + z_c = \lambda_0/\lambda_i$. The total shift is:

$$1 + z = \frac{\lambda_0}{\lambda_e} = (1+z_t)(1+z_c) \tag{C.1}$$

Let us denote by m'_{λ_0} , m''_{λ_0} 6the apparent magnitudes at proper distance *R* and Δ respectively, and by M_{λ_0} 7the absolute magnitude at luminosity distance 10 pc. Our problem is to compute $m''_{\lambda_0} - M_{\lambda_0}$8. Firstly, the magnitude definition (A.6) between points *I* and *O* gives:

$$m'_{\lambda_0}(R) - m''_{\lambda_0}(\Delta) = -2.5 \ln \frac{f'_{\lambda_0}(\mathrm{R})}{f''_{\lambda_0}(\Delta)} \tag{C.2}$$

Now, the flux $f'_{\lambda_0}(R)$ at some wavelength λ_0 can be related to the emitter's luminosity *L(r)* at radius r, by the tired light formula (B.1):

$$f'_{\lambda_0}(R) = \frac{1}{(1+z_t)^2} \frac{1}{4\pi \mathrm{R}^2} L_{\lambda_0/(1+z_t)} \tag{C.3}$$

where *r* has been neglected before *R*. Next, the flux at *O* may be computed by applying the cosmological formula (A.4) between *I* and *O*, assuming a fictive source at *I* of luminosity *L′* and radius *R*:

$$f''_{\lambda_0}(\Delta) = \frac{1}{(1+z_c)^3} \frac{1}{4\pi\Delta^2} L'_{\lambda_0/(1+z_c)} \tag{C.4}$$

where *R* has been neglected before *Δ*, the latter being determined as a function of z_c via equation (A.5). The problem has been transferred to the evaluation of *L′* at *I*. Since the universe does not depart significantly from a Euclidean universe between E and I, we are allowed to use the Euclidean relation:

$$L'_\lambda(R) = 4\pi R^2 f'_\lambda(R) \tag{C.5}$$

Thus (C.4) becomes:

$$f''_{\lambda_0}(\Delta) \approx \frac{1}{(1+z_c)^3} \left(\frac{R}{\Delta}\right)^2 f'_{\lambda_0/(1+z_c)} \tag{C.6}$$

But (C.3) relates *f′* to *L*, so that (C.6) may finally be written:

$$f''_{\lambda_0}(\Delta) \approx \frac{(1+z_t)}{(1+z)^3} \frac{1}{4\pi\Delta^2} f'_{\lambda_0/(1+z)} \tag{C.7}$$

where use has been made of (C.1). Substitution of (C.7) and (C.3) into (C.2) furnishes:

$$m''_{\lambda_0}(\Delta) - m'_{\lambda_0}(R) = 2.5 \ln\left(\frac{L_{\lambda_0/(1+z_t)}}{L_{\lambda_e}}\right) + 5 \ln\left(\frac{\Delta}{R}\right) + 7.5 \ln(1+z_c) \tag{C.8}$$

Another equation is needed to relate m' to the absolute magnitude. It derives from the tired light formula (B.2):

$$m'_{\lambda_0}(R) - M_{\lambda_0} = 5(\ln(R) - 1) + 5 \ln(1+z_t) + 2.5 \ln\left(\frac{L_{\lambda_0}}{L_{\lambda_0/(1+z_t)}}\right) + A_{\lambda_0} \tag{C.9}$$

Adding (C.8) and (C.9) yields the desired equation:

$$m''_{\lambda_0}(\Delta) - M_{\lambda_0} = 5\big(\ln\big(\Delta(z_c)\big) - 1\big) + 2.5 \ln(1+z_c) + 5.0 \ln(1+z) + K^s_{\lambda_0}(z) + A_{\lambda_0} \tag{C.10}$$

with as before:

$$K^s_{\lambda_0}(z) = 2.5 \ln \frac{L_{\lambda_0}}{L_{\lambda_e}} \tag{C.11}$$

This reduces to the cosmological formula (A.7) when $z = z_c$. It should be noticed that the selective term has not changed, which was expected since it depends only on the total shift *z*. However, the non-selective term has been slightly modified, which justifies a posteriori our decision to extract it from the total reddening correction for comparison. It must be stressed again that *Δ* is computed via (A.5) with z_c, the cosmological part of redshift only.

For completion, the same relations are written in frequency units. The tired light formula (C.3) translates to:

$$f'_{\nu_0}(R) = \frac{1}{4\pi \mathrm{R}^2} L_{\nu_0/(1+z_t)} \tag{C.12}$$

and the cosmological formula (C.4) becomes:

$$f''_{\nu_0}(\Delta) \approx \frac{1}{(1+z_c)} \frac{1}{4\pi\Delta^2} L'_{\nu_0/(1+z_c)}(R) \tag{C.13}$$

Thus, the same kind of calculation yields:

$$m''_{\nu_0}(\Delta) - M_{\nu_0} = 5\big(\ln\big(\Delta(z_c)\big) - 1\big) + 2.5\ln(1+z_c) + K^s_{\nu_0}(z) + A_{\nu_0} \tag{C.14}$$

With $K^s_{\nu_0}(z) = 2.5\ \ln\frac{L_{\nu_0}}{L_{\nu_e}}9$. When $z = z_c$, this again reduces to the usual cosmological formula:

$$m_{\lambda_0}(\Delta) - M_{\nu_0} = 5\big(\ln\big(\Delta(z)\big) - 1\big) + 2.5\ln(1+z) + K^s_{\nu_0}(z) + A_{\nu_0} \tag{C.15}$$

BIBLIOGRAPHY

Adams T.F., (1977), Ap. J. Suppl. Series **33,** 19.
Alladin S.M., (1965), Ap. J. **141,** 768.
Ambartsumian V.A., (1958), in *La structure et l'évolution de l'Univers*, 11ième conseil de physique Solvay, ed. R. Stoops, Bruxelles, p.24.
Ambartsumian V.A., (1961), Astron. J. **66**, 536.
Ambartsumian V.A., (1965), in *The Structure and Evolution of Galaxies*, 13th Solvay Conference on Physics, University of Brussels, Interscience Publishers.
Antonucci R.R.J., (1993), Ann. Rev. Astron. Astrophys. **31**, 473.
Antonucci R.R.J. and Miller J.S., (1985), Ap. J. **297**, 621.
Arakelian M.A., (1971), Astrofizika **7**, 457.
Arp H., (1966), Ap. J. Suppl. Series **14**, 1.
Arp H., (1967), Ap. J. **148**, 321.
Arp H., (1968), Publ. Astron. Soc. Pacific **80**, 129.
Arp H., (1969), Astron. Astrophys. **3,** 418.
Arp H., (1970), Astron. J. **75,** 1.
Arp H., (1971a), Astrophys. Letters **9,** 1.
Arp H., (1971b), Astrophys. Letters. **7**, 221.
Arp H., (1972), in *External Galaxies and Quasi-Stellar Objects*, IAU Symposium 44, ed. D.S. Evans, p.380.
Arp H., (1976), Ap. J. (Letters) **207**, L147.
Arp H., (1977), in *L'évolution des galaxies et ses implications cosmologiques*, Colloqium No.263, ed. C. Balkowsky and B.E. Westerlund, Paris, CNRS, p. 377.
Arp H., (1980), Ap. J. **239**, 469.
Arp H., (1981), Ap. J. **250**, 31.
Arp H., (1983), Ap. J. **271**, 479.
Arp H., (1987), *Quasar, Redshift and Controversies*, Interstellar Media, Berkeley.
Arp H., (1990a), Astrophys. Space Sci. **167**, 183.
Arp H., (1990b), IEEE transactions on Plasma Science **18**, 77.
Arp H. and Burbidge G., (1990), Ap. J. **353**, L1.
Arp H., Burbidge G., Hoyle F., Narlikar J.V. and Wickramasinghe N.C., (1990), Nature **346**, 807.
Arp H. and Sulentic J.W., (1979), Ap. J. **229**, 496.
Arp H. and Sulentic J.W., (1985), Ap. J. **291**, 88.
Arp H., Sulentic J.W. and Di Tullio, G., (1979), Ap. J. **229**, 489.
Arp H., Surdej J. and Swings J.P., (1984), Astron. Astrophys. **138**, 179.
Bahcall N.A., (1977), Ann. Rev. Astron. Astrophys. **15**, 505.
Bahcall J.N., Jannuzi B.T., Schneider D.P., Hartig G.F. and Jenkins E.B., (1992), Ap. J. **398**, 495.
Bailey M.E. and Clube S.V.M., (1978), Nature **275**, 278.
Balick B. and Heckman T.M., (1982), Ann. Rev. Astron. Astrophys. **20**, 431.
Balick B. and Heckman T.M., (1983), Ap. J. **265**, L1.
Balkowski C., (1973), Astron. Astrophys. **29**, 43.
Barthel P.D., (1987), in *Superluminal Radio Sources*, ed. Zensus J.A. and Pearson T.J., Cambridge University Press, p.148.
Beichman C. A. et al., (1985), Ap. J. **293**, 148.
Beichman C.A., Soifer B.T., Helou G., Chester T.J., Neugebauer G., Gillett F.C. and Low F.J., (1986), Ap. J. **308**, L1.
Bekenstein J.D. and Milgrom M., (1984), Ap. J. **286**, 7.
Bergeron J. and Kundth D., (1984), M.N.R.A.S **207**, 263.
Binney J. and Tremaine S., (1987), *Galactic Dynamics*, Princeton university Press.
Bjorken J.D. and Drell S.D., (1964), *Relativistic Quantum Mechanics*, McGraw-Hill.
Blades J.C., (1987), in *QSO Absorption Lines: Probing the Universe*, Proceedings of the QSO Absorption Line Meeting, Baltimore, May 19-21 1987, ed. J.C. Blades, D.A Turnshek and C.A Norman, Cambridge University Press.
Bottinelli L. and Gouguenheim L., (1974), Astron. Astrophys. **33**, 269.
Boroson T.A. and Oke J.B., (1984), Ap. J. **281**, 535.
Boroson T.A., Persson S.E. and Oke J.B., (1985), Ap. J. **293**, 120.
Boroson T.A. and Green R.F., (1992), Ap. J. Suppl. Series **80**, 109.
Boskenberg A. and Sargent W.L.W., (1978), Ap. J. **220**, 42.
Bosma A., (1978), Ph.D. Thesis, University of Groningen.
Bowen D.V., Pettini M., Penston M.V. and Blades J.C., (1991a), Mon. Not. R. Astron. Soc. **248**, 153.
Bowen D.V., Pettini M., Penston M.V. and Blades J.C., (1991b), Mon. Not. R. Astron. Soc. **249**, 145.
Bradt H.V., Burke B.F., Canizares C.R., Greenfield P.E., van Paradijs J. and Koski A.T., (1978), Ap. J. (Letters) **226**, L111.
Brandt J.C., (1960), Ap. J. 131, **293**.
Brandt J.C. and Belton M.J.S., (1962), Ap. J. **136**, 352.
Bregman J.N. et al., (1981), Nature **293**, 714.
Brown R.L. and Lo K.Y., (1982), Ap. J. **253**, 108.

Browne I., (1987), in *Superluminal Radio Sources*, ed. Zensus J.A. and Pearson T.J., Cambridge University Press, p.111.
Burbidge G., (1967), Nature **216**, 1287.
Burbidge G., (1979), Nature **282**, 451.
Burbidge G., (1980), in *IAU Symposium 92*, eds. Abell G.O. and Peebles P.J.E., Doordrecht, Reidel, p.99.
Burbidge E.M., Burbidge G., Solomon P.M. and Strittmatter P.A., (1971), Ap. J. **170**, 233.
Burbidge G., Hewitt A., Narlikar J.V. and Das Gupta P., (1990), Ap. J. Suppl. Series, **74,** 675; **BHNDG**.
Burstein, D. and Heiles C., (1978), Ap. J. **225**, 40.
Caldwell N. and Philips M.M., (1981), Ap. J. **244**, 447.
Carilli C.L., van Gorkom J.H. and Stocke J.T., (1989), Nature **338**, 134.
Cecil G. and Stockton A., (1985), Ap. J. **288**, 201.
Clube S.V.M., (1978), Vistas in Astronomy **22**, 77.
Clube S.V.M., (1983), in *Quasars and Gravitational Lenses*, Proceedings of the 24 th. Liège Astrophysical Colloqium, p.393.
Cocke W.J., (1983), Astrophys. Letters **23**, 239.
Cocke W.J., (1985), Ap. J. **288**, 22.
Cocke W.J. and Tifft W.G., (1983), Ap. J. **268**, 56.
Crawford M.K., Genzel R., Harris A.I., Jaffe D.T., Lacy J.H., Lutgen J.B., Serabyn E. and Townes C.H., (1985), Nature **315**, 467.
Crenshaw D.M. and Blackwell Jr. J.H., (1990), Ap. J. **358**, L37.
Dai Wen-sai, Liu Ru-liang and Hu Fu-xing, (1979), Chinese Astronomy **3,** 31; (1978), Acta Astron. Sinica **19**, 24; **DLH**.
Davies R.D. et al., (1976), Mon. Not. R. Astron. Soc. **177**, 319.
DerSarkissian M., (1984), Nuovo Cimento (Letters) **40**, 390
DerSarkissian M., (1986a), Astrophys. Space Sci. **126**, 185.
DerSarkissian M., (1986b), Astrophys. Space Sci. **126**, 409.
de Vaucouleurs, G. and de Vaucouleurs A., (1964), *Reference Catalogue of Bright Galaxies*, University of Texas Press, Austin.
Dressler A., (1976), Ph. D Thesis, University of California, Santa Cruz.
Dressler A., (1980), Ap. J. Suppl. series **42**, 565.
Dressler A. and Richstone D.O., (1988), Ap. J. **324**, 701.
Driessen P., (1983), *Einstein versus Bohr,* Journal « l'intermédiaire », revue pour cadres et dirigeants, 3, p.1, 4 février 1983.
Driessen P., (1986), *Einstein-Cartan Theory with a Geometrized Contortion Tensor*, in the abstracts of the 11th. conference on General Relativity and Gravitation, Stockholm, July 6-12, 1986, p.78.
Driessen P., (1991), Fractal Space-Time, non-published. This paper had a tormented history: it was first submitted to Astrophysics & Space Science, September 2, 1991, under the name "Fractal Space-Time". A lengthy reviewal process ensued with no less than four referees. None wanted to accept it or refuse it. Finally, the editor Zdenek Kopal accepted it, in August 12, 1992. However, I had found an error and I asked Kopal to stop the publication process. I resubmitted it in considerably improved form, in June 8 1994, under the name "A Fractal Universe Model". But, in the meantime, Kopal had died, and the new editor, J.E. Dyson, argued that, since it was a revised version, it should go through the reviewing process again. After six months, it came back with a refusal in March 21, 1995, with the comment from the referee that it was "not credible". Finally, I published it in the viXra archive when it became available (see Driessen 2015, below).
Driessen P., (2015), *A Fractal Universe Model*, viXra.org: 1510.0124.
Driessen P., (2020), *A Fractal Model of Particles*, viXra.org: 2005.0268.
Eckers R.D., Fanti R., Lari C. and Parma P., (1978), Nature **276**, 588.
Faber S.M. and Gallagher J.S., (1976), Ap. J. **204**, 365.
Faber S.M. and Gallagher J.S., (1979), Ann. Rev. Astron. Astrophys. **17**, 135.
Fabian A.C., Nulsen P.E.J. and Canizares C.R., (1984), Nature **310**, 733.
Fabricant D. and Gorenstein P., (1983), Ap. J. **267**, 535.
Field G.B., Arp H. and Bahcall J.N., (1973), *The Redshift Controversy*, Benjamin, Reading, Massachussets.
Gaskell C.M., (1983), in *Quasars and Gravitational Lenses*, Proceedings of the 24 th. Liège Astrophysical Colloqium, p.473.
Gehren T., Fried J., Wehinger P.A. and Wyckoff S., (1984), Ap. J. **278**, 11.
Genzel, R. and Townes C.H., (1987), Ann. Rev. Astron. Astrophys. **25,** 377.
Georgi H. and Glashow S.L., (1974), Phys. Rev. (Letters) **32,** 438.
Giovanelli R. and Haynes M.P., (1989), Ap. J. (Letters) **346**, L5.
Gower A., Gregory P.C., Hutchings J.B. and Unruh W.G., (1982), Ap. J. **262**, 478.
Grandi S.A. and Osterbrock D.E., (1978), Ap. J. **220**, 783.
Haschick A.D. and Burke B.F., (1975), Ap. J. (Letters) **200**, L137.
Hawkins M.R.S., (1978), Mon. Not. R. Astron. Soc. **182**, 361.
Heckman T.M., (1978), Publ. Astron. Soc. Pacific **90**, 241.
Heckman T.M., (1987), in *IAU Symposium 121*, *Observational Evidences of Activity of Galaxies*, eds. E. Khachikian, K. Fricke and J. Melnick, Reidel, Doordrecht.
Heckman T.M., Bothum G.D., Balick B. and Smith E.P., (1984), Astron. J. **89**, 958.
Heckman T.M., Miley G.K., Balick B. van Breugel W.J.M. and Butcher H.R., (1982), Ap. J. **262**, 529.
Heidmann N., (1968), Astrophys. Letters **3**, 153.
Henry J.P., Becklin E.E and Telesco C.M., (1984), Ap. J. **280**, 98.
Hine R.G. and Longair M.S., (1979), Mon. Not. R. Astron. Soc. **188**, 111.
Hodge P.W., (1963), Astron. J. **68**, 237; 470

Hodge P.W., (1970), in *IAU Symp. 44*, Uppsala, Sweden.
Holmberg E.B., (1958), Medd. Lunds Astron. Obs. II, **136**.
Hoyle F., (1965), Nature **208**, 111.
Hoyle F. and Burbidge G., (1966), Ap. J. **144**, 534.
Hoyle F., Burbidge G. and Sargent W.L.W., (1966), Nature **209**, 751.
Huchra J. and Sargent W.L.W., (1973), Ap. J. **186**, 433.
Hutchings J.B., Crampton D. and Campbell B., (1984), Ap. J. **280**, 41.
Hutchings J.B., Campbell B. and Crampton D. (1982), Ap. J. **261**, L23.
Hutchings J.B., Crampton D. and Campbell B. and Pritchet C., (1981), Ap. J. **247**, 710.
Jaakkola T., (1971), Nature **234**, 534.
Jaakkola T., Donner K.J. and Teerikorpi P., (1975), Astrophys. Space Sci. **37**, 301.
Keel W.C., (1983), Ap. J. **269**, 466.
Kellerman K.I. et al., (1977), Ap. J. **214**, L61.
Kormendy J., (1988), Ap. J. **325**, 128.
Kristian J., (1973), Ap. J. (Letters) **179**, L61.
Kronberg P.P., Burbidge E.M., Smith H.E. and Strom R.G., (1977), Ap. J. **218**, 8.
Laing R.A., (1981), Mon. Not. R. Astron. Soc. **195**, 261.
Lawrence A., (1987), Publ. Astron. Soc. Pacific **99**, 309.
Liakhovets, (1986), in *Abstracts of the 11 th. conference on General Relativity and Gravitation*, July 6-12 1986, Stockholm, Sweden, p.152.
Lin D.N.C. and Lynden-Bell D., (1982), Mon. Not. R. Astron. Soc. **198**, 707.
Linfield R., (1981), Ap. J. **250**, 464.
Liu Yong-Zhen, Deng Zu-Gan and Cao Sheng-Lin, (1984), Astrophys. Space Sci. **116**, 215.
Lonsdale C.J. and Morison I., (1983), Mon. Not. R. Astron. Soc. **203**, 833.
López-Corredoira M. and C. M. Gutiérrez C. M., (2002) Astron. & Astrophys. Lett., **390-3**, L15.
Lynden-Bell D., (1969), Nature **223**, 690.
Lynden-Bell D., (1971), Mon. Not. R. Astron. Soc. **155**, 119.
Lynden-Bell D. and Pringle J.E., (1974), Mon. Not. R. Astron. Soc. **168**, 603.
Malkan M.A., (1984), Ap. J. **287**, 555.
Mandelbrot B.B., (1982), *The Fractal Geometry of Nature*, San Francisco, Freeman.
Meisenheimer K. and Röser H.-J., (1986), Nature **319**, 459.
Miley G.K. and Miller J.S., (1979), Ap. J. (Letters) **228**, L55.
Milgrom M., (1983), Ap. J. **270**, 371.
Mirabel I.F., Rodriguez L.F., Cordier B., Paul J. and Lebrun F., (1992), Nature **358**, 215.
Muradyan R.M., (1980), Astrophys. Space Sci. **69**, 339.
Narlikar J.V., (1986), in *IAU Symposium 119*, *Quasars*, eds. Swarup G. and Kapahi V.K., p.463.
Narlikar J.V. and Das P.K., (1980), Ap. J. **240**, 401.
Neff S.G., Hutchings J.B. and Gower A.C., (1989), Astron. J. **97**, 1291.
Nordsieck K.H., (1973a), Ap. J. **184**, 719.
Nordsieck K.H., (1973b), Ap. J. **184**, 735; **NS**.
Oemler A. Jr., (1976), Ap. J. **209**, 693.
Oke J.B. and Sandage A., (1968), Ap. J. **154**, 21.
Oldershaw R.L., (1985), Internat. J. Gen. Systems, **10**, 235.
Oldershaw R.L., (1986a), Internat. J. Gen. Systems, **12**, 137.
Oldershaw R.L., (1986b), Astrophys. Space Sci. **126**, 203.
Oldershaw R.L., (1986c), Astrophys. Space Sci. **126**, 199.
Oldershaw R.L., (1986d), Internat. J. Gen. Systems **13**, 67.
Oldershaw R.L., (1987), Ap. J. **322**,34.
Orr M. and Browne I., (1982), Mon. Not. R. Astron. Soc. **200**, 1067.
Osterbrock D.E., (1977), Ap. J. **215**, 733.
Ostriker J.P., (1977), in *Evolution of Galaxies and Stellar Populations*, eds. R.B. Larson and B.M. Tinsley, New Heaven, Yale University Observatory, p. 369.
Ostriker J.P. and Peebles P.J.E., (1973), Ap. J. **186**, 467.
Owen F.N. and O'Dea, C., (1983), Bull. A.A.S. **14**, 949.
Porcas R.W., (1987), in *Superluminal Radio Sources*, ed. Zensus J.A. and Pearson T.J., Cambridge University Press, p.12.
Rieke G.H., Lebofsky M.J. and Kinman T.D., (1979), Ap. J. (Letters) **232**, L151.
Rieke G.H. and Rieke M.J., (1988), Ap. J. **330**, L33.
Roberts M.S., (1976), Comments on Astrophys. **6**, 105.
Romanishin W. and Hintzen, P., (1989), Ap. J. **341**, 41.
Röser H.-J. and Meisenheimer K., (1986), Astron. Astrophys. **154**, 15.
Rowan-Robinson M., (1972), Nature **236**, 112.
Rowan-Robinson M., (1973), Astron. Astrophys. **23**, 331.
Rubin V.C., Ford W.K. and Thonnard N., (1978), Ap. J. (Letters) **225**, L107.

Rudnick L. and Edgar B.K., (1984), Ap. J. **279**, 74.
Sandage A.R., (1966), Ap. J. **146**, 13.
Sandage A.R., (1972a), Ap. J. **173**, 485.
Sandage A.R., (1972b), Ap. J. **178**, 25.
Sandage A.R., (1973), Ap. J. **180**, 687.
Sandage A.R., (1988), Ann. Rev. Astron. Astrophys. **26**, 561.
Sandage A.R. and Cacciari C., (1990), Ap. J. **350**, 645.
Sanders R.H. and Prendergast K.H., (1974), Ap. J. **188**, 489.
Sandage A.R. and Visvanathan, N., (1978), Ap. J. **225**, 742.
Sanders R.H., (1981), Ap. J. **244**, 820.
Sanders R.H., (1986), Mon. Not. R. Astron. Soc. **223**, 539.
Sanders R.H. and Bania T.M., (1976), Ap. J. **204**, 341.
Sanders D.B., Soifer B.T., Elias J.H., Madore B.F., Matthews K., Neugebauer G. and Scoville N.Z., (1988), Ap. J. **325**, 74.
Sarazin, C. L., (1986), Rev. Mod. Phys. **58**, 1.
Sarazin, C. L. and O'Connell, (1983), Ap. J. **268**, 552.
Sargent W.L.W., (1972), Ap. J. **173**, 7.
Schmidt M., (1976), Ap. J. (Letters) **209**, L55.
Schwarz M.P., (1979), Ph.D. thesis, Australian National University.
Schweizer F., (1980), Ap. J. **237**, 303.
Schweizer F., (1982), Ap. J. **252**, 455.
Serabyn E., Lacy J.H., Townes C.H. and Bharat R., (1987), Ap. J. **326**, 171.
Setti G. and Woltjer L., (1973), Ann. N.Y. Acad. Sci. **224**, 8.
Setti G. and Woltjer L., (1977), Ap. J. **218**, L33.
Shklovsky, I.S., (1962), Astron. Zh. **39**, 591.
Shklovsky, I.S., (1971), Astrophys. Letters **10**, 5.
Simkin S.M., Su H.J. and Schwarz M.P., (1980), Ap. J. **237**, 404.
Sistero R.F., (1983) Astrophys. Letters **23**, 235.
Sivaram C. and Sinha K.P., (1979), Phys. Reports **51**, 111.
Steiner J.E. (1981), Ap. J. **250**, 469.
Stockton A. N., (1978), Ap. J. **223**, 747.
Stockton A. N., Wyckoff S. and Wehinger P.A. (1979), Ap. J. **231**, 673.
Sulentic J.W., (1981), Ap. J. (Letters) **244**, L53.
Sulentic J.W., (1983a), Ap. J. **265**, L49.
Sulentic J.W., (1983b), in *Quasars and Gravitational Lenses*, Proceedings of the 24 th. Liège Astrophysical Colloqium, p.360.
Sulentic J.W., (1983c), Ap. J. (Letters) **265**, L49.
Sulentic J.W., (1986), Ap. J. **304**, 617.
Sulentic J.W., (1988), in *New Ideas in Astronomy*, ed. Bertola F., Sulentic J.W. and Madore B.F., Cambridge University Press, p.123.
Sulentic J.W. and Arp H.C., (1987a), Ap. J. **319**, 687.
Sulentic J.W. and Arp H.C., (1987b), Ap. J. **319**, 693.
Takase B. (1967), Publ. Astron. Soc. Japan **19**, 427.
Takase B. and Kinoshita H., (1967), Publ. Astron. Soc. Japan **19,** 409; **TK**.
Terlevich R., and Melnick, J. (1985), Mon. Not. R. Astron. Soc. **213**, 841.
Terrell J., (1964), Science **145**, 918.
Terrell J., (1966), Science **154**, 1281.
Thorne K.S., Price R.H. and MacDonald D.A., (1986), *Black Holes: The Membrane Paradigm*, Yale University Press, Newhaven.
Tifft W.G., (1972), Ap. J. **175**, 613.
Tifft W.G., (1976), Ap. J. **206**, 38.
Tifft W.G., (1978), Ap. J. **221**, 756.
Tifft W.G., (1980), Ap. J. **236**, 70.
Tifft W.G., (1982a), Ap. J. **257**, 442.
Tifft W.G., (1982b), Ap. J. **262**, 44.
Tifft W.G. and Cocke W.J., (1984), Ap. J. **287**, 492.
Toomre A., (1963), Ap. J. **138**, 385.
Toomre A., (1977), in *Evolution of Galaxies and Stellar Populations*, eds. R.B. Larson and B.M. Tinsley, New Haeven, Yale University Observatory, p. 401.
Toomre A. and Toomre J., (1972), Ap. J. **178**, 623.
Trimble V., (1987), Ann. Rev. Astron. Astrophys. **25**, 425.
Tully, R.B., (1988), *Nearby Galaxies Catalogue*, Cambridge University Press; TU
Turnshek D.A, (1987), in *QSO Absorption Lines: Probing the Universe*, Proceedings of the QSO Absorption Line Meeting held in Baltimore, May 19-21 1987, eds. J.C. Blades, D.A Turnshek and C.A Norman, p. 17.
Valentijn E.A and Casertano S., (1988), Astron. Astrophys. **206**, 27.
van der Kruit P.C., Oort J.H. and Mathewson D.S., (1972), Astron. Astrophys. **21,** 169.

Vigier J.P., (1988), in New Ideas in Astronomy, Proceedings of a Conference held in honour of Arp's 60th birthday, Venice, May 5-7, 1987, p. 257.
Vorontsov-Velyaminov B., (1961), Astron. J. **66**, 551.
Webster A., (1982), Mon. Not. R. Astron. Soc. **200**, 47.
Weedman D.W., (1970), Ap. J. (Letters) **161**, L113.
Weedman D.W., (1971), Astrophys. Letters **9**, 49.
Weedman D.W., (1973), Ap. J. **183**, 29.
Weedman D.W., (1976), Quart. J. R. Astron. Soc. **17**, 227.
Weedman D.W., (1977), Ann. Rev. Astron. Astrophys. **15**, 69.
Weedman D.W., (1980), Ap. J. **237**, 326.
Wehinger P.A and Wyckoff S., (1978), Mon. Not. R. Astron. Soc. **184**, 335.
Wesson P.S., (1981), Phys. Rev. **D23**, 1730.
Wiita P.J. and Siah M.J., (1981), Ap. J. **243**, 710.
Wilson A.S. and Heckman T.M., (1985), in *Astrophysics of Active Galaxies and Quasi-Stellar Objects*, ed. by J.S. Miller (Mill Valley, CA: University Science Books), p. 39.
Wolf R.A. and Bahcall J.N., (1972), Ap. J. **176**, 559.
Wyckhoff S., Wehinger P.A and Gehren T., (1981), Ap. J. **247**, 750.
Zaritsky D., Olszewski E.W., Schommer R.A., Peterson R.C., Aaronson M., (1989), Ap. J. **345**, 759.
Zensus J.A., (1987), in *Superluminal Radio Sources*, ed. Zensus J.A. and Pearson T.J., Cambridge University Press, p.26.
Zwicky F. and Karpowicz M., (1966), Ap. J. **146**, 43.